Geographic, Hydrologic, and Geochemical Characterization of Ra Contaminated Groundwater in Wisconsin

A Final Report prepared for the State of Wisconsin Groundwater Research and Monitoring Program

Madeleine Mathews[1], Sean R. Scott[2], Madeline B. Gotkowitz[3], and Matthew Ginder-Vogel[1]*

1. Environmental Chemistry and Technology Program, Department of Civil and Environmental Engineering, University of Wisconsin – Madison, Madison, WI
2. Wisconsin State Laboratory of Hygiene, Madison, WI
3. Montana Bureau of Mines and Geology, Butte, MT

Table of Contents

Project Summary
Title: Geographic, Hydrologic, and Geochemical Characterization of Ra Contaminated Groundwater in Wisconsin

Project ID: DNR236

Investigators:
Principle Investigator: Matthew Ginder-Vogel, Associate Professor, Dept. of Civil and Environmental Engineering, University of Wisconsin – Madison

Co-Principal Investigator: Madeleine Gotkowitz, Research Division Chief/Professor, Montana Bureau of Mines and Geology (previously affiliated with the Wisconsin Geological and Natural History Survey)

Co-Principal Investigator: Florence Udenby, Graduate student, Dept. of Civil and Mineral Engineering, University of Toronto (previously affiliated with the Wisconsin Department of Natural Resources)

Research Assistant: Madeleine Mathews, Doctoral Candidate, Environmental Chemistry and Technology Program, University of Wisconsin – Madison

Period of Contract: 07/01/2018 - 06/30/2020

Background/Need:
Groundwater, an important source of drinking water in Wisconsin, is susceptible to contamination by naturally occurring metals and radionuclides (e.g., radium). Many wells open to the Cambrian-Ordovician aquifer system (COAS) in Wisconsin source water containing radium (Ra) levels measuring at or above the maximum contaminant level (MCL) of the combined activity of ^{226}Ra and ^{228}Ra. Regional groundwater quality trends are useful to predict Ra occurrence across the Midwestern US; however, complex contaminant-solid phase associations make it difficult to use these trends at the state or municipal level. Here, we aim to develop a conceptual understanding of the major sources of Ra to groundwater throughout the COAS in Wisconsin, using sequential extractions examining Ra-solid phase associations as well as temporal and spatial analysis of long-term datasets.

Objectives: (1) Identification and characterization of geographically distributed wells with elevated dissolved Ra. (2) Quantify the Ra leaching potential of solids associated with elevated dissolved Ra concentrations. (3) Provide a geographically and geochemically relevant basis for management decisions.

Methods:
In this study, we quantify ultra-trace radium (Ra) levels in from a series of sequential extractions of aquifer solids sourced from the COAS in Wisconsin, using multi-collector inductively coupled plasma mass spectrometry (MC-ICPMS) techniques. Examined stratigraphic units include the Maquoketa shale, Galena dolostone, St. Peter sandstone, and Tunnel City sandstone. The quantification of parent isotope ^{238}U via MC-ICPMS allows for comparison of parent/daughter

activity ratios, providing information on potential mobilization of Ra from the site of parent decay. Additionally, spatial and temporal trends in radium concentrations in groundwater from the COAS in Wisconsin were evaluated with a Wisconsin Department of Natural Resources compliance dataset, collected from public water supplies. Thorough documentation of methods and all collected data are fully described in Appendices B and C.

Results and Discussion:
Quantification of the Ra leaching potential of selected stratigraphic units reveals that local geochemistry plays a major role in Ra partitioning from aquifer solids to the aqueous system in the COAS in Wisconsin. Comparison of whole-rock parent (^{238}U) and daughter (^{226}Ra) isotope activities indicates that Ra remains close to the site of ^{238}U decay in all examined stratigraphic units as the $^{238}U/^{226}Ra$ ratio is not significantly different from the equilibrium value. However, the $^{238}U/^{226}Ra$ ratios in the Maquoketa shale and St Peter sandstone sample groups also are not significantly different from twice the equilibrium value, indicating Ra leaching. Across the examined stratigraphy, Ra levels vary. For example, average whole-rock ^{226}Ra activity is 70 ± 10 mBq/cm^3 in the Maquoketa shale while average whole-rock ^{226}Ra is 6 ± 1 mBq/cm^3 in the St Peter sandstone. Radium in the cumulative non-HF digested fractions, or the more geochemically-mobile portion, also varied across stratigraphic units. Specifically, 63% of the more geochemically-mobile ^{226}Ra in the Maquoketa shale is measured in the acido-soluble fraction with 37% in the reducible fraction, in comparison to only 6% of the more geochemically-mobile ^{226}Ra in the Tunnel City sandstone is measured in the acido-soluble fraction with 94% in the reducible fraction.

Additionally, analysis of long-term trends in Ra levels in Wisconsin groundwater demonstrates differing trends at the state scale in comparison to trends determined for individual municipalities. Specifically, statistically significant increasing trends in combined radium activity ($^{226}Ra + ^{228}Ra$) for portions of the aquifer confined by the Maquoketa shale unit ($p < 10^{-15}$, $n = 211$) as well as the aquifer system where the Maquoketa shale is not present ($p < 10^{-15}$, $n = 340$). At the municipal scale, increasing radium trends is also observed in the communities of Sussex ($p < 10^{-15}$, $n = 98$) and Brookfield ($p < 10^{-15}$, $n = 35$) in Wisconsin, with and a decreasing trend in the city of Waukesha ($p < 10^{-9}$, $n = 176$).

Conclusions/Implications/Recommendations:
This study develops a combined geochemical and hydrologic conceptual model describing Ra release from, and potential sequestration in, in the COAS in Wisconsin in order to provide a scientific basis for strategies to minimize Ra in drinking water sourced from groundwater. Particularly, we demonstrate the influence of local factors on Ra mobilization in the COAS in Wisconsin, where it depends on both reactive solid-phases present in bedrock stratigraphy and on local geochemical conditions influencing solid-phase-Ra interactions. This suggests that changes in geochemical conditions (e.g., competitive ion exchange) impacts Ra partitioning from solid-phase to the aqueous system differently across stratigraphic units. We also display the value of using water quality compliance datasets for investigating contaminant trends both spatially and temporally; it is important to keep in mind geographic scale and context in examining Ra trends.

Key Words: Radium, groundwater, geochemistry, water quality, publicly available datasets, trend analysis

Appendix A: Awards, Publications, Reports, Patents, Presentations, Students

Publications, Reports and Patents:

Mathews, M.; Scott, S. R.; Gotkowitz, M. B.; Ginder-Vogel, M., Association of radionuclide isotopes with aquifer solids in the Midwestern Cambrian-Ordovician aquifer system. *ACS Earth and Space Chemistry* **2021**.

Dematatis, M.; Plechacek, A.; Mathews, M.; Wright, D. B.; Udenby, F.; Gotkowitz, M. B.; Ginder-Vogel, M., Spatial and temporal variability of radium in the Wisconsin Cambrian-Ordovician aquifer system. *AWWA Water Science* **2020**.

Presentations:

Madeleine Mathews, Sean Scott, Madeline Gotkowitz, Matthew Ginder-Vogel; "*Isotopic analysis of radionuclide presence at discrete intervals in the Midwestern Cambrian-Ordovician aquifer system."* Presentation at GSA – 2020 Annual Meeting; October 28, 2020.

Madeleine Mathews, Madeline Gotkowitz, Sean Scott, Matthew Ginder-Vogel; "*Radionuclide association with aquifer solids in the Midwestern Cambrian-Ordovician aquifer system.*" Presentation at GSA – 2019 Annual Meeting; September 25, 2019.

Madeleine Mathews, Madeline Gotkowitz, Matthew Ginder-Vogel; *"Radionuclide Sorption to Aquifer Solids in the Midwestern Cambrian-Ordovician aquifer system."* Presentation at: AWRA Wisconsin Section – 2019 Annual Meeting; March 1, 2019.

Amy Plechacek, Marie Dematatis, Madeleine Mathews, Florence Olson, Madeline Gotkowitz, Matthew Ginder-Vogel; "Geologic and Geochemical Conditions Affecting Radium Mobility in the Wisconsin Cambrian- Ordovician Aquifer System." Poster presentation at: AWRA Wisconsin Section – 2019 Annual Meeting; February 28, 2019.

Awards:

The initial results of this research were leveraged to obtain student funding from the Grainger Wisconsin Distinguished Graduate Fellowship.

Students:

Madeleine Mathews – Doctoral Candidate in the Environmental Chemistry and Technology Program at UW – Madison
mmathews2@wisc.edu, 660 N. Park St., Madison, WI 53706

Appendix B: Publication - Association of radionuclide isotopes with aquifer solids in the Midwestern Cambrian-Ordovician aquifer system

Madeleine Mathews[1], Sean R. Scott[2], Madeline B. Gotkowitz[3], and Matthew Ginder-Vogel[1]*

1. Environmental Chemistry and Technology Program, Department of Civil and Environmental Engineering, University of Wisconsin – Madison, Madison, WI
2. Wisconsin State Laboratory of Hygiene, Madison, WI
3. Montana Bureau of Mines and Geology, Butte, MT

*Corresponding author. Tel.: (608) 262-0768; E-mail address: matt.ginder-vogel@wisc.edu

Adapted from: Mathews, M.; Scott, S. R.; Gotkowitz, M. B.; Ginder-Vogel, M., Association of radionuclide isotopes with aquifer solids in the Midwestern Cambrian-Ordovician aquifer system. *ACS Earth and Space Chemistry* **2021**.

ACS EARTH AND SPACE CHEMISTRY

http://pubs.acs.org/journal/aesccq

Article

Association of Radionuclide Isotopes with Aquifer Solids in the Midwestern Cambrian−Ordovician Aquifer System

Madeleine Mathews, Sean R. Scott, Madeline B. Gotkowitz, and Matthew Ginder-Vogel*

Cite This: https://dx.doi.org/10.1021/acsearthspacechem.0c00279

Read Online

ACCESS | Metrics & More | Article Recommendations | Supporting Information

ABSTRACT: Groundwater, an important source of drinking water globally, is susceptible to contamination by naturally occurring metals and radionuclides. Regional trends in groundwater quality are useful in predicting the occurrence of contaminants but are difficult to translate to local scales due to complex contaminant−solid phase associations. Here, the aqueous phase of sequential extractions is analyzed using multicollector inductively coupled plasma mass spectrometry techniques to quantify ultratrace radium (Ra) levels in operationally defined fractions of the aquifer solids. Results demonstrate that local-scale geochemistry drives Ra partitioning to groundwater in the U.S. Midwestern Cambrian−Ordovician aquifer system. Analysis of whole-rock extractions indicates that parent and daughter isotope activity ratios indicate that Ra remains close to the site of ^{238}U decay in most stratigraphic units, where the $^{238}U/^{226}Ra$ ratio is similar to the equilibrium value; however, other stratigraphic units display isotope ratios indicative of Ra leaching. Additionally, Ra varies in prevalence across examined stratigraphy, in both whole-rock and sequential extractions; the average whole-rock ^{226}Ra activity is 70 ± 10 mBq/cm^3 in the Maquoketa shale in comparison to 6 ± 1 mBq/cm^3 in the St Peter sandstone. This suggests that Ra mobilization depends on both the reactive solid phases present in the stratigraphy and the influence of local geochemical conditions on solid phase−contaminant interactions. Variation in geochemical conditions, such as redox or competitive ion exchange, affects Ra partitioning to groundwater differently across stratigraphy, depending on initial solid-phase associations.

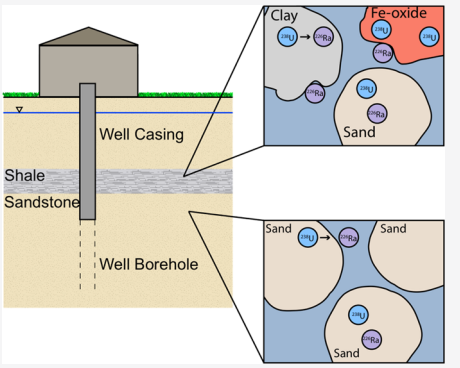

KEYWORDS: *groundwater, contamination, Midwestern Cambrian−Ordovician aquifer system, radium, ICP-MS*

INTRODUCTION

Groundwater is a major source of drinking water worldwide, with an estimated 2.5 billion people relying solely on groundwater for daily water needs.[1] The presence of contaminants affects the quantity of groundwater available for drinking, as degraded water quality dictates overall water availability.[2,3] Regulatory and research efforts often focus on prevention and/or remediation of anthropogenic contaminants in groundwater; however, naturally occurring contaminants (e.g., Ra, As) are already present within many aquifer systems and can be mobilized by changes in geochemical conditions.[4−11] In many cases, water quality is degraded by naturally occurring constituents, increasing water stress within a community and thus requiring expensive water treatment or alternate water sources.[12,13] Local-scale spatial variability (e.g., within a municipality) in well water quality, combined with annual and decadal temporal variation, also complicates management of municipal well fields.[14] A better understanding of processes controlling naturally occurring contaminant speciation and partitioning within aquifer systems may contribute to maintaining groundwater as a potable water resource.[15,16]

Determining the processes controlling the distribution of naturally occurring contaminants within a heterogeneous aquifer is challenging, in part because complex flow paths within regional aquifer systems, and local flow paths impacted by groundwater pumping, affect subsequent contaminant partitioning into the groundwater. *In situ* solid phase−contaminant associations are also difficult to ascertain, as many studies examine water samples from municipal wells, which are screened over long intervals across heterogeneous groundwater systems. Naturally occurring contaminants in aquifers and aquitards are often associated with reactive solid-phase surfaces and when released degrade water quality.[17,18] For some radiogenic contaminants, alpha decay can eject daughter nuclides from the mineral lattice into the aqueous phase (e.g., ^{226}Ra from the ^{238}U decay chain).[19] Geochemical factors, including changes in redox conditions and/or total dissolved solids (TDS), influence contaminant partitioning to aquifer solids through processes including precipitation/dissolution and sorption/desorption.[4,7,20−27] Competition for

Received: October 14, 2020
Revised: December 16, 2020
Accepted: December 17, 2020

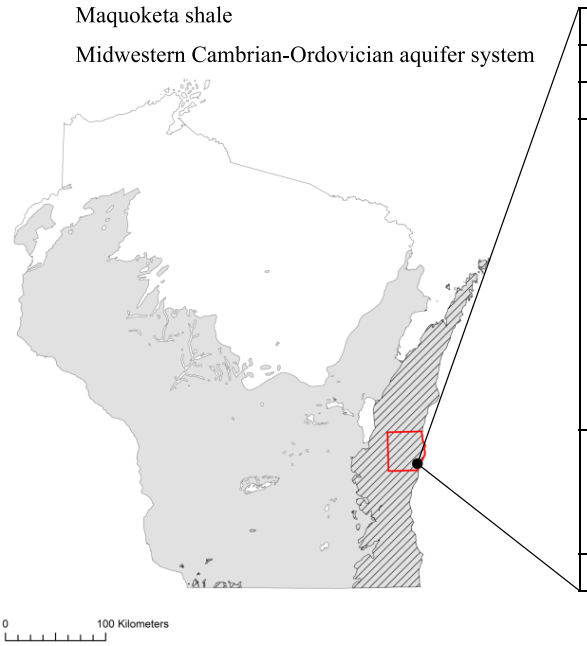

Geologic time	Stratigraphic unit (depth below surface)*
Pleistocene	Glacial drift (0 - 40 m)
Silurian	Niagara dolostone (40 - 226 m)
Ordovician	**Maquoketa shale** (226 - 296 m) Subsampled depth: 294 m
	Galena dolostone (296 - 332 m) Subsampled depth: 307 m
	Decorah dolostone (332 - 340 m)
	Platteville dolostone (340 - 360 m)
	St Peter sandstone (360 - 417 m) Subsampled depth: 379 m
Cambrian	**Tunnel City sandstone** (417 - 549 m) Subsampled depth: 423 m
	Mt. Simon sandstone (549 - 570 m)
Precambrian	Crystalline bedrock

*Table not to scale

Figure 1. Midwestern Cambrian−Ordovician aquifer system extent in Wisconsin (gray), and the portion confined by the Maquoketa shale (diagonal lines). The inset shows the location of the borehole in Sheboygan Co., and the representative stratigraphy at the drill site. Stratigraphy in bold are the units examined in this study, with specified subsampled depth.

sorption sites at a high ionic strength results in a decrease in the sorption capacity for specific, naturally occurring contaminants, resulting in contaminant partitioning into the aqueous phase.[17,28−31] Additionally, the dissolution and/or absence of iron (Fe) and manganese (Mn) oxides due to anoxic aquifer conditions can cause elevated levels of associated contaminants.[4,7,19,21,23,32]

Radium (Ra) is one example of a naturally occurring contaminant that degrades groundwater quality upon partitioning to the aqueous phase. Radium is a naturally occurring radionuclide found at elevated levels in regionally important groundwater systems, including the Midwestern Cambrian−Ordovician (MCOAS) and the North Atlantic Coastal Plain aquifer systems.[4,7] Since long-term ingestion of water containing elevated Ra can result in osteosarcoma and other bone diseases, the US Environmental Protection Agency regulates Ra in drinking water with a maximum contaminant level (MCL) of 185 mBq/L (5 pCi/L) for the combination of the two major isotopes, ^{226}Ra and ^{228}Ra. Guidelines from the World Health Organization recommend an individual dose criterion of 0.1 mSv for total radionuclides in drinking water consumption for 1 year, where mSv is a unit of radiation dose measuring the health impact of ionizing radiation on the human body.[16,33−37]

Geochemical interactions between Ra and aquifer solids in groundwater systems affect Ra partitioning to the aqueous system.[38] In the laboratory, Ra sorption to solid phases such as clay and transition-metal oxides (e.g., Fe, Mn) has been verified.[39−43] At the laboratory scale, contaminant−solid interactions can be examined via sequential extraction of rock core obtained from aquifer systems to determine contaminant distribution between various solid phases. Due to the low concentrations of concern, counting methods used to analyze Ra in solution often require large sample volumes (>500 mL) and/or generate relatively high analytical detection limits, which limits applicability in situations where sample volume is limited.[44−47] Analytical techniques such as multi-collector inductively coupled plasma mass spectrometry (MC-ICPMS) can measure isotopes of contaminants at ultratrace levels in the small sample volumes produced by laboratory experiments.[48−50]

Analysis of leachate from sequential extractions provides information about the association of ^{226}Ra and ^{238}U with aquifer solids, and about the mobility of daughter isotopes from the site of parent decay.[51,52] Here, we use MC-ICPMS to quantify ^{226}Ra associated with various fractions of aquifer solids from sequential extraction experiments examining multiple stratigraphic units from the MCOAS. The sensitivity of the MC-ICPMS technology provides quantitative results to examine partitioning from ultratrace Ra levels in MCOAS solids. This work enables examination of Ra availability across different types of bedrock, to better understand the influence of geochemical factors on Ra release to groundwater in aquifer systems.

MATERIALS AND METHODS

Midwestern Cambrian−Ordovician Aquifer System. The MCOAS underlies a large portion of the Midwestern United States, including parts of Minnesota, Iowa, Missouri, Illinois, Indiana, and Wisconsin. More than 630 million gallons per day of groundwater is withdrawn for public and domestic water supply.[53] The Cambrian and Ordovician sedimentary bedrock is largely composed of permeable marine sandstones and carbonate rock; the clastic rocks are typically cemented by calcite ($CaCO_3$) and dolomite ($(Ca,Mg)CO_3$). In some locations, these permeable and prolific aquifers are separated by locally or regionally confining shale aquitards. Crystalline Precambrian basement rock underlies this groundwater system. A large portion of the Cambrian and Ordovician formations are regionally confined by the Maquoketa shale, particularly in eastern Wisconsin, and throughout the formation's extent in Iowa, Illinois, Indiana, and Missouri. Groundwater below the

https://dx.doi.org/10.1021/acsearthspacechem.0c00279
ACS Earth Space Chem. XXXX, XXX, XXX−XXX

Maquoketa shale is typically anoxic, with an estimated groundwater age ranging from 6000 to 40 000 years before present.[54,55] Elevated Ra commonly occurs in groundwater obtained from this confined system.[32] Broad geochemical trends associated with elevated Ra include low dissolved oxygen and elevated TDS.[4,7,23,52,56] Sampling at discrete intervals within the MCOAS suggests similar geochemical trends related to elevated Ra in the groundwater.[38]

Sample Selection and Preparation. This study examined a core collected in 1961 from a regionally confined portion of the MCOAS in Sheboygan County, Wisconsin. Subsamples examined include the lower Maquoketa shale, the Galena dolostone, the St Peter sandstone, and sandstone of the Tunnel City Group (Figure 1). At this location, the subsample of the Maquoketa shale was taken from the Scales Member, which consists primarily of gray dolomitic shale with 0.1% total organic carbon and some fine disseminated iron sulfides. It is underlain by the Galena Formation, a massive dolostone with occasional vugs and chert nodules. The fine- to medium-grained, clean quartz sandstone of the St Peter Formation is poorly cemented where sampled. The 132 m thickness of Tunnel City Group has heterogeneous lithology, consisting primarily of sandstone and glauconitic sandstone, with minor amounts of quartzite and interbedded dolomite; a glauconitic sandstone interval was sampled for this experiment (Figure 1).

Subsamples of each stratigraphic unit were selected from the core and prepared for the experiment. Although the ∼150 mm diameter core was stored under atmospheric conditions, visual inspection for Fe oxidation rinds revealed the extent of oxidation was limited to <3 mm on the core's outer edge. To obtain samples representative of the regionally confined aquifer system, we cut into the middle of each core length and removed the oxidized edges. After preparation, samples were kept in an anoxic environment where each was pulverized, then finely ground by agate mortar and pestle. Samples were then sieved through a 1 mm mesh into 500 mL centrifuge tubes. Each depth was subsampled in triplicate to account for heterogeneity within individual samples.

Sequential Extractions. Sequential extractions were conducted at room temperature in an anoxic chamber (Table 1). The first extraction targeted water-soluble metals, using synthetic groundwater composed of a saturated solution of trace-metal-grade calcium carbonate ($CaCO_3$) in ultrapure water, purged with nitrogen gas until anoxic, then the solution was brought to ∼pH 8 with trace-metal-grade hydrochloric acid (HCl). A rock-to-extractant mass ratio of 1:10 was initially utilized: 200 mL of each extracting reagent was added to 20 g of the prepared bedrock sample. The solution was then shaken for less than a minute and then kept undisturbed for 16 h. Each sample was then centrifuged at 4000 rpm for 30 min, and the supernatant was filtered with a 0.45 μm PTFE membrane filter. The filtrate was then preserved with trace-metal-grade nitric acid (HNO_3) to pH < 2. The second extraction used 1 M trace-metal-grade acetic acid added to the solid from the previous step and targeted sorbed metals and metals associated with carbonate minerals; however, it is possible that some Fe and Mn (hydr) oxides may dissolve in this step.[57] This suspension was also shaken, then kept undisturbed for 16 h before centrifuging and filtering, as previously described. The third extracting reagent was 0.04 M hydroxylamine hydrochloride in 25% v/v acetic acid and targeted remaining Mn oxide and some Fe oxides with hydroxylamine hydrochloride as the reducing agent.[57−62] After addition of 200 mL of the extracting reagent to the remaining solid, the samples were shaken and then kept undisturbed for 16 h at room temperature, after which each was centrifuged and filtered as in previous steps.[63−65] Note that barite is not a targeted mineral in these extractions, since the low dissolved sulfate content of the system indicates that it is undersaturated. X-ray diffraction analysis of aquifer solids subsamples from before and after the extraction was conducted to further examine changes in crystalline mineral phases (Figures S2−S9).

Table 1. Sequential Extraction and Digestion Methods[a]

fraction	targeted associations	reagent	temperature, time
water-soluble	water-soluble ions	calcium carbonate (saturated)	RT, 16 h
acido-soluble	sorbed metals, carbonate minerals[57]	1 M acetic acid	RT, 16 h
reducible	Mn and Fe oxides	0.04 M hydroxylamine hydrochloride in 25% v/v acetic acid	RT, 16 h
HF-digested	residual metals; mineral lattice	conc. HF, HNO_3, HCl	100−110 °C, 24 h

[a]RT = room temperature.

Whole-Rock Digestion. The remaining solids were dried and then completely digested at the conclusion of the sequential extraction. Each sample was baked at 50 °C until dry. Next, 0.5 g dry weight of each was placed into a clean Teflon bottle, to which 2 mL of concentrated trace-metal-grade HNO_3 and 1 mL of concentrated trace-metal-grade hydrochloric acid (HCl) were added and then heated at ∼100 °C in a block heater overnight. After initial heating, 1 mL of concentrated trace-metal-grade hydrofluoric acid (HF) and 3 mL of ultrapure water were added to all samples; all samples were then heated at 100−110 °C for an additional 24 h.[64] The containers were cooled to room temperature, then 1 mL of HCl and 1 mL of ultrapure water were added to the digestion liquid, and samples were heated uncapped from 105 to 85 °C. An addition of 4 mL of concentrated HNO_3 was added to each sample and heated uncapped from 105 to 95 °C; this step was repeated until few or no solids were observed in the samples. Hydrofluoric acid was added to any samples with visible silicate minerals and samples were heated; then, the series of evaporations were repeated. Finally, the samples were diluted with 50 mL of ultrapure water and 50 mL of saturated boric acid solution.[64,66]

General Chemical Analysis. Alkalinity and pH were determined for the water-soluble samples. A PerkinElmer Optima 4300 DV inductively coupled plasma optical emission spectrometer was used to analyze for bulk metals (e.g., Ca, Mg, Na, Mn, Fe, Ba, Sr) in all samples. Isotopic analysis for Ra parent isotopes ^{238}U and ^{232}Th was conducted using a Thermo Scientific ELEMENT2 high-resolution inductively coupled plasma mass spectrometer at the Wisconsin State Laboratory of Hygiene Trace Elements Clean Laboratory.

Preparation for Ra Isotopic Analysis. Each aqueous sample from the sequential extractions was purified through a series of columns prior to Ra isotopic analysis.[67] Column volume (CV) is contingent on sample volume, specified for each column purification step below. The resins were stored in dilute acid; to fill a column, the resin was shaken to suspend and an appropriate volume of the slurry was added to the column via a pipette. Initially, each sample was evaporated to

https://dx.doi.org/10.1021/acsearthspacechem.0c00279
ACS Earth Space Chem. XXXX, XXX, XXX−XXX

dryness, dissolved in one CV of conc. HNO_3, and taken to dryness again. Then, the dried sample was dissolved in one CV of conc. HNO_3 and one CV of ultrapure water (e.g., ~7 M HNO_3) and heated at ~110 °C under reflux.

The first column isolated the cations from the rest of the sample. Here, typical CVs were 2 mL of AG1-X8 (100−200 mesh) anion exchange resin. The addition of the sample load (e.g., sample dissolved in 2 CV ~7 HNO_3) and subsequent 1.5 CV of ~7 M HNO_3 washes containing Ra were collected and taken to dryness. One CV conc. HCl was added and then taken to dryness prior to purification on the second column.

The second column separated the Ra + barium (Ba) fraction from the majority of the matrix elements from the isolated cation fraction from the first column; here, typical CVs were 2 mL of AG50W-X8 (200−400 mesh) cation exchange resin. Each dried sample collected from the first column was dissolved in one CV of 1 M HCl for loading onto the column and heated at ~110 °C under reflux. Five progressively stronger washes of HCl were passed through the column, until the Ra fraction was collected in 4.5 CV of 6 M HCl, followed by 2 CV of 8 M HCl; the Ra fraction was determined via elution chemistry. The Ra + Ba fraction was taken to dryness, and one CV of conc. HNO_3 was added; then, the sample was taken to dryness again for the third column.

The third and fourth columns removed Ba remaining in the sample after the second column purification. To separate the Ra and Ba, 0.5 mL of Eichrom SrSpec resin settled over 0.2 mL of Eichrom Prefilter inert resin beads was used. The sample was dissolved in 0.5 CV of 3 M HNO_3 for loading onto the column. Once loaded, one CV of 3 M HNO_3 was passed through; then, the Ra fraction was eluted with five CV of 3 M HNO_3 and collected. The collected samples were then evaporated. The column was then cleaned with two alternating washes of ultrapure water and 3 M HNO_3; then, the SrSpec column procedure was repeated for complete Ba removal.

The final column removed ^{228}Th produced via decay during the sample purification process. It was similar to the first column, but with one CV equal to 1 mL of AG1-X8 resin. After the fifth column, the samples were evaporated; then, 100 μL of 16 M HNO_3 was added and heated at 145 °C to decompose organic residue from the resin. After evaporation, 25 μL of 16 M HNO_3 was added and the samples were briefly (<5 min) heated at 130 °C; 0.5 mL of ultrapure water was then added to each sample during the preparation for isotopic composition measurements.

Radium Isotopic Analyses. Mean beam intensities of ^{226}Ra were measured using the Neptune Plus MC-ICPMS at the Wisconsin State Laboratory of Hygiene. Isotope ratios were measured using a single SEM/RPQ detector in dynamic mode. Total yields were determined using a calibration curve created from dilutions of the NIST4967A ^{226}Ra solution standard. Ra standard yields and isotope ratios were used to calculate the activities of ^{226}Ra in the samples; these were converted to number of atoms, from which Ra activities were calculated. The detector was calibrated before each analytical session using a dilute tuning solution containing ^{238}U. A rock standard (USGS SBC-1) was digested in the same manner as the other HF-digested rocks and run through the purification columns and analyzed on the MC-ICPMS. Final ^{226}Ra activities were corrected using a factor of 0.59 based on an average of yields determined from the NIST4967A and SBC-1 standards processed by column purification alongside samples. Uncertainty in ^{226}Ra activities is calculated from the standard deviation of the measured beam intensity.

RESULTS

Whole-Rock ^{226}Ra and ^{238}U. Although not the primary objective of this work, the whole-rock ^{238}U/^{226}Ra ratio is an essential measurement to understanding how the total amount of Ra varies across different stratigraphic units (Table 2). Note

Table 2. Measured Whole-Rock Radionuclide Activities Per Sample, as a Sum of All Fractions[a]

stratigraphic unit	depth (m)	^{238}U (mBq/g rock)	^{226}Ra (mBq/g rock)
Maquoketa shale−1	294	94 ± 1	88 ± 1
Maquoketa shale−2	294	98 ± 1	75 ± 4
Maquoketa shale−3	294	104 ± 1	59 ± 2
Galena dolostone−1	307	74.6 ± 0.7	58.98 ± 0.09
Galena dolostone−2	307	66.7 ± 0.5	61 ± 1
Galena dolostone−3	307	72.8 ± 0.8	56 ± 1
St Peter sandstone−1	379	10.2 ± 0.2	5 ± 1
St Peter sandstone−2	379	8.5 ± 0.2	7.7 ± 0.3
St Peter sandstone−3	379	9.2 ± 0.2	6.5 ± 0.3
Tunnel City sandstone−1	423	18.6 ± 0.2	15 ± 1
Tunnel City sandstone−2	423	18.0 ± 0.1	22 ± 1
Tunnel City sandstone−3	423	20.4 ± 0.3	18.6 ± 0.4
SBC-1	SRM	64.8 ± 0.7	65 ± 1

[a]Uncertainty represents instrumental error. Units are mBq/cm^3 aquifer unless otherwise specified. SRM = Standard reference material.

that here we define activity (A) as the radioactive decay of a nuclide

$$A = N^*\lambda \quad (1)$$

where N is the number of atoms and λ is the radioactive decay constant; the number of atoms per g rock is first converted to dpm then to mBq per cm^3 aquifer, using bulk rock properties for porosity and dry bulk density (Table S1). The activity ratio is defined as the ratio of whole-rock daughter and parent nuclide activities (e.g., ^{226}Ra and ^{238}U); whole-rock activities are the sum of the radionuclide from each experimental fraction. The Maquoketa shale has the highest content of radionuclides; whole-rock ^{238}U activities average 99 ± 5 mBq/cm^3 from three samples, with average whole-rock ^{226}Ra activity of 70 ± 10 mBq/cm^3, where the uncertainty represents standard deviation (results from individual samples provided in Table 2). The St Peter sandstone samples have the lowest amount measured, with 9.3 ± 0.9 mBq/cm^3 average whole-rock ^{238}U activities, and 6 ± 1 mBq/cm^3 average whole-rock ^{226}Ra activities. Whole-rock radionuclide content in the Galena dolostone and Tunnel City are between that of the Maquoketa shale and St Peter sandstone. Radionuclide levels in the Galena dolostone are closer to the Maquoketa shale than the St Peter sandstone, with average whole-rock ^{238}U activity of 71 ± 4 mBq/cm^3, and whole-rock ^{226}Ra activity of 59 ± 3 mBq/cm^3. The Tunnel City sandstone is similar to the St Peter sandstone, with 19 ± 1 mBq/cm^3 average whole-rock ^{238}U activity and 19 ± 4 mBq/cm^3 average whole-rock ^{226}Ra activity. Overall, stratigraphy with greater whole-rock ^{238}U activity also contains greater whole-rock ^{226}Ra activity.

The whole-rock ^{238}U/^{226}Ra activity ratio for each stratigraphic unit is compared to an equilibrium value determined from the ^{238}U/^{226}Ra ratio for the standard reference material

https://dx.doi.org/10.1021/acsearthspacechem.0c00279
ACS Earth Space Chem. XXXX, XXX, XXX−XXX

(SRM) SBC-1, a value of 0.94. Student's *t*-test was conducted on each sample group to compare differences between the whole-rock $^{238}U/^{226}Ra$ ratio and the equilibrium value.[68] The $^{238}U/^{226}Ra$ ratio increases as either ^{238}U is added or ^{226}Ra is removed from the system; therefore, the Student's *t*-test was also conducted for the value 1.88, which is twice the equilibrium value. Samples from the Galena dolostone have an average whole-rock $^{238}U/^{226}Ra$ activity ratio of 1.2 ± 0.1, where uncertainty represents the standard deviation (Figure 2). The whole-rock $^{238}U/^{226}Ra$ ratio for samples in the Maquoketa shale and St Peter sandstone varies (averaging 1.4 ± 0.4 and 1.5 ± 0.5, respectively). The Tunnel City sandstone samples have an average whole-rock $^{238}U/^{226}Ra$ ratio of 0.84 ± 0.04. There is no significant difference between the whole-rock $^{238}U/^{226}Ra$ ratio for each sample group, and the equilibrium value of 0.94 ($p > 0.05$ for all groups). The whole-rock $^{238}U/^{226}Ra$ ratios for the Maquoketa shale and St Peter sandstone are also not significantly different from twice the equilibrium value of 1.88 ($p > 0.05$), while the whole-rock $^{238}U/^{226}Ra$ ratios for the Tunnel City and Galena are significantly different from 1.88 ($p < 0.05$).

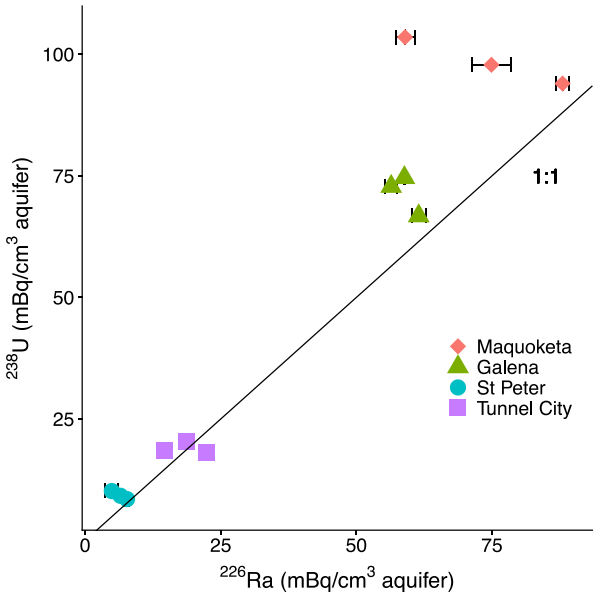

Figure 2. Total ^{238}U and ^{226}Ra activities per volume of aquifer sampled in each bedrock unit. The black line represents a 1:1 activity ratio. The error bars represent instrumental uncertainty.

Activity of ^{226}Ra in Targeted Extractions. The amount of ^{226}Ra in the final, HF-digested fraction is similar for all stratigraphic units; however, the amount of ^{226}Ra in the less recalcitrant fractions (e.g., water-soluble, acido-soluble, reducible fractions) varies by stratigraphic unit (Figure 3a,b). For all samples, the majority of ^{226}Ra is in the HF-digested fraction: 99% for Galena dolostone (58 ± 2 mBq/cm^3), 98% for Maquoketa shale (70 ± 10 mBq/ cm^3), 92% for St Peter sandstone (6 ± 1 mBq/ cm^3), and 94% for Tunnel City sandstone (17 ± 4 mBq/ cm^3). In the Maquoketa shale, the ^{226}Ra removed prior to HF digestion distributes between the water-soluble (0.2%), acido-soluble (63%), and reducible (37%) fractions (0.004 ± 0.001, 1.01 ± 0.08, and 0.6 ± 0.1 mBq/cm^3, respectively). For the non-HF-digested fraction, the Galena dolostone and St Peter sandstone are more similar in terms of ^{226}Ra content in the reducible fraction at 60 and 59%, respectively (Table S2). However, for the non-HF-digested portion, ^{226}Ra in the Galena dolostone is largely found in the acido-soluble fraction (63%), compared to the St Peter sandstone where most of the ^{226}Ra is found in the reducible fraction (77%,). Most of the non-HF-digested ^{226}Ra in the Tunnel City sandstone unit is in the reducible fraction (94%, or 1.1 ± 0.3 mBq/cm^3), with the water-soluble and acido-soluble fractions containing much less (0.4 and 6%, or 0.0047 ± 0.0005 and 0.06 ± 0.03 mBq/cm^3, respectively). Although

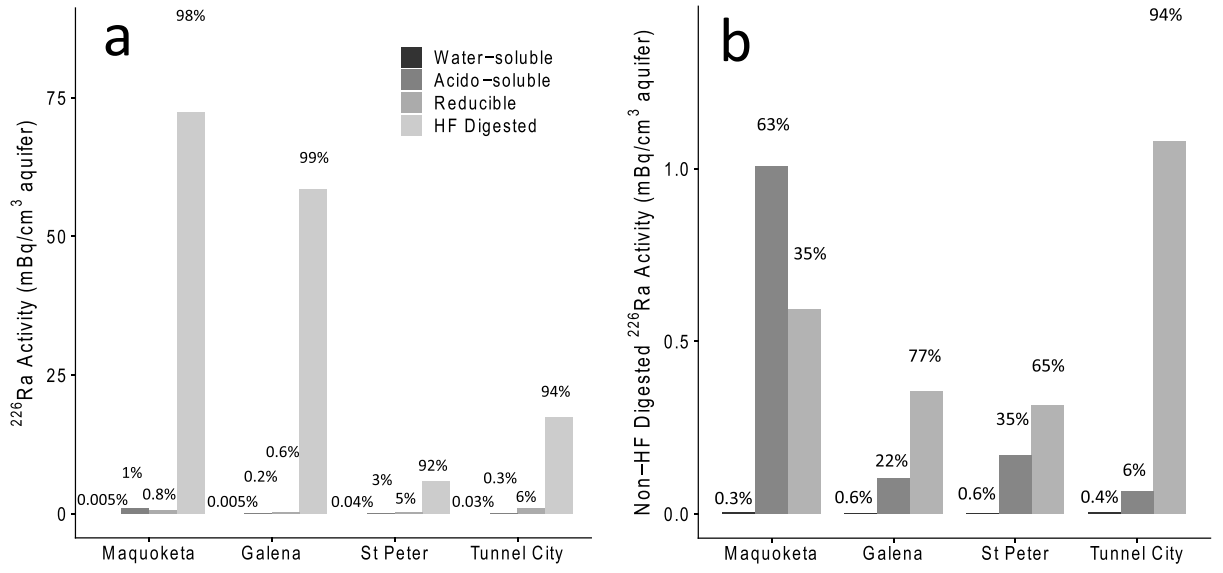

Figure 3. Average ^{226}Ra per aquifer volume, separated into sequential extraction and digestion fractions for each stratigraphic unit. (a) Distribution across all fractions including the digestion. Percentage values indicate the proportion of the specified fraction in comparison to the total ^{226}Ra for the stratigraphic unit. (b) Distribution within each stratigraphic unit for the non-HF-digested fractions. Percentage values indicate the proportion of the specified fraction in comparison to the total non-HF-digested ^{226}Ra for the stratigraphic unit. In both, the error bars represent sample variability. Note different *y*-axis ranges.

https://dx.doi.org/10.1021/acsearthspacechem.0c00279
ACS Earth Space Chem. XXXX, XXX, XXX−XXX

>85% of ^{238}U is associated with the HF-digested fraction, ^{238}U distribution across fractions also varies by stratigraphic unit (Figure S1).

Geochemistry of Water-Soluble Fraction. The leachate from the water-soluble fraction follows a similar chemistry for the examined stratigraphic units, although trace-metal concentrations vary (Figure 4 and Table S3). Dissolved

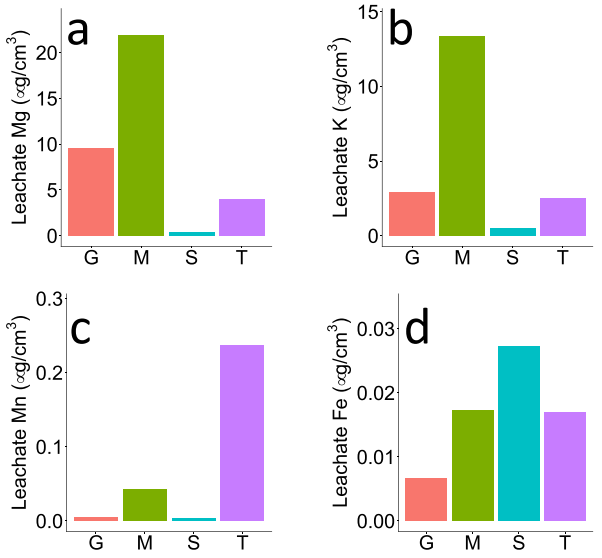

Figure 4. Geochemical indicators determined in the water-soluble fraction for each stratigraphic unit. Note different *y*-axis ranges. Uncertainty represents the standard deviation of individual samples. G = Galena dolostone, M = Maquoketa shale, S = St Peter sandstone, T = Tunnel City sandstone.

magnesium (Mg^{2+}) in the water-soluble fraction leachate varies in concentration across the Maquoketa shale, Galena dolostone, St Peter sandstone, and Tunnel City sandstone (22 ± 2, 9.5 ± 0.7, 0.4 ± 0.1, and 4 ± 1 $\mu g/cm^3$ respectively). Dissolved potassium (K^+) is similar, with the greatest concentration in the Maquoketa shale (13 ± 1 $\mu g/cm^3$), similar concentrations for the Galena dolostone and Tunnel City sandstone (2.9 ± 0.2, 2.5 ± 0.5 $\mu g/cm^3$), and a much smaller concentration in the St Peter sandstone (0.5 ± 0.1 $\mu g/cm^3$). Dissolved iron (Fe(II)) ranges from 0.007 ± 0.004 to 0.027 ± 0.004 $\mu g/cm^3$. More variability is observed in dissolved manganese (Mn(II)) concentrations, ranging from 0.24 ± 0.06 $\mu g/cm^3$ in the Tunnel City sandstone to 0.0031 ± 0.0003 $\mu g/cm^3$ in the St Peter Sandstone.

DISCUSSION

Sources of ^{226}Ra to Groundwater. Possible sources of Ra to groundwater include ejection from alpha recoil, as well as desorption from or dissolution of Ra bearing solid phases; geochemical factors influencing these processes vary greatly in their relative time scales (Figure 5). While Ra is present across the stratigraphic units examined in this study, the large majority is retained within the aquifer solids. This suggests the low aqueous Ra activities typically observed in MCOAS groundwater result from immobilization within, or association with, aquifer solid phases, rather than absence of Ra from the system (Figure 3a). As the overall aquifer system is close to secular equilibrium, alpha recoil by parent isotopes does not appear to partition ^{226}Ra into the aqueous system at elevated levels, although some indication of ^{226}Ra leaching may be

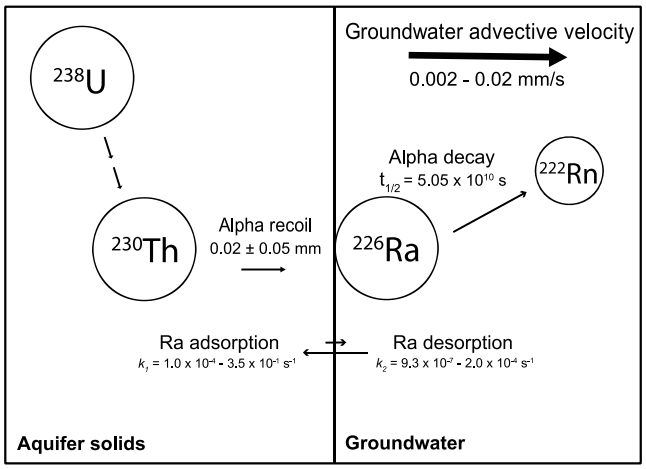

Figure 5. Conceptual diagram depicting the time scales of geochemical processes influencing Ra associations with aquifer solids in the MCOAS. Estimates of alpha recoil distance,[69] ^{226}Ra decay constant,[83] average groundwater transport,[84] and first-order rate constants for Ra adsorption−desorption in natural fresh to brackish groundwater[76,82] are included.

indicated by disequilibrium observed in some stratigraphic units. Some possible explanations for equilibrium observed in the overall aquifer system are that ^{226}Ra may eject out of the mineral lattice to associate with aquifer solids or eject into solution but rapidly repartition to the solid-phase surface. The location of the parent isotope within the mineral lattice is also important, as it is estimated that ^{226}Ra is only ejected at a distance of 0.02 ± 0.05 mm by alpha recoil, which suggests that it could remain within the original solid depending on grain size (Figure 5).[19,69] The solids digested in the HF fraction are not easily modified or dissolved under typical aquifer conditions, so geochemical changes in the aquifer system will not impact release of ^{226}Ra from this portion of the aquifer material. Therefore, ^{226}Ra present in groundwater is likely due to the impact of local geochemical conditions on ^{226}Ra found in the water-soluble, acido-soluble, and reducible fractions.

While sequential extractions provide information about the association of ^{226}Ra with portions of the aquifer solids, it is challenging to examine Ra in groundwater at the field or experimental scale, due to ultratrace analyte concentrations present amidst complex geochemical and hydrologic interactions. MC-ICPMS is beneficial for analyzing aqueous Ra at environmentally relevant concentrations and volumes.[48−50] For aqueous analysis, the large sample volume and wide range of detection limits make many EPA-approved methods (e.g., gamma spectrometry, ICPMS, liquid scintillation counting) difficult to use smaller-scale experiments.[44−47] Many of these methods use decay counting methods to analyze for aqueous ^{226}Ra and require at least a sample size of 1 L with detection limits for these methods ranging from 0.37−37 mBq/L (0.01−1.0 pCi/L).[70]

Potential ^{226}Ra Leaching. The stratigraphic units examined in this study formed during the Ordovician and Cambrian geologic eras, more than 443 million years ago; therefore, secular equilibrium is expected in the whole-rock samples.[19,21,71−74] Comparison of parent and daughter nuclide activities (e.g., mBq/cm^3 ^{238}U and mBq/cm^3 ^{226}Ra) provides information about potential ^{226}Ra leaching from the site of parent decay in the aquifer system (Figure 2). Secular

https://dx.doi.org/10.1021/acsearthspacechem.0c00279
ACS Earth Space Chem. XXXX, XXX, XXX−XXX

equilibrium, where parent and daughter nuclides reach equivalent activities, occurs in parent−daughter systems that have not been impacted by transport (e.g., removal of the daughter isotope) for a time period that is significantly longer than the daughter isotope half-life. As the half-life of the parent isotope ^{238}U (4.5×10^9 years) is much longer than the half-life of its daughter isotope, ^{226}Ra (1.6×10^3 years), after ~2 million years and in the absence of transport processes, ^{238}U and ^{226}Ra isotope activities should be equivalent.[75]

^{226}Ra leaching potential varies by stratigraphic unit, where some units are more likely to support ^{226}Ra transport.[20,24,25,27,76] As there is not a significant difference between the whole-rock $^{238}U/^{226}Ra$ equilibrium value of 0.94 and the average ratios determined for the four stratigraphic units examined in this study ($p > 0.05$ for all sample groups), the overall aquifer system is close to secular equilibrium (Figure 2). However, for the Maquoketa shale and the St Peter sandstone sample groups, the whole-rock $^{238}U/^{226}Ra$ ratios are not significantly different from twice the equilibrium value (i.e., 1.88), which suggests disequilibrium and therefore potential Ra leaching. The observed disequilibrium in these units is likely due to Ra removal mechanisms that promote the partitioning of ^{226}Ra to the aqueous system, such as damage of the mineral lattice due to alpha recoil, or changes in available sorption sites.

Association of ^{226}Ra with Aquifer Solids. In all stratigraphic units, most ^{226}Ra and ^{238}U are in the HF-digested fraction (>90% for ^{226}Ra, >85% for ^{238}U), indicating that the majority of these radionuclides are encased within the solid (Figures 3 and S1)[77] and will not readily partition to the aqueous system due to geochemical changes (Figure 3a). The absolute quantity of ^{226}Ra varies across stratigraphic units, ranging from an average of 70 ± 10 mBq/cm^3 aquifer in the Maquoketa shale to an average of 6 ± 1 mBq/cm^3 aquifer in the St Peter sandstone (Table 2). Elevated Ra concentrations in shale layers are frequently observed; this may be in part due to the enriched presence of clay minerals and/or increased parent isotope levels.[19,78−81] It is important to consider potential hydrologic interactions between stratigraphic units with elevated Ra (e.g., Maquoketa shale) and units containing lower amounts of Ra (e.g., St Peter sandstone), as introduced changes in water chemistry (e.g., elevated TDS, anoxic conditions) due to intra-stratigraphy flow patterns may influence conditions promoting Ra leaching.

Geochemical Influences on ^{226}Ra Leaching. Geochemical processes like dissolution, desorption, or ion exchange within the aquifer system can result in the release of Ra associated with the non-HF-digested fractions (e.g., the water-soluble, acido-soluble, and reducible fractions). Some solid phases associated with the various fractions suggest that the dissolution of key minerals release ^{226}Ra, including Mn- and Fe-(hydr)oxides associated with the reducible fraction.[59] The large proportion of ^{226}Ra present in the Tunnel City sandstone reducible fraction ^{226}Ra (94%) indicates that Mn- and Fe-(hydr)oxide are likely an important control on ^{226}Ra partitioning in this unit. Additionally, a large portion of the ^{226}Ra (63%) is released in the acido-soluble fraction in the Maquoketa shale. This suggests that Ra may be present as easily desorbed surface complexes or with carbonate minerals, since these are the phases targeted by this extraction.[61] The Galena dolostone and St Peter sandstone have similar volume-normalized quantities of ^{226}Ra in the acido-soluble fraction (0.10 ± 0.2 and 0.17 ± 0.07 mBq/L, respectively) and the reducible fraction (0.36 ± 0.06 and 0.32 ± 0.07 mBq/L, respectively). The slightly larger acido-soluble fraction in the St Peter sandstone may contribute to the increased leachability of ^{226}Ra observed in the greater $^{238}U/^{226}Ra$ ratio for the St Peter samples, suggesting a greater amount of weakly sorbed Ra in the St Peter sandstone than in the Galena dolostone.

Evaluation of leachate chemistry from the water-soluble fraction of the sequential extractions provides further information about the critical factors controlling Ra partitioning from solid to aqueous phase (e.g., redox state). The St Peter sandstone has the smallest amounts of Mg^{2+}, Mn(II), and K^+, but the largest amounts of Fe(II) in comparison to the other stratigraphic units. The cycling of trace metals like Fe(II) through geochemical factors like precipitation and redox changes may control Ra partitioning in the St Peter sandstone (Figure 4). Similarly, the Tunnel City sandstone has larger amounts of Fe(II) and Mn(II); this supports sequential extraction data in that transition-metal oxides are likely major controls for Ra partitioning in this unit. Additionally, the presence of cations like Mg^{2+} and K^+ in water leachate, such as in the Maquoketa shale or Galena dolostone, suggests that sorption site competition between these cations and Ra is likely occurring in these units. Notably, the Maquoketa shale water leachate has a similar amount of Fe(II) as the Tunnel City sandstone water leachate. If transition-metal oxides are present in the Maquoketa shale, Mg^{2+} and K^+ likely compete for the sorption sites present in those minerals in this unit.

Geochemical conditions such as elevated TDS and reducing conditions impact available sorption sites within aquifer solids; these conditions have been observed to increase dissolved Ra activity in the MCOAS.[4,7,19,20,23,38] The variation in ^{226}Ra−solid association in the non-HF-digested fractions across stratigraphic units implies that geochemical conditions (e.g., redox conditions, TDS level, pH) within each formation have different effects on ^{226}Ra partitioning into the aqueous system, particularly impacting sorption (Figure 3b). While sorption is a reversible process, first-order rate constants for Ra adsorption, 1.0×10^{-4}−3.5×10^{-1} s^{-1}, are much larger than for desorption, 9.3×10^{-7}−2.0×10^{-4} s^{-1} (Figure 5).[76,82] Both of these rate constants are also orders of magnitude smaller than the half-life of ^{226}Ra (5.05×10^{10} s); ^{226}Ra will experience sorption and desorption many times before undergoing radioactive decay. However, this depends on geochemical conditions which might enhance either sorption or desorption. Phases affected by reducing redox conditions may dissolve and/or be absent depending on redox conditions, causing fewer sorption sites to be present.[40−43] Elevated TDS in groundwater results in increased sorption site competition, and fewer available sites for Ra sorption.[28,29] For example, the impact of high TDS in the Maquoketa shale is more likely to result in elevated Ra in the groundwater in comparison to high TDS in the St Peter sandstone, due to higher levels of ^{226}Ra and greater association of ^{226}Ra with the water-soluble and acido-soluble fractions in the Maquoketa shale (Figure 3b). Additionally, ^{226}Ra is emitted via alpha recoil 0.02 ± 0.05 mm from the site of parent decay.[69] Not only will geochemical reactions like sorption affect the presence of ^{226}Ra in groundwater, but also the proximity of parent nuclides to Ra sorption sites is also important to consider. This suggests that the impact of specific geochemical conditions varies in importance across stratigraphy.

Comparison of the exchangeable ^{226}Ra in the examined stratigraphic units with the maximum contaminant level (MCL) of 185 mBq/L for total aqueous ^{226}Ra and ^{228}Ra

https://dx.doi.org/10.1021/acsearthspacechem.0c00279
ACS Earth Space Chem. XXXX, XXX, XXX−XXX

Table 3. Mass Balance for Total Exchangeable ^{226}Ra Associated with Each Stratigraphic Unit[a]

stratigraphic unit	est. porosity	total exchangeable ^{226}Ra (mBq/cm^3)	total exchangeable ^{226}Ra (mBq/L)	partition coefficient	^{226}Ra in water (%)
Maquoketa shale	0.08	1.6 ± 0.2	$2.0 \times 10^{-4} \pm 2 \times 10^{-3}$	0.009 ± 0.001	0.9 ± 0.1
Galena dolostone	0.05	0.46 ± 0.04	$9.2 \times 10^{-3} \pm 8 \times 10^{-2}$	0.020 ± 0.002	2.0 ± 0.2
St Peter sandstone	0.12	0.5 ± 0.1	$4 \times 10^{-3} \pm 1 \times 10^{-3}$	0.05 ± 0.01	5 ± 1
Tunnel City sandstone	0.17	1.1 ± 0.3	$7 \times 10^{-3} \pm 2 \times 10^{-3}$	0.03 ± 0.02	3 ± 1

[a]Partition coefficient is estimated at the maximum contaminant level (185 mBq/L ^{226}Ra). ^{226}Ra in water is in relation to total exchangeable ^{226}Ra. Uncertainty represents the standard deviation of individual samples.

activities further develops how hydrologic and geochemical conditions will influence ^{226}Ra mobilization across different bedrock units. Specifically, we calculated a mass balance designed to examine what percentage of ^{226}Ra would be in the water in comparison to the exchangeable ^{226}Ra associated with the aquifer solids for each stratigraphic unit (Table 3). ^{226}Ra activities were converted from mBq/cm^3 to mBq/L, with the addition of 185 mBq/L of aqueous ^{226}Ra to compare the MCL to the overall exchangeable ^{226}Ra content, via eq 2

$$^{226}\mathrm{Ra}_{\mathrm{ex,\ aq}} = \frac{\mathrm{MCL} + (^{226}\mathrm{Ra}_{\mathrm{ex}})\left(\frac{1 \times 10^{-6}\ \mathrm{cm}^3}{\mathrm{m}^3}\right)}{n \times 1000\ \mathrm{m}^3/\mathrm{L}} \quad (2)$$

where ^{226}Ra$_{ex, aq}$ is the total exchangeable ^{226}Ra estimated for an aqueous system, in mBq/L; MCL is the Ra maximum contaminant level at 185 mBq/L of ^{226}Ra; ^{226}Ra$_{ex}$ is the total exchangeable ^{226}Ra, in mBq/cm^3; and n is porosity. The partition coefficient, D, is calculated by eq 3

$$D = \frac{\mathrm{MCL}}{^{226}\mathrm{Ra}_{\mathrm{ex,\ aq}}} \quad (3)$$

These calculations determine variation between each stratigraphic unit and the percent ^{226}Ra estimated to be in the aqueous fraction at the MCL. The St Peter sandstone has the greatest amount of ^{226}Ra estimated to be in the aqueous system, while the Maquoketa shale has the least amount (5 ± 1 and 0.9 ± 0.1%, respectively). Stratigraphic units like the Maquoketa shale likely have greater sorption capacity, resulting in a smaller D value and less ^{226}Ra in the aqueous phase in comparison to overall solid-phase associations. Sandstone units like the St Peter have a larger percentage of ^{226}Ra in the aqueous phase in relation to the total ^{226}Ra; this suggests that if Ra is present within the St Peter sandstone, it is more likely that it will be in the aqueous phase than in the Maquoketa shale. The range of partition coefficients among these four stratigraphic units further confirms that the geochemical associations available within a stratigraphic unit are major controls for ^{226}Ra mobilization and that this control varies across different types of bedrock.

Our study demonstrates an innovative approach, combining sequential extraction experiments on aquifer solids with sensitive analytical techniques (e.g., MC-ICPMS) to examine contaminant interactions in groundwater. For radioactive contaminants, examining isotopic processes such as secular equilibrium can reveal further information about transport within an aquifer system. Secular equilibrium between ^{226}Ra and ^{238}U in the examined stratigraphic units suggests that ^{226}Ra leaching depends on available solid-phase associations, and varies with different stratigraphic units (Figure 2). While geochemical associations between Ra and solid phases are therefore important controls on contaminant mobility, this association varies across stratigraphy as demonstrated by the assorted distribution of Ra across non-HF-digested fractions (Figure 3b). Local-scale geochemical variation within stratigraphic units can result in Ra partitioning from the aquifer solids to the aqueous system, through processes such as desorption and mineral dissolution or absence.

Some limitations of this study include use of geochemical leachate rather than groundwater samples and assumptions about reactive solid-phase associations based on the sequential extractions. While extraction experiments provide valuable information about analyte−rock interactions, they are limited via experimental controls in comparison to the complex interactions occurring in aquifer systems. It is recognized that the identification of direct Ra−mineral associations is more specific to examining Ra interactions with particular minerals present within bedrock. Nonetheless, the quantification of Ra−solid interaction via sequential extractions targets the fractions of aquifer materials expected to have the largest impact on Ra partitioning to the aqueous phase in this portion of the MCOAS.

Environmental Implications. Local geochemistry controls the partitioning of Ra and other contaminants to the aqueous system. Some bedrock formations have elevated levels of contaminants that partition more easily to groundwater (e.g., Ra in the Maquoketa shale); changing geochemical conditions at an individual well can influence the partitioning of contaminants at that site. Physical well features may also affect the quality of water pumped across bedrock formation, such as casing depth, total well depth, and relative transmissivity of sedimentary layers. Additionally, changes in well pumping rates can change hydraulic gradients, and as a result can alter groundwater flow paths and impact metal mobility by introducing new geochemical conditions.[85] Examples of this include drawing groundwater containing elevated dissolved solids to a different part of the aquifer system or inducing flow of oxygenated, recently recharged water across Ra-enriched shale aquitards. Such changes may affect the presence of solid phase, releasing sorbed contaminants into the aqueous system.[85]

Understanding the impact of local geochemistry and changes in groundwater flow systems on Ra partitioning can inform well construction and ultimately reduce the uptake of naturally occurring contaminant by wells. While geochemical trends that affect contaminant partitioning are apparent at the regional scale (e.g., Ra in the MCOAS), prediction of local-scale contaminant concentrations is complicated by the influence of local geochemistry, lithologic heterogeneity, and wells open to multiple stratigraphic units. Use of sensitive methods that identify ultra-trace-level Ra concentrations demonstrates that local geochemistry is a major control on Ra release to the aqueous system. These data will support development of geochemical and hydrologic models to assess the influence of groundwater withdrawal on the partitioning of contaminants to groundwater in systems such as the MCOAS, where

https://dx.doi.org/10.1021/acsearthspacechem.0c00279
ACS Earth Space Chem. XXXX, XXX, XXX−XXX

interbedded shale, sandstone, and carbonates affect contaminant mobility within heavily used aquifer systems.

■ ASSOCIATED CONTENT

Supporting Information

The Supporting Information is available free of charge at https://pubs.acs.org/doi/10.1021/acsearthspacechem.0c00279.

Select geophysical parameters and calculation (Table S1); exchangeable ^{226}Ra (Table S2); average ^{238}U per aquifer volume (Figure S1); analyte concentrations from water-soluble leachate (Table S3); and XRD patterns of select samples (Figures S2−S9) (PDF)

■ AUTHOR INFORMATION

Corresponding Author

Matthew Ginder-Vogel − *Environmental Chemistry and Technology Program, Department of Civil and Environmental Engineering, University of Wisconsin−Madison, Madison, Wisconsin 53711, United States;* orcid.org/0000-0001-9183-1931; Phone: (608) 262-0768; Email: matt.ginder-vogel@wisc.edu

Authors

Madeleine Mathews − *Environmental Chemistry and Technology Program, Department of Civil and Environmental Engineering, University of Wisconsin−Madison, Madison, Wisconsin 53711, United States*

Sean R. Scott − *Wisconsin State Laboratory of Hygiene, Madison, Wisconsin 53718, United States*

Madeline B. Gotkowitz − *Montana Bureau of Mines and Geology, Butte, Montana 59701, United States*

Complete contact information is available at: https://pubs.acs.org/10.1021/acsearthspacechem.0c00279

Notes

The authors declare no competing financial interest.

■ ACKNOWLEDGMENTS

The authors thank the Wisconsin State Laboratory of Hygiene for support and training in multicollector inductively coupled plasma mass spectrometry techniques, and specifically Joel Overdier for uranium analysis. The samples in this report are curated at the Wisconsin Geological and Natural History Survey's (WGNHS) core repository. The authors thank WGNHS, particularly Carsyn Ames, Esther Stewart, and Pat McLaughlin, for providing access to samples from core 60000086, descriptions, and lab facilities. Laboratory assistance provided by Gabrielle Campagnola, Amy Plechacek, James Lazarcik, and Lily Schacht was greatly appreciated. Thanks also go to Lily Schacht and Amy Plechacek for providing excellent insight into the writing of the manuscript. Funding for this project is provided by the Wisconsin Groundwater Research and Monitoring Program as well as the Wisconsin Department of Natural Resources. M.M. was supported by funding from the Grainger Wisconsin Distinguished Graduate Fellowship.

■ REFERENCES

(1) WWAP (United Nations World Water Assessment Programme). *The United Nations World Water Development Report 2015: Water for a Sustainable World*; UNESCO: Paris, 2015.

(2) Liu, J.; Liu, Q.; Yang, H. Assessing water scarcity by simultaneously considering environmental flow requirements, water quantity, and water quality. *Ecol. Indic.* **2016**, *60*, 434−441.

(3) Zeng, Z.; Liu, J.; Savenije, H. H. G. A simple approach to assess water scarcity integrating water quantity and quality. *Ecol. Indic.* **2013**, *34*, 441−449.

(4) Stackelberg, P. E.; Szabo, Z.; Jurgens, B. C. Radium mobility and the age of groundwater in public-drinking-water supplies from the Cambrian-Ordovician aquifer system, north-central USA. *Appl. Geochem.* **2018**, *89*, 34−48.

(5) Grützmacher, G.; Kumar, P. J. S.; Rustler, M.; Hannappel, S.; Sauer, U. Geogenic groundwater contamination—definition, occurrence and relevance for drinking water production. *Zbl. Geol. Paläont. Teil I* **2013**, *1*, 69−75.

(6) Fendorf, S.; Wielinga, B. W.; Hansel, C. M. Chromium Transformations in Natural Environments: The Role of Biological and Abiological Processes in Chromium(VI) Reduction. *Int. Geol. Rev.* **2000**, *42*, 691−701.

(7) Szabo, Z.; dePaul, V. T.; Fischer, J. M.; Kraemer, T. F.; Jacobsen, E. Occurrence and geochemistry of radium in water from principal drinking-water aquifer systems of the United States. *Appl. Geochem.* **2012**, *27*, 729−752.

(8) Polizzotto, M. L.; Harvey, C. F.; Li, G.; Badruzzman, B.; Ali, A.; Newville, M.; Sutton, S.; Fendorf, S. Solid-phases and desorption processes of arsenic within Bangladesh sediments. *Chem. Geol.* **2006**, *228*, 97−111.

(9) Polizzotto, M. L.; Harvey, C. F.; Sutton, S. R.; Fendorf, S. Processes conducive to the release and transport of arsenic into aquifers of Bangladesh. *Proc. Natl. Acad. Sci. U.S.A.* **2005**, *102*, 18819.

(10) Oden, J. H.; Szabo, Z. *Arsenic and radionuclide occurrence and relation to geochemistry in groundwater of the Gulf Coast Aquifer System in Houston, Texas, 2007−11*; 2016.

(11) Berg, M.; Trang, P. T. K.; Stengel, C.; Buschmann, J.; Viet, P. H.; Van Dan, N.; Giger, W.; Stüben, D. Hydrological and sedimentary controls leading to arsenic contamination of groundwater in the Hanoi area, Vietnam: The impact of iron-arsenic ratios, peat, river bank deposits, and excessive groundwater abstraction. *Chem. Geol.* **2008**, *249*, 91−112.

(12) Stuyfzand, P. J.; Raat, K. J. Benefits and hurdles of using brackish groundwater as a drinking water source in the Netherlands. *Hydrogeol. J.* **2010**, *18*, 117−130.

(13) Great Lakes-St. Lawrence River Basin Water Resources Council, Final Decision. In 2016.

(14) Dematatis, M.; Plechacek, A.; Mathews, M.; Wright, D. B.; Udenby, F.; Gotkowitz, M. B.; Ginder-Vogel, M. Spatial and temporal variability of radium in the Wisconsin Cambrian-Ordovician aquifer system. *AWWA Water Sci.* **2020**, *2*, No. e1171.

(15) Muehe, E.; Kappler, A. Arsenic mobility and toxicity in South and Southeast Asia−a review on biogeochemistry, health and socio-economic effects, remediation and risk predictions. *Environ. Chem.* **2014**, *11*, 483−495.

(16) Aieta, E. M.; Singley, J. E.; Trussell, A. R.; Thorbjarnarson, K. W.; McGuire, M. J. Radionuclides in Drinking Water: An Overview. *J. - Am. Water Works Assoc.* **1987**, *79*, 144−152.

(17) Vinson, D. S.; Tagma, T.; Bouchaou, L.; Dwyer, G. S.; Warner, N. R.; Vengosh, A. Occurrence and mobilization of radium in fresh to saline coastal groundwater inferred from geochemical and isotopic tracers (Sr, S, O, H, Ra, Rn). *Appl. Geochem.* **2013**, *38*, 161−175.

(18) Izbicki, J. A.; Wright, M. T.; Seymour, W. A.; McCleskey, R. B.; Fram, M. S.; Belitz, K.; Esser, B. K. Cr(VI) occurrence and geochemistry in water from public-supply wells in California. *Appl. Geochem.* **2015**, *63*, 203−217.

(19) International Atomic Energy Agency. The environmental behaviour of radium: revised edition *Technical Reports Series No. 476* 2014, 476 44 51.

(20) Tricca, A.; Porcelli, D.; Wasserburg, G. J. Factors controlling the groundwater transport of U, Th, Ra, and Rn. *J. Earth Syst. Sci.* **2000**, *109*, 95−108.

(21) Vinson, D. S.; Lundy, J. R.; Dwyer, G. S.; Vengosh, A. Implications of carbonate-like geochemical signatures in a sandstone aquifer: Radium and strontium isotopes in the Cambrian Jordan aquifer (Minnesota, USA). *Chem. Geol.* **2012**, *334*, 280−294.
(22) Gilkeson, R. H.; Specht, S. A.; Cartwright, K.; Griffin, R. A.; Larson, T. E., Geologic studies to identify the source for high levels of radium and barium in Illinois ground-water supplies: a preliminary report. 1978.
(23) Grundl, T.; Cape, M. Geochemical factors controlling radium activity in a sandstone aquifer. *Ground Water* **2006**, *44*, 518−527.
(24) Reynolds, B. C.; Wasserburg, G. J.; Baskaran, M. The transport of U- and Th-series nuclides in sandy confined aquifers. *Geochim. Cosmochim. Acta* **2003**, *67*, 1955−1972.
(25) Tricca, A.; Wasserburg, G. J.; Porcelli, D.; Baskaran, M. The transport of U-and Th-series nuclides in a sandy unconfined aquifer. *Geochim. Cosmochim. Acta* **2001**, *65*, 1187−1210.
(26) Felmlee, J. K.; Cadigan, R. A. *Radium and Uranium Concentrations and Associated Hydrogeochemistry in Ground Water in Southwestern Pueblo County, Colorado*; 79-974; 1979.
(27) Vinson, D. S.; Vengosh, A.; Hirschfeld, D.; Dwyer, G. S. Relationships between radium and radon occurrence and hydrochemistry in fresh groundwater from fractured crystalline rocks, North Carolina (USA). *Chem. Geol.* **2009**, *260*, 159−171.
(28) Nathwani, J. S.; Phillips, C. R. Adsorption of 226Ra by soils in the presence of Ca2+ ions. Specific adsorption (II). *Chemosphere* **1979**, *8*, 293−299.
(29) Tamamura, S.; Takada, T.; Tomita, J.; Nagao, S.; Fukushi, K.; Yamamoto, M. Salinity dependence of 226Ra adsorption on montmorillonite and kaolinite. *J. Radioanal. Nucl. Chem.* **2014**, *299*, 569−575.
(30) Tomita, J.; Satake, H.; Fukuyama, T.; Sasaki, K.; Sakaguchi, A.; Yamamoto, M. Radium geochemistry in Na−Cl type groundwater in Niigata Prefecture, Japan. *J. Environ. Radioact.* **2010**, *101*, 201−210.
(31) Krishnaswami, S.; Bhushan, R.; Baskaran, M. Radium isotopes and 222Rn in shallow brines, Kharaghoda (India). *Chem. Geol.* **1991**, *87*, 125−136.
(32) Luczaj, J.; Masarik, K. Groundwater Quantity and Quality Issues in a Water-Rich Region: Examples from Wisconsin, USA. *Resources* **2015**, *4*, 323−357.
(33) Evans, R. D. Radium poisoning: a review of present knowledge. *Am. J. Public Health Nations Health* **1933**, *23*, 1017−1023.
(34) Guse, C. E.; Marbella, A. M.; George, V.; Layde, P. M. Radium in Wisconsin drinking water: an analysis of osteosarcoma risk. *Arch. Environ. Health* **2002**, *57*, 294−303.
(35) Cohn, P.; Skinner, R.; Burger, S.; Falgiano, J.; Klotz, J.Radium in Drinking Water and the Incidence of Osteosarcoma: A Report to the New Jersey Department of Environmental Protection. 2003.
(36) Canu, I. G.; Laurent, O.; Pires, N.; Laurier, D.; Dublineau, I. Health effects of naturally radioactive water ingestion: the need for enhanced studies. *Environ. Health Perspect.* **2011**, *119*, 1676−1680.
(37) World Health Organization. *Guidlines for Drinking-Water Quality: Fourth Edition Incorporating the First Addendum*; Geneva, 2017.
(38) Mathews, M.; Gotkowitz, M.; Ginder-Vogel, M. Effect of geochemical conditions on radium mobility in discrete intervals within the Midwestern Cambrian-Ordovician aquifer system. *Appl. Geochem.* **2018**, *97*, 238−246.
(39) Alhajji, E.; Al-Masri, M. S.; Khalily, H.; Naoum, B. E.; Khalil, H. S.; Nashawati, A. A Study on Sorption of 226Ra on Different Clay Matrices. *Bull. Environ. Contam. Toxicol.* **2016**, *97*, 255−260.
(40) Ames, L. L.; McGarrah, J. E.; Walker, B. A.; Salter, P. F. Uranium and radium sorption on amorphous ferric oxyhydroxide. *Chem. Geol.* **1983**, *40*, 135−148.
(41) Bassot, S.; Mallet, C.; Stammose, D. Experimental Study and Modeling of the Radium Sorption onto Goethite. *MRS Proc.* **2000**, *663*, 1081.
(42) Chen, M. A.; Kocar, B. D. Radium Sorption to Iron (Hydr)oxides, Pyrite, and Montmorillonite: Implications for Mobility. *Environ. Sci. Technol.* **2018**, *52*, 4023−4030.
(43) Sajih, M.; Bryan, N. D.; Livens, F. R.; Vaughan, D. J.; Descostes, M.; Phrommavanh, V.; Nos, J.; Morris, K. Adsorption of radium and barium on goethite and ferrihydrite: A kinetic and surface complexation modelling study. *Geochim. Cosmochim. Acta* **2014**, *146*, 150−163.
(44) Charette, M. A.; Dulaiova, H.; Gonneea, M. E.; Henderson, P. B.; Moore, W. S.; Scholten, J. C.; Pham, M. K. GEOTRACES radium isotopes interlaboratory comparison experiment. *Limnol. Oceanogr.* **2012**, *10*, 451−463.
(45) Nathwani, J. S.; Phillips, C. R. Rates of leaching of radium from contaminated soils: An experimental investigation of radium bearing soils from Port Hope, Ontario. *Water, Air, Soil Pollut.* **1978**, *9*, 453−465.
(46) van Es, E. M.; Russell, B. C.; Ivanov, P.; Read, D. Development of a method for rapid analysis of Ra-226 in groundwater and discharge water samples by ICP-QQQ-MS. *Appl. Radiat. Isot.* **2017**, *126*, 31−34.
(47) Jia, G.; Jia, J. Determination of radium isotopes in environmental samples by gamma spectrometry, liquid scintillation counting and alpha spectrometry: a review of analytical methodology. *J. Environ. Radioact.* **2012**, *106*, 98−119.
(48) Geibert, W.; Rodellas, V.; Annett, A.; van Beek, P.; Garcia-Orellana, J.; Hsieh, Y.-T.; Masque, P. 226Ra determination via the rate of 222Rn ingrowth with the Radium Delayed Coincidence Counter (RaDeCC). *Limnol. Oceanogr.* **2013**, *11*, 594−603.
(49) Copia, L.; Nisi, S.; Plastino, W.; Ciarletti, M.; Povinec, P. P. Low-level 226Ra determination in groundwater by SF-ICP-MS: optimization of separation and pre-concentration methods. *J. Anal. Sci. Technol.* **2015**, *6*, No. 22.
(50) Sharabi, G.; Lazar, B.; Kolodny, Y.; Teplyakov, N.; Halicz, L. High precision determination of 228Ra and 228Ra/226Ra isotope ratio in natural waters by MC-ICPMS. *Int. J. Mass Spectrom.* **2010**, *294*, 112−115.
(51) Fleischer, R. L. Alpha-recoil damage: Relation to isotopic disequilibrium and leaching of radionuclides. *Geochim. Cosmochim. Acta* **1988**, *52*, 1459−1466.
(52) Weaver, T. R.; Bahr, J. Geochemical evolution in the Cambrian-Ordovician sandstone aquifer, eastern Wisconsin: 1. Major ion and radionuclide distribution. *Ground Water* **1991**, *29*, 350−356.
(53) Stackelberg, P. E. *Groundwater Quality in the Cambrian-Ordovician Aquifer System, Midwestern United States*; 2017-3056; Reston, VA, 2017; p 4.
(54) Young, H. L.; Siegel, D. I. Hydrogeology of the Cambrian-Ordovician Aquifer System in the Northern Midwest, United States *U.S. Geological Survey Professional Paper 1405-B 99* 1992.
(55) Young, H. L. *Summary of Ground-Water Hydrology of the Cambrian-Ordovician Aquifer System in the Northern Midwest, United States*; US Department of the Interior, US Geological Survey, 1992; Vol. *1405*.
(56) Weaver, T. R.; Bahr, J. M. Geochemical evolution in the Cambrian-Ordovician sandstone aquifer, eastern Wisconsin: 2. Correlation between flow paths and ground-water chemistry. *Ground Water* **1991**, *29*, 510−515.
(57) Kaakinen, J.; Kuokkanen, T.; Kujala, K.; Välimäki, I.; Jokinen, H. The Use of a Five-stage Sequential Leaching Procedure for Risk Assessment of Heavy Metals in Waste Rock Utilized in Railway Ballast. *Soil Sediment Contam.* **2012**, *21*, 322−334.
(58) Fujikawa, Y.; Fukui, M. Variations in adsorption mechanisms of radioactive cobalt and cesium in rocks. *J. Contam. Hydrol.* **1991**, *8*, 177−195.
(59) Chao, T. T. Selective Dissolution of Manganese Oxides from Soils and Sediments with Acidified Hydroxylamine Hydrochloride. *Soil Sci. Soc. Am. J.* **1972**, *36*, 764−768.
(60) Robinson, G. D. Sequential chemical extractions and metal partitioning in hydrous Mn—Fe-oxide coatings: Reagent choice and substrate composition affect results. *Chem. Geol.* **1984**, *47*, 97−112.
(61) Leermakers, M.; Mbachou, B. E.; Husson, A.; Lagneau, V.; Descostes, M. An alternative sequential extraction scheme for the

https://dx.doi.org/10.1021/acsearthspacechem.0c00279
ACS Earth Space Chem. XXXX, XXX, XXX−XXX

determination of trace elements in ferrihydrite rich sediments. *Talanta* **2019**, *199*, 80−88.
(62) Suresh, P. O.; Dosseto, A.; Handley, H. K.; Hesse, P. P. Assessment of a sequential phase extraction procedure for uranium-series isotope analysis of soils and sediments. *Appl. Radiat. Isot.* **2014**, *83*, 47−55.
(63) Wang, X.; Xu, S.; Zhang, B.; Zhao, S. Deep-penetrating geochemistry for sandstone-type uranium deposits in the Turpan−Hami basin, north-western China. *Appl. Geochem.* **2011**, *26*, 2238−2246.
(64) Sawhney, B. L.; Stilwell, D. E. Dissolution and elemental analysis of minerals, soils, and environmental samples. In *Quantitative Methods in Soil Mineralogy*; Amonette, J. E.; Zelazny, L. W., Eds. SSSA: Madison, WI, 1994; pp 49−82.
(65) Mester, Z.; Sturgeon, R. *Sample Preparation for Trace Element Analysis*; Elsevier, 2003; Vol. *XLI*, p 1286.
(66) Muratli, J. M.; McManus, J.; Mix, A.; Chase, Z. Dissolution of fluoride complexes following microwave-assisted hydrofluoric acid digestion of marine sediments. *Talanta* **2012**, *89*, 195−200.
(67) Sims, K. W. W.; Hart, S. R.; Reagan, M. K.; Blusztajn, J.; Staudigel, H.; Sohn, R. A.; Layne, G. D.; Ball, L. A.; Andrews, J. 238U-230Th-226Ra-210Pb-210Po, 232Th-228Ra, and 235U-231Pa constraints on the ages and petrogenesis of Vailulu'u and Malumalu Lavas, Samoa. *Geochem., Geophys., Geosyst.*, 2008, *9*, 4 DOI: 10.1029/2007GC001651.
(68) de Winter, J. Using the Student's t-test with extremely small sample sizes. *Practical Assessment, Research & Evaluation* **2013**, *18*.
(69) Sturchio, N. C.; Banner, J. L.; Binz, C. M.; Heraty, L. B.; Musgrove, M. Radium geochemistry of ground waters in Paleozoic carbonate aquifers, midcontinent, USA. *Appl. Geochem.* **2001**, *16*, 109−122.
(70) Office of Environmental Policy and Assistance - Air, W. a. R. D. E. *Compendium of EPA-approved Analytical Methods for Measuring Radionuclides in Drinking Water*; US Department of Energy, 1998.
(71) Ostrom, M. E. Paleozoic Stratigraphic Nomenclature for Wisconsin. *Wisconsin Geological and Natural History Survey Information Circular 8* 1967.
(72) Stern, T. W.; Stieff, L. R. Part 13. RADIUM-URANIUM EQUILIBRIUM AND RADIUM-URANIUM AGES OF SOME *US Geological Survey Professional Paper* 1959, 320 151.
(73) Pietruszka, A. J.; Carlson, R. W.; Hauri, E. H. Precise and accurate measurement of 226Ra−230Th−238U disequilibria in volcanic rocks using plasma ionization multicollector mass spectrometry. *Chem. Geol.* **2002**, *188*, 171−191.
(74) Michel, J. Redistibution of uranium and thorium series isotopes during isovolumetric weathering of granite. *Geochim. Cosmochim. Acta* **1984**, *48*, 1249−1255.
(75) IUPAC. *Compendium of Chemical Terminology*; Blackwell Scientific Publications: Oxford, 1997.
(76) Krishnaswami, S.; Graustein, W. C.; Turekian, K. K.; Dowd, J. F. Radium, thorium and radioactive lead isotopes in groundwaters: Application to the in situ determination of adsorption-desorption rate constants and retardation factors. *Water Resour. Res.* **1982**, *18*, 1663−1675.
(77) Webster, I. T.; Hancock, G. J.; Murray, A. S. Modelling the effect of salinity on radium desorption from sediments. *Geochim. Cosmochim. Acta* **1995**, *59*, 2469−2476.
(78) Iyengar, M. A. R. The natural distribution of radium. *The Environmental Behaviour of Radium* **1990**, *1*, 59−128.
(79) Warner, N. R.; Christie, C. A.; Jackson, R. B.; Vengosh, A. Impacts of shale gas wastewater disposal on water quality in western Pennsylvania. *Environ. Sci. Technol.* **2013**, *47*, 11849−11857.
(80) Haluszczak, L. O.; Rose, A. W.; Kump, L. R. Geochemical evaluation of flowback brine from Marcellus gas wells in Pennsylvania, USA. *Appl. Geochem.* **2013**, *28*, 55−61.
(81) Rowan, E. L.; Engle, M. A.; Kirby, C. S.; Kraemer, T. F. Radium content of oil-and gas-field produced waters in the Northern Appalachian Basin (USA): Summary and discussion of data. *US Geological Survey Scientific Investigations Report* 2011, *5135*2011 31.
(82) Swarzenski, P. W.; Baskaran, M.; Rosenbauer, R. J.; Edwards, B. D.; Land, M. A combined radio-and stable-isotopic study of a California coastal aquifer system. *Water* **2013**, *5*, 480−504.
(83) Porcelli, D. The behavior of U-and Th-series nuclides in groundwater. *Rev. Mineral. Geochem.* **2003**, *52*, 317.
(84) Borchardt, M. A.; Bradbury, K. R.; Gotkowitz, M. B.; Cherry, J. A.; Parker, B. L. Human enteric viruses in groundwater from a confined bedrock aquifer. *Environ. Sci. Technol.* **2007**, *41*, 6606−6612.
(85) Ayotte, J. D.; Szabo, Z.; Focazio, M. J.; Eberts, S. M. Effects of human-induced alteration of groundwater flow on concentrations of naturally-occurring trace elements at water-supply wells. *Appl. Geochem.* **2011**, *26*, 747−762.

https://dx.doi.org/10.1021/acsearthspacechem.0c00279
ACS Earth Space Chem. XXXX, XXX, XXX−XXX

Supporting Information

Association of radionuclide isotopes with aquifer solids in the Midwestern Cambrian-Ordovician aquifer system

Madeleine Mathews[1], Sean Scott[2], Madeline B. Gotkowitz[3], and Matthew Ginder-Vogel[1]*

1. Environmental Chemistry and Technology, Department of Civil and Environmental Engineering, University of Wisconsin – Madison, Madison, WI
2. Wisconsin State Laboratory of Hygiene, Madison, WI
3. Montana Bureau of Mines and Geology, Butte, MT

*Corresponding author. Tel.: (608) 262-0768; E-mail address: matt.ginder-vogel@wisc.edu

Table of Contents

Table S1. Select geophysical parameters for examined rock core. Note that porosity and dry bulk density were measured for the specific core; caution would need to be applied when extrapolating these values to the entire unit due to variability of cementation and grain size distribution within geologic units. [1]

Formation	Depth for geophysical properties (m)	Porosity	Dry bulk density (g/cm^3)
Maquoketa Shale	230	0.08	2.58
Galena Dolostone	326	0.05	2.69
St Peter Sandstone	395	0.12	2.33
Tunnel City Sandstone	423	0.17	2.20

Aquifer volume calculation:

Formation: Maquoketa Shale
Total ^{226}Ra (pCi/g rock): 0.8 ± 0.2

^{226}Ra per aquifer volume (water-soluble fraction) = $\frac{mBq\ ^{226}Ra}{g\ rock} * porosity$

^{226}Ra per aquifer volume (acido-soluble, reducible, HF digested fractions) =

$$\frac{mBq\ ^{226}Ra}{g} * (1 - porosity) * Dry\ bulk\ density(\frac{g}{cm^3})$$

Table S2. Distribution of ^{226}Ra across the non-HF digested fractions.

Sample	Fraction	Non-HF digested ^{226}Ra (mBq/cm^3)	Non-HF digested ^{226}Ra (%)	Non-HF digested ^{238}U (mBq/cm^3)	Non-HF digested ^{238}U (%)
Maquoketa Shale	Water-soluble	0.004 ± 0.001	0.2	0.010 ± 0.002	0.1
	Acido-soluble	1.00 ± 0.08	63	5 ± 1	77
	Reducible	0.6 ± 0.1	37	1.5 ± 0.2	23
Galena Dolostone	Water-soluble	0.0027 ± 0.0009	0.6	0.0039 ± 0.0003	0.07
	Acido-soluble	0.10 ± 0.02	22	3.4 ± 0.4	58
	Reducible	0.36 ± 0.06	77	2.41 ± 0.02	42
St Peter Sandstone	Water-soluble	0.0027 ± 0.0007	0.6	0.0027 ± 0.0003	1
	Acido-soluble	0.17 ± 0.07	35	0.13 ± 0.01	63
	Reducible	0.32 ± 0.07	64	0.07 ± 0.01	36
Tunnel City Sandstone	Water-soluble	0.0047 ± 0.0005	0.4	0.017 ± 0.003	0.6
	Acido-soluble	0.06 ± 0.03	6	1.8 ± 0.4	66
	Reducible	1.1 ± 0.3	94	0.89 ± 0.04	33

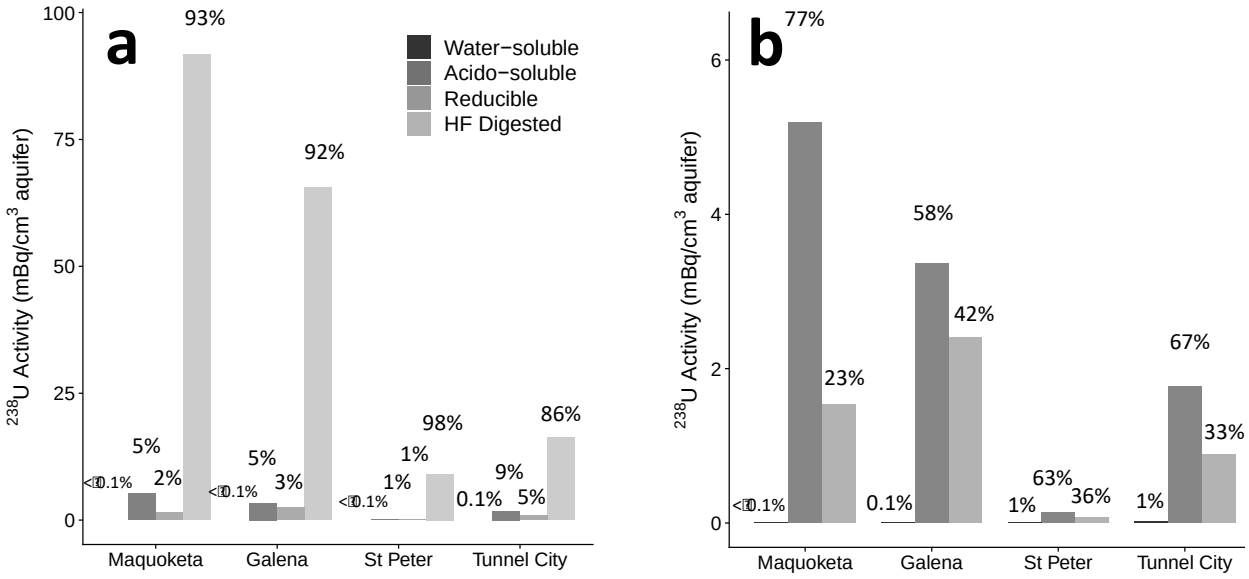

Figure S1. Average ^{238}U per aquifer volume, separated into sequential extraction and digestion fractions for each stratigraphic unit. (a) shows distribution across all fractions including the digestion. Percentage values indicate the proportion of the specified fraction in comparison to the total ^{238}U for the stratigraphic unit. (b) shows the distribution within each stratigraphic unit for the non-HF digested fractions. Percentage values indicate the proportion of the specified fraction in comparison to the total non-HF digested ^{238}U for the stratigraphic unit. In both, error bars represent sample variability. Note different y-axis ranges.

Table S3. Analyte concentrations from water-soluble leachate, for each stratigraphic unit. Uncertainty is attributed to instrumental error.

Stratigraphic Unit	Mg^{2+} ($\mu g/cm^3$)	Fe(II) ($\mu g/cm^3$)	Mn(II) ($\mu g/cm^3$)	K^{+} ($\mu g/cm^3$)
Maquoketa shale	22 ± 2	0.02 ± 0.02	0.043 ± 0.004	13 ± 1
Galena dolostone	9.5 ± 0.7	0.007 ± 0.004	0.0048 ± 0.0002	2.9 ± 0.2
St Peter sandstone	0.4 ± 0.1	0.027 ± 0.004	0.0031 ± 0.0003	0.5 ± 0.1
Tunnel City	4 ± 1	0.02 ± 0.01	0.24 ± 0.06	2.5 ± 0.5

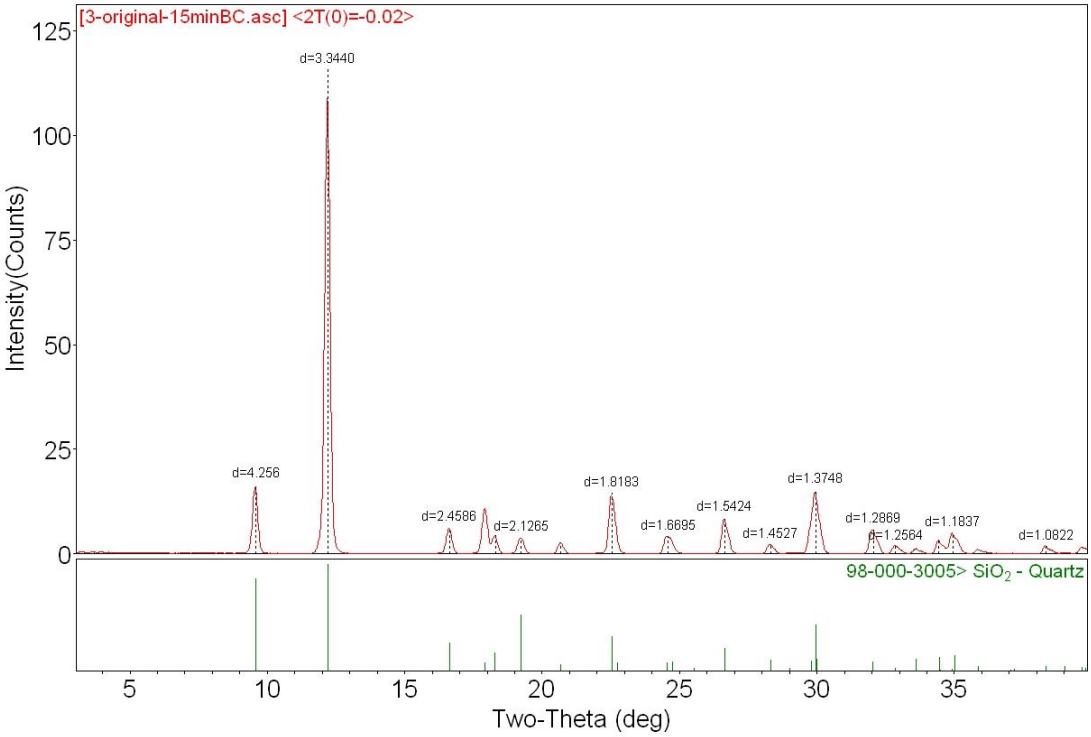

Figure S2. X-ray diffraction (XRD) data for a selected sample from the Tunnel City rock samples, prior to the sequential extraction.

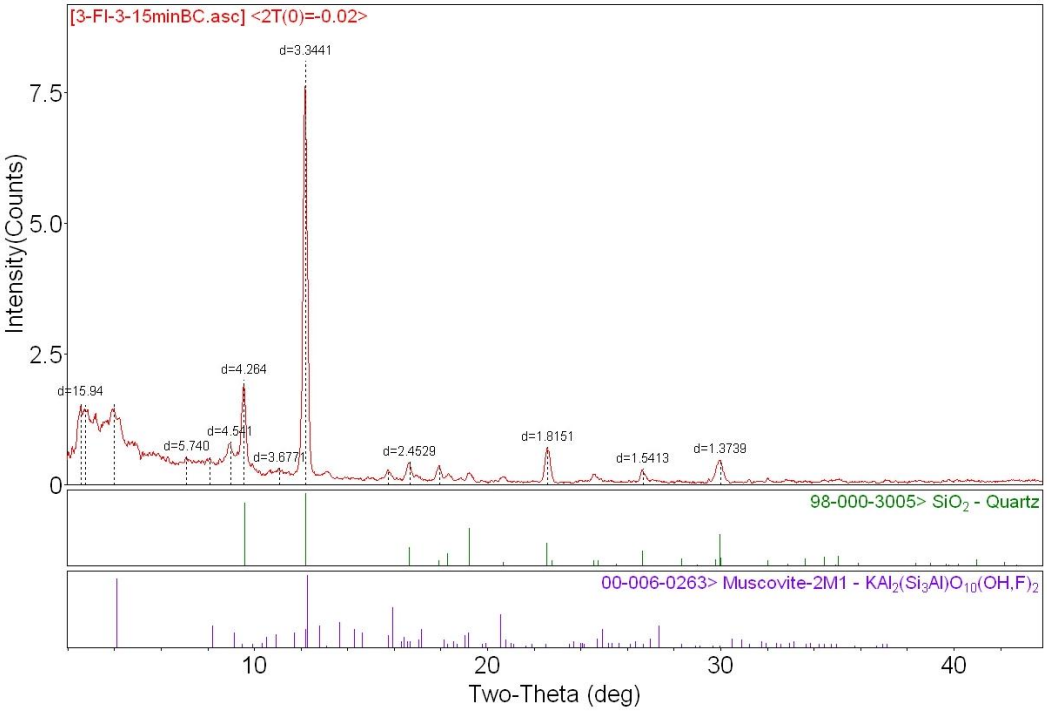

Figure S3. X-ray diffraction (XRD) data for a selected sample from the Tunnel City rock samples, after the sequential extraction.

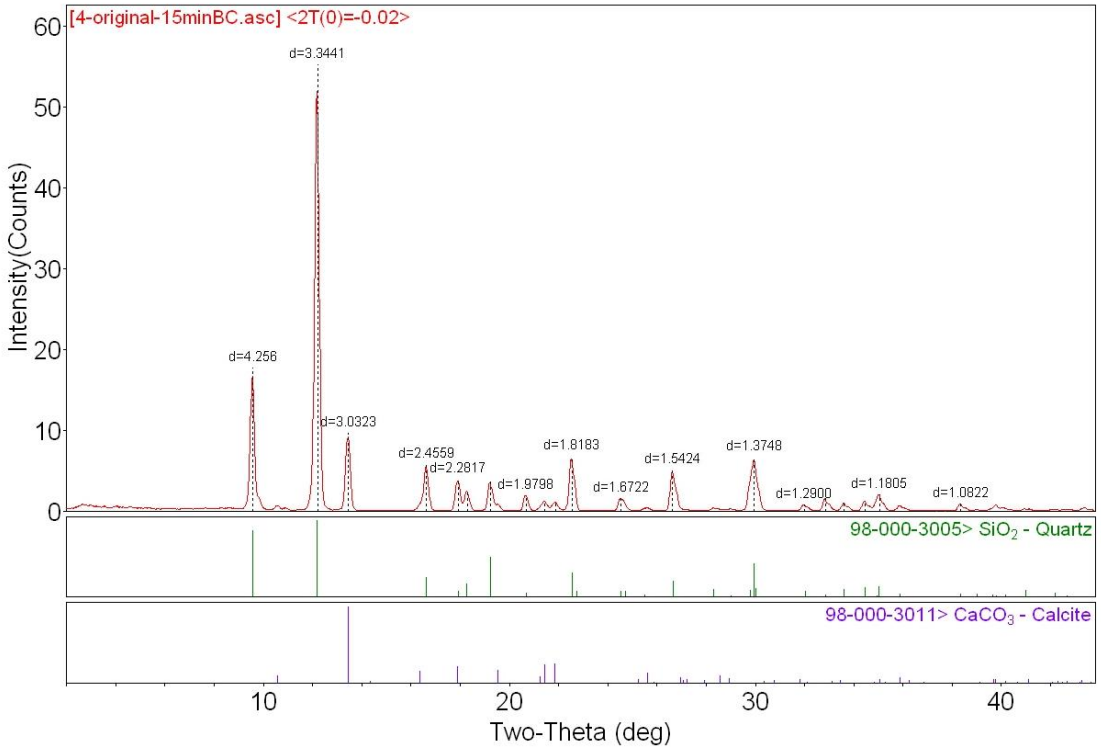

Figure S4. X-ray diffraction (XRD) data for a selected sample from the St Peter rock samples, prior to the sequential extraction.

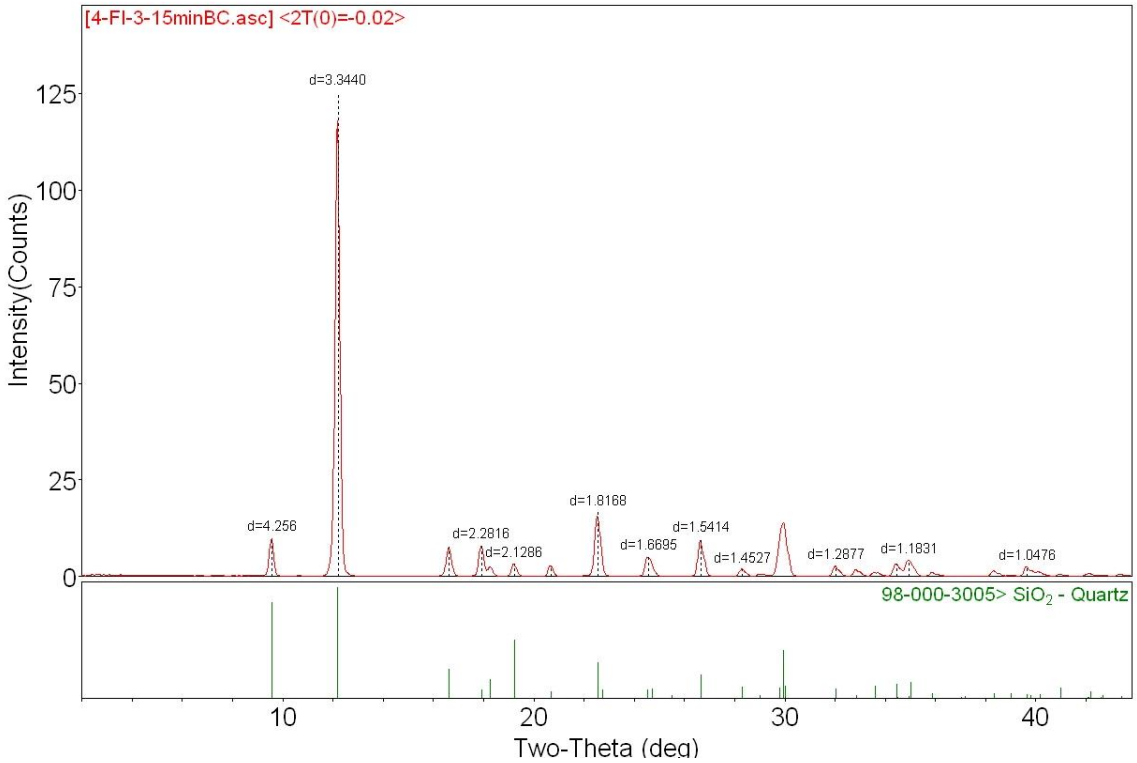

Figure S5. X-ray diffraction (XRD) data for a selected sample from the St Peter rock samples, after the sequential extraction.

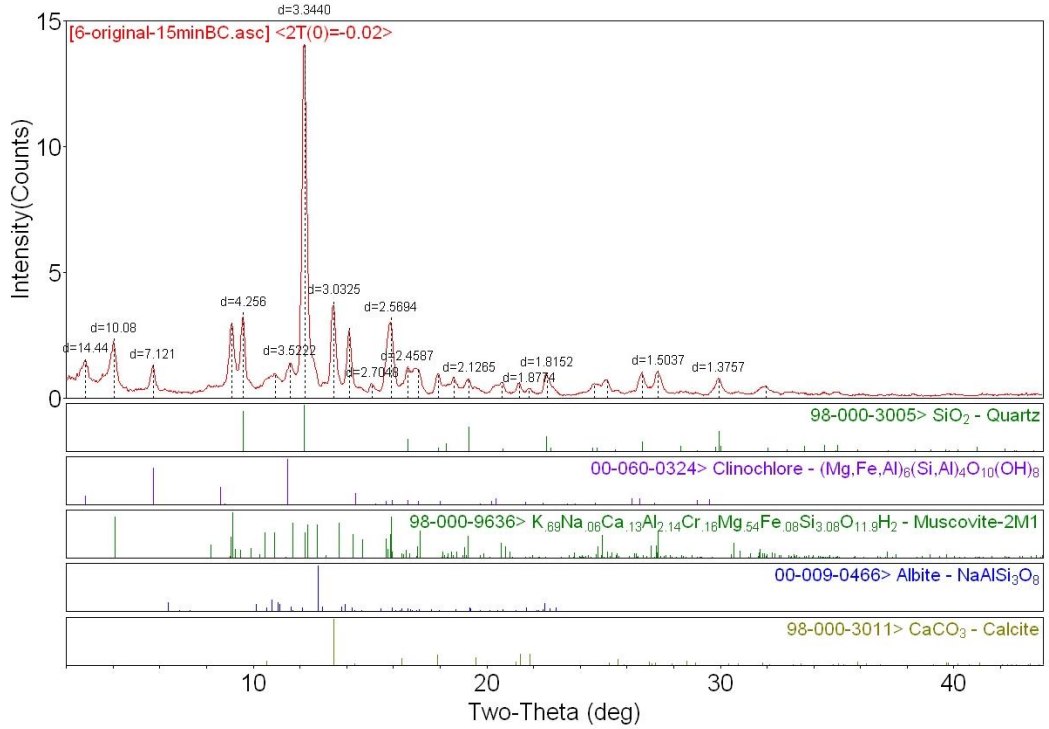

Figure S6. X-ray diffraction (XRD) data for a selected sample from the Maquoketa rock samples, prior to the sequential extraction.

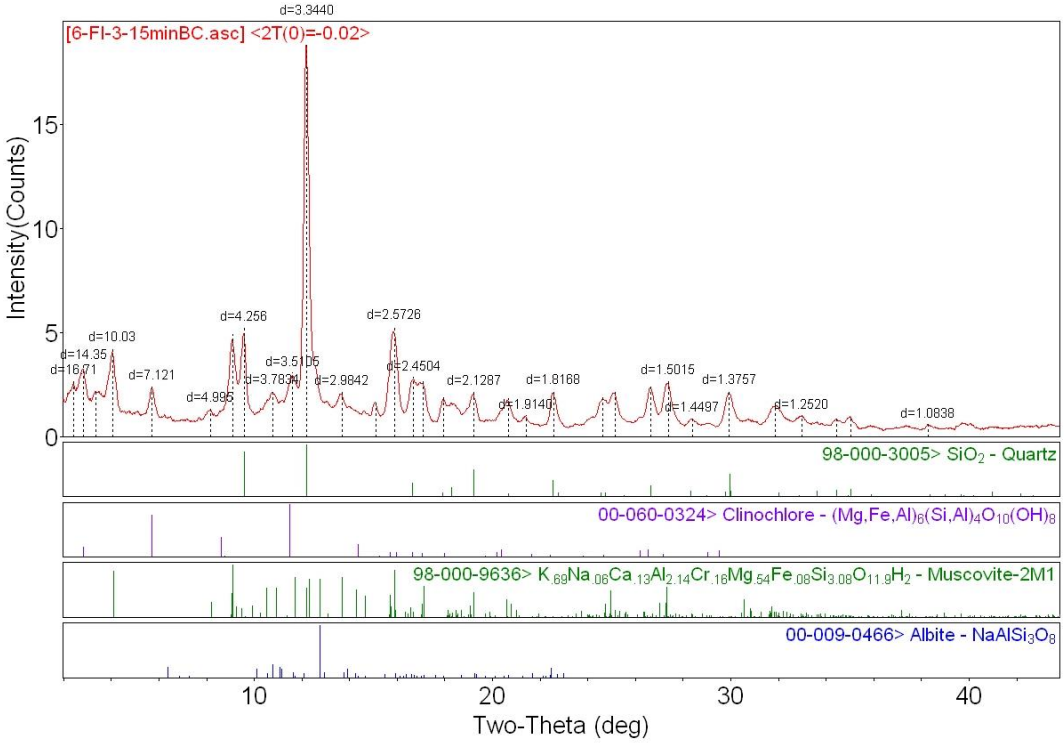

Figure S7. X-ray diffraction (XRD) data for a selected sample from the Maquoketa rock samples, after the sequential extraction.

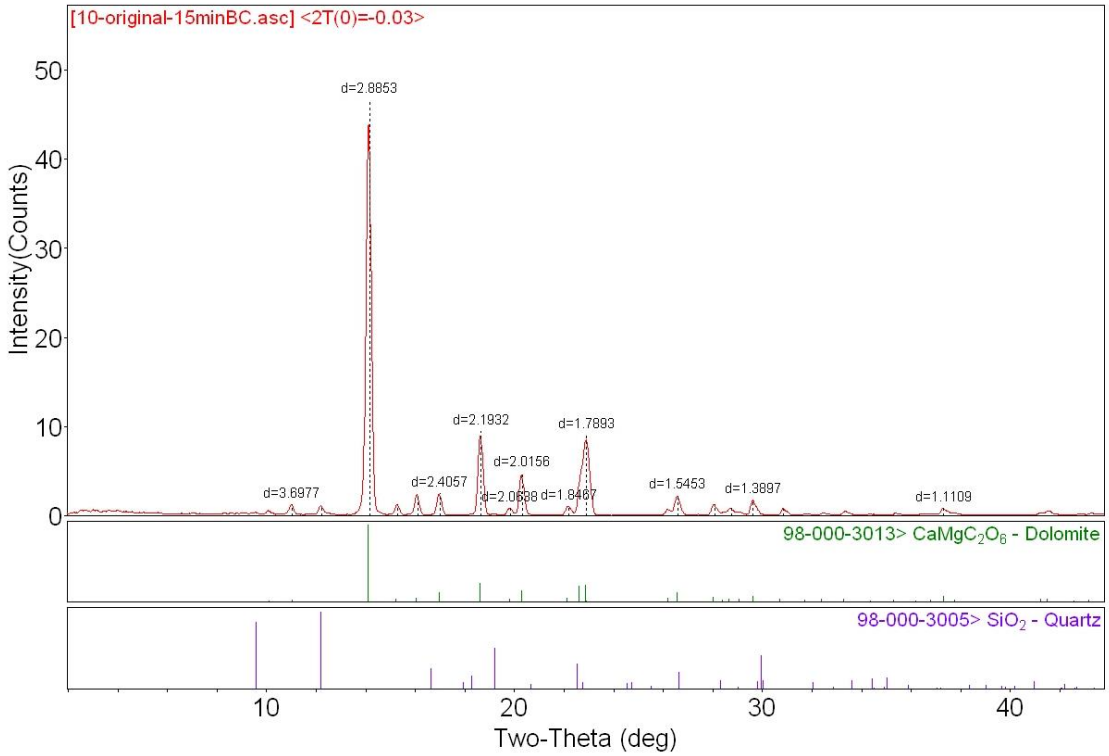

Figure S8. X-ray diffraction (XRD) data for a selected sample from the Galena rock samples, prior to the sequential extraction.

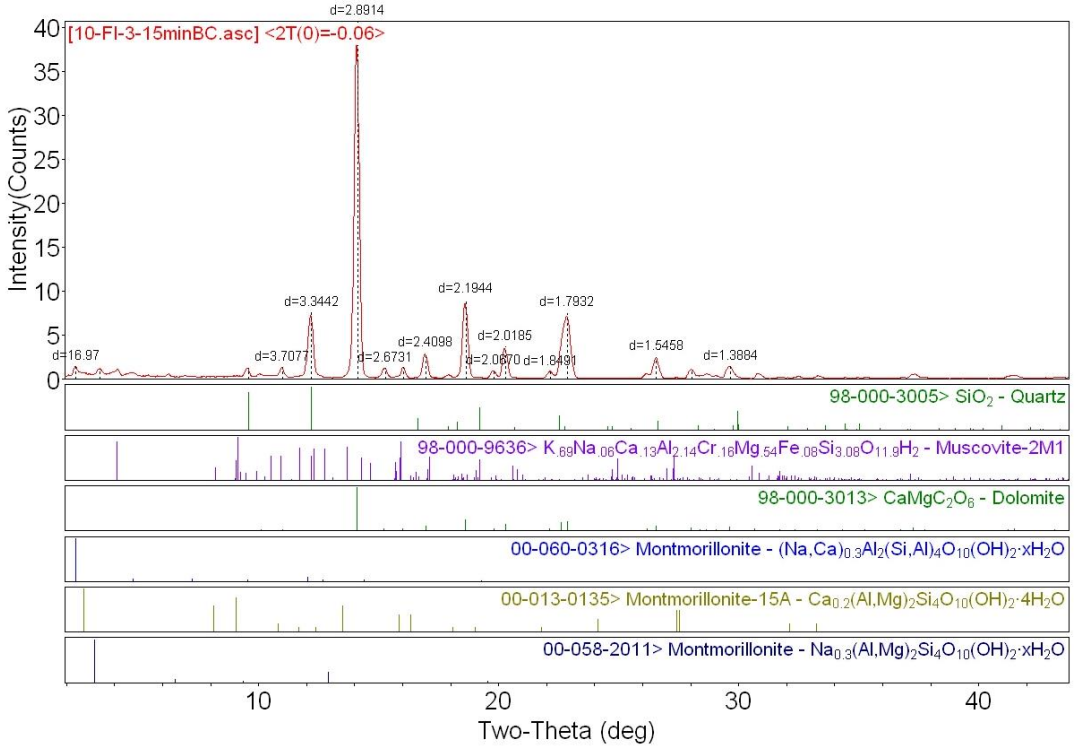

Figure S9. X-ray diffraction (XRD) data for a selected sample from the Galena rock samples, after the sequential extraction.

References

1. Porosities and densities of Wisconsin's aquifers and aquitards. https://wgnhs.wisc.edu/maps-data/data/rock-properties/porosity-density-measurements-data/

Appendix C: Publication - Spatial and temporal variability of radium in the Wisconsin Cambrian-Ordovician aquifer system

Marie Dematatis[1], Amy Plechacek[2], Madeleine Mathews[2], Daniel Wright[1], Florence Udenby[3], Madeline Gotkowitz[4,5], Matthew Ginder-Vogel[1,2]

1. Department of Civil and Environmental Engineering, University of Wisconsin-Madison, Madison, WI 53706, United States
2. Environmental Chemistry and Technology Program, University of Wisconsin-Madison, Madison, WI 53706, United States
3. Wisconsin Department of Natural Resources, Madison, WI 53707, United States
4. Wisconsin Geological and Natural History Survey, Madison, WI 53706
5. Current Affiliation: Montana Bureau of Mines and Geology, Butte, MT 59701, United States

Adapted from: Dematatis, M.; Plechacek, A.; Mathews, M.; Wright, D. B.; Udenby, F.; Gotkowitz, M. B.; Ginder-Vogel, M., Spatial and temporal variability of radium in the Wisconsin Cambrian-Ordovician aquifer system. *AWWA Water Science* **2020**.

Received: 26 September 2019 | Revised: 10 January 2020 | Accepted: 14 January 2020

DOI: 10.1002/aws2.1171

AWWA WATER SCIENCE

ORIGINAL RESEARCH

Spatial and temporal variability of radium in the Wisconsin Cambrian–Ordovician aquifer system

Marie Dematatis[1] | **Amy Plechacek**[2] | **Madeleine Mathews**[2] | **Daniel B. Wright**[1] | **Florence Udenby**[3] | **Madeline B. Gotkowitz**[4] | **Matthew Ginder-Vogel**[1,2]

[1]Department of Civil and Environmental Engineering, University of Wisconsin-Madison, Madison, Wisconsin

[2]Environmental Chemistry and Technology Program, University of Wisconsin-Madison, Madison, Wisconsin

[3]Wisconsin Department of Natural Resources, Madison, Wisconsin

[4]Montana Bureau of Mines and Geology, Butte, Montana

Correspondence
Matthew Ginder-Vogel, Water Science and Engineering Laboratory, 660 North Park Street, Madison, WI 53706.
Email: mgindervogel@wisc.edu

Present address
Madeline B. Gotkowitz, Montana Bureau of Mines and Geology, Butte, MT, 59701

Funding information
Wisconsin Department of Natural Resources; Wisconsin Groundwater Coordinating Council; National Science Foundation Graduate Research Fellowship Program, Grant/Award Number: DGE-1747503

Abstract

Compliance monitoring of contaminants in public drinking water supplies results in publicly available data sets that are maintained by state agencies and useful for investigating changes in water quality. In this study, spatial and temporal trends in naturally occurring radium (combined $^{226}Ra + {}^{228}Ra$) concentrations in groundwater from the Midwestern Cambrian–Ordovician aquifer system were evaluated with a Wisconsin Department of Natural Resources compliance data set. Average combined Ra from 2000 to 2018 in the Midwestern Cambrian–Ordovician aquifer system increased from 5.5 to 7.9 pCi/L in the confined region and from 4.8 to 6.6 pCi/L in the unconfined region. On a local scale, the data demonstrate increasing radium in the communities of Sussex ($n = 98$) and Brookfield ($n = 35$), and a decreasing trend in nearby Waukesha ($n = 176$). This study demonstrates the utility of compliance data sets for investigating water quality trends and the importance of geographic scale in examining such data.

KEYWORDS

drinking water, groundwater, publicly available data sets, radium, trend analysis, water quality

1 | INTRODUCTION

Groundwater is an important source of drinking water in the United States. In 2015, 15.2 bgd were withdrawn at public water supply wells (Dieter et al., 2018). Because of state and federal regulation of public drinking water systems, U.S. government agencies typically maintain publicly available data sets that encompass water use, water quality, and well construction records. These data sets provide opportunities to examine trends pertaining to the quantity and quality of groundwater used for drinking water in the United States. For example, long-term data sets were analyzed to indicate that wells in the United States are being drilled deeper more often than shallower (Perrone & Jasechko, 2019). It will be important to assess corresponding temporal trends in groundwater use and quality; ultimately, findings such as these can help guide decision-making for water resource management. In this study, a long-term, publicly available data set maintained by the Wisconsin Department of Natural Resources (DNR) is used to investigate the utility of this type of data analysis to examine important questions about regional

water quality. This data set includes naturally occurring combined-radium (e.g., $^{226}Ra + ^{228}Ra$) measurements from wells drawing from the Midwestern Cambrian–Ordovician aquifer system (MCOAS) in Wisconsin.

The MCOAS, a regional aquifer system (with both confined and unconfined features) primarily consisting of sandstone and dolostone and extending across parts of Wisconsin, Minnesota, Illinois, Iowa, Missouri, and Indiana, is a critical drinking water source in the Midwest. In 2014, 631 mgd were withdrawn from the MCOAS for combined public supply and domestic use (e.g., private residential wells; Arnold et al., 2017). However, the water associated with the MCOAS has higher levels of naturally occurring Ra compared with most U.S. aquifer systems (Gilkeson, Specht, Cartwright, Griffin, & Larson, 1978; Szabo, dePaul, Fischer, Kraemer, & Jacobsen, 2012). The Maquoketa Shale forms a regional confining unit for a large portion of the MCOAS. Groundwater sampled from beneath the Maquoketa Shale has been shown to have higher average Ra than groundwater from wells completed in the regionally unconfined portion of the MCOAS (Stackelberg, Szabo, & Jurgens, 2018; Szabo et al., 2012). However, local confining units in underlying aquifers can also promote geochemical conditions that are associated with elevated Ra in groundwater (Grundl & Cape, 2006; Mathews, Gotkowitz, & Ginder-Vogel, 2018; Stackelberg et al., 2018; Szabo et al., 2012; Young & Siegel, 1992).

Radium occurs naturally in aquifer systems, it is emitted via alpha decay from parent isotopes of uranium and thorium (e.g., ^{238}U and ^{232}Th; International Atomic Energy Agency, 2014). Ingestion of the radionuclide Ra over long time periods has been shown to be associated with osteosarcoma and other bone disease (Cohn, Skinner, Burger, Falgiano, & Klotz, 2003; Evans, 1933; Guse, Marbella, George, & Layde, 2002; Mays, Rowland, & Stehney, 1985). Accordingly, the U.S. Environmental Protection Agency (USEPA) has set a maximum contaminant level (MCL) of 5 pCi/L for the combination of the two major isotopes, ^{226}Ra and ^{228}Ra. Municipalities must follow USEPA guidelines for monitoring and reporting combined-Ra levels. Sampling requirements are complex: sampling frequency varies depending on combined-Ra levels, and multiple sampling points may be possible for a single well if a treatment system is installed (USEPA, 2000, 2001). Filtering the data set associated with combined-Ra monitoring is challenging, as it must address the complex sampling frequency and ensure accurate representation of the aquifer system (e.g., including only untreated samples).

Many water utilities struggle with combined-Ra MCL exceedances for drinking water wells completed in the MCOAS, in particular in the confined portion of the aquifer in southeast Wisconsin (Wisconsin Department of Natural Resources, 2013, 2019). For example, the city of Waukesha is seeking to improve drinking water quality, following years of aquifer depletion and elevated combined Ra (Figure 1). Waukesha received approval from the Great Lakes Compact Council in 2016 to source drinking water from Lake Michigan, with the stipulation that an equal volume of treated wastewater is returned to the lake's watershed (Great Lakes–St. Lawrence River Basin Water Resources Council, 2016). With Waukesha's project costs approaching US$300 million, smaller nearby communities such as Brookfield and Sussex are seeking economical alternative methods, such as well construction aimed at avoiding elevated combined Ra in the subsurface, to maintain compliance with the combined-Ra MCL (Behm, 2018). As communities investigate the issue of avoiding groundwater elevated in Ra, questions about trends in combined-Ra activities across the

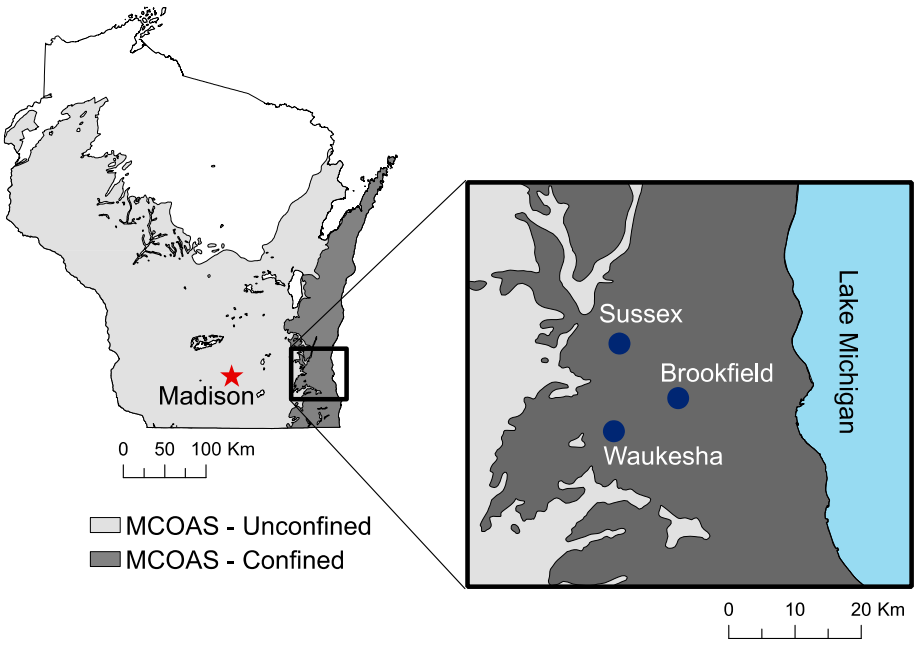

FIGURE 1 Location of the municipalities of Waukesha, Sussex, and Brookfield relative to the unconfined and confined portions of the Midwestern Cambrian–Ordovician aquifer system (MCOAS) in Wisconsin. The location of Madison is shown for reference

region and within nearby communities in southeast Wisconsin begin to emerge (Figure 1).

The temporal variability of combined-Ra levels in the MCOAS in Wisconsin at the regional and individual water utility scales is examined using the Wisconsin Department of Natural Resources' (DNR) Public Drinking Water System compliance data set. Previous studies examine Ra levels at geographic scales ranging from the entire MCOAS (Siegel, 1989; Stackelberg et al., 2018; Szabo et al., 2012; Wilson, 2012), to more specific regions within the aquifer system (Grundl & Cape, 2006; Weaver & Bahr, 1991), and to the local scale (Mathews et al., 2018). In contrast, the present study examines trends in maximum combined-Ra measurements in hydrogeologically defined regions of the MCOAS in Wisconsin, and at the scale of water utility well fields in southeast Wisconsin. This is important, as it elucidates the opportunity to answer pertinent questions related to applied water quality issues, using long-term drinking water quality data sets. Nonparametric statistical methods allow robust analysis of samples collected at varied sampling frequencies, and provide quantitative estimates of changing levels of combined Ra over time in the MCOAS.

2 | MATERIALS AND METHODS

2.1 | Data sources and selection

Temporal trends in combined-Ra activities for wells drawing from the MCOAS in Wisconsin were investigated by obtaining data from the existing state agency water quality database. Groundwater combined-Ra data were retrieved from the publicly available Wisconsin DNR drinking water quality data set (Wisconsin Department of Natural Resources, 2018). Records for untreated, unblended water samples with a combined-Ra measurement and associated, state-assigned, unique well identifier were selected from an initial data set containing 42,249 records. Data were further refined to exclude duplicate records (e.g., samples from the same well on the same day with the same combined measurement). A sampling period from 2000 to 2018 was chosen because of the limited number of records prior to this period. If a well was sampled more than once in a given year, the maximum combined-Ra value was selected, as this is the value reported for compliance. These combined-Ra data by unique well number were joined with a geospatial data set of well locations using ArcMap from ArcGIS Desktop (Release 10.6, Environmental Systems Research Institute, Redlands, CA).

It is important to have knowledge of well construction and associated lithology because it gives information about each well open interval. The Wisconsin Geological and Natural History Survey (WGNHS) well record geodatabase was used in this study to obtain information about well locations, unique well numbers, geologic logs, well construction reports, and depth-to-bedrock attributes. Data were further limited to include only wells with associated combined-Ra data completed only in MCOAS bedrock, excluding any wells completed in unconsolidated sand and gravel deposit, or those missing depth-to-bedrock data. Groundwater samples from wells open only to unconsolidated sand-and-gravel deposits were not considered representative of the MCOAS. Further details about data filtering and processing are provided in the Supporting Information.

Well type in the data set were classified by the hydrogeologic regions, MCOAS-unconfined and MCOAS-confined, based on the presence or absence of the regionally confining Maquoketa Shale (Figure 1). Although these classifications do not capture the complexity of local aquifer conditions, they provide a basis for evaluating trends in water quality relative to the presence or absence of the regional confining unit. For MCOAS-confined, the data set was limited to bedrock wells located in the geographic extent of the Maquoketa Shale with intervals open only to the regionally confined, deep portion of the MCOAS below the confining shale layer.

The open interval of each well in this region was determined from well completion data contained in geologic logs developed by WGNHS and drillers' well construction reports retrieved from the Wisconsin DNR. Where the regional confining unit is present, wells open to the underlying Cambrian and Ordovician aquifers were classified as regionally confined. To the west, where the Maquoketa Shale is absent, wells open to Cambrian and Ordovician aquifers were classified as regionally unconfined. Presence of local confining units was not considered. For wells associated only with a driller's well construction report, the driller's lithologic descriptions were interpreted by comparing them with the depth and thickness of the Maquoketa Shale documented in geologic logs for nearby wells. Combined-Ra sampling records from three wells were excluded from the analysis because of either missing geologic information or the well being open both to the confined and unconfined aquifers. The final data used for the following analyses are provided in Tables S1 and S2.

2.2 | Regional-scale analyses

Combined-Ra data were grouped and analyzed by region to investigate trends within different hydrogeologic settings. Regions of interest were created with a Wisconsin bedrock-geology geospatial data set developed by WGNHS. Wells with associated combined-Ra data were selected by location for each region in ArcMap. The resulting MCOAS data set used for regional analyses consisted of 551 raw water records

from 268 wells (i.e., 189 MCOAS-unconfined wells and 79 MCOAS-confined wells) spanning January 2000 to April 2018. Raw water is water sampled directly from a tap at a wellhead, prior to any treatment or storage tank. Only raw-water records were considered to ensure samples were representative of local aquifer conditions. The data set includes results from wells with statuses of active, inactive, or temporarily out of service.

Nonparametric Theil–Sen linear regressions were performed on the regionally confined and unconfined MCOAS data sets to assess combined-Ra trends across the state (Sen, 1968; Theil, 1992). Compared with linear regression using ordinary least squares, Theil–Sen linear regression is less sensitive to outliers because the median is used to estimate the slope rather than a weighted mean and can therefore be expected to provide more robust inferences in conditions of irregular sampling frequency. This allowed for accurate interpretation of this data set, which included an increased number of sample measurements in more recent years. All Theil–Sen regressions were executed in R using the *mblm* and *zyp* packages (Bronaugh & Werner, 2013; Komsta, 2013; R Core Team, 2018). Averages for each region were calculated for five-year intervals with the exception of the most recent time period, for which the average was calculated for the interval from January 2015 to April 2018 (time of combined-Ra data retrieval).

2.3 | Local-scale analyses

Theil–Sen regressions were also performed on combined-Ra data for each of three water utilities in Waukesha County, Wisconsin, to assess local-scale temporal trends. The data set for the Sussex, Brookfield, and Waukesha water utilities consists of wells drawing from the regionally confined portion of the MCOAS (Figure 1). Data were limited to samples designated as raw water, investigation, grab, and check samples collected from March 2002 to February 2019 (Sussex and Brookfield) and from May 2000 to March 2019 (Waukesha). All available combined-Ra measurements from wells in the confined system for these utilities were initially included, including multiple measurements from a single well within a given year. The data set was then limited to samples representative of the aquifer system by excluding samples collected following radionuclide or iron removal, filtration, and those samples consisting of blended water from multiple wells.

3 | RESULTS AND DISCUSSION

3.1 | Regional-scale results

Nonparametric Theil–Sen linear regression reveals increasing combined-Ra activity for both the MCOAS-confined ($p < .001$, $n = 211$) and MCOAS-unconfined ($p < .001$, $n = 340$; Figure S1). For the MCOAS-unconfined region, the average (SD) combined-Ra activities range from 4.8 ± 2.9 pCi/L in 2000–2004 to 6.6 ± 2.8 pCi/L in 2015–2018 (Table 1). For the MCOAS-confined region, the average confined-Ra activities range from 5.5 ± 3.3 pCi/L in 2000–2004 to 7.9 ± 5.0 pCi/L in 2015–2018. The MCOAS-confined consistently exhibits higher average combined-Ra than the MCOAS-unconfined. This aligns with previous findings of elevated combined-Ra in the confined portion of the MCOAS relative to the unconfined portion (Stackelberg et al., 2018; Szabo et al., 2012; Figure 2).

3.2 | Local-scale results

Radium trends vary at the local scale within the regionally confined portion of the MCOAS in the data subset, based on the Theil–Sen regression analysis for the municipal wells in Sussex, Brookfield, and Waukesha. Combined-Ra levels for the municipal water utilities of Sussex and

TABLE 1 Regional time period averages, medians, and standard deviations for combined Ra in the MCOAS-unconfined and the MCOAS-confined

Region	Time period	Average combined Ra (pCi/L)	Median combined Ra (pCi/L)	*SD*
MCOAS-unconfined	2000–2004	4.8	4.6	2.9
	2005–2009	4.0	3.7	2.8
	2010–2014	5.1	5.3	2.9
	2015–2018	6.6	6.4	2.8
MCOAS-confined	2000–2004	5.5	4.8	3.3
	2005–2009	6.1	5.8	2.8
	2010–2014	7.7	6.5	6.7
	2015–2018	7.9	7.3	5.0

Abbreviation: MCOAS, Midwestern Cambrian–Ordovician aquifer system.

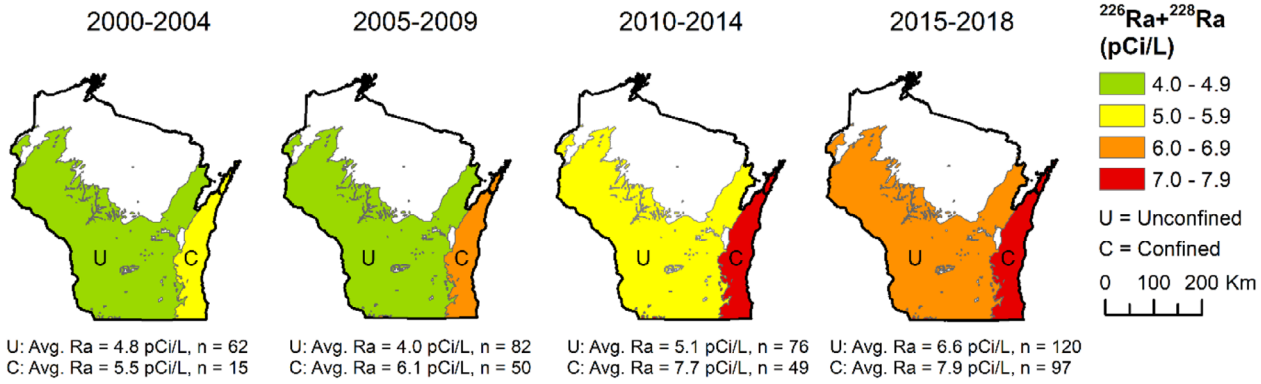

FIGURE 2 Average combined-radium (^{226}Ra + ^{228}Ra) activity in pCi/L from 2000 to 2018 in the regionally unconfined (U) and regionally confined (C) portions of the Midwestern Cambrian–Ordovician aquifer system in Wisconsin. The number of combined-Ra records averaged for a region in a given time period is represented by *n*

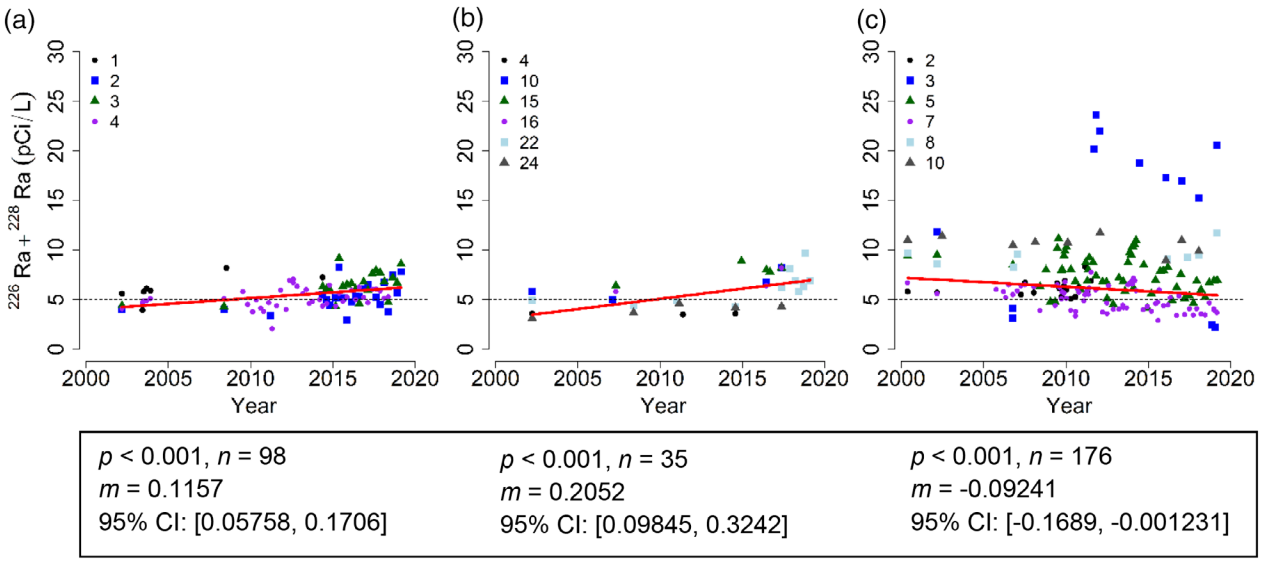

FIGURE 3 Well-specific combined-radium (^{226}Ra + ^{228}Ra) data for water utility wells drawing from the regionally confined Midwestern Cambrian–Ordovician aquifer system in the Wisconsin municipalities of (a) Sussex; (b) Brookfield; and (c) Waukesha. Legend indicates local well identification number. Theil–Sen linear regressions are denoted by the bold red lines, all resulting in $p < .001$. The associated number of samples (n), regression slope, and 95% confidence interval (CI) are noted

Brookfield approach the MCL at the beginning of the study period (2002) with initial averages of 4.2 and 4.4 pCi/L, respectively; this supports increasing trends over time ($p < .001$, $n = 98$ and $p < .001$, $n = 35$, respectively; Figure 3). Radium levels in Waukesha are well above the MCL at the beginning of the data subset (2000) with an initial average of 8.5 pCi/L, and demonstrate a decreasing trend over time ($p < .001$, $n = 176$; Figure 3). Theil–Sen regression analysis was also performed on individual wells for each municipality (Figure S2).

Examination of combined-Ra levels for individual wells in the three municipalities demonstrates variable trends over time for each well. In Sussex, combined-Ra activities for all four municipal wells drawing from the confined MCOAS appear to have increased (Figure 3a). Combined Ra seems to have increased in most Brookfield wells but has remained relatively constant in well 4 (Figure 3b). Wells in Waukesha exhibit variable combined-Ra trends, with individual wells generally increasing, decreasing, or remaining relatively constant in combined-Ra levels (Figure 3c). For example, Waukesha well 3 experiences dramatic fluctuations in combined-Ra activities over the time period, with the highest measurement of 23.6 pCi/L in 2011 and lowest of 2.2 pCi/L in 2019.

These results emphasize the importance of examining large, publicly available data sets at multiple levels. Analyzing data for the entire aquifer system identifies broad trends; however, inspection at the municipality or individual well

scale demonstrates the effect that local conditions have on Ra mobility. Differences in well construction, aquifer geochemistry, and transport result in spatial and temporal variability in combined-Ra levels.

4 | CONCLUSION

Availability of a long-term, publicly accessible data enabled examination of combined-Ra trends over time in the MCOAS of Wisconsin. Within the data subset limited to best represent wells within both MCOAS-unconfined and MCOAS-confined, combined-Ra levels appear to be increasing over time in the MCOAS at the regional scale, but there are variable trends at the local scale. This work demonstrates the importance of considering spatial scale when interrogating a water quality database, since local geochemical and physical conditions may influence contaminant mobility and differ from relative regional-scale conditions.

Use of the Wisconsin DNR's database required significant processing to ensure consistency in sampling locations and accurate representation of the MCOAS. Understanding definitions of sample type (e.g., raw water), sampling source designations, and selecting data appropriate for the examining the long-term trend of combined Ra in the MCOAS in Wisconsin supports accurate interpretation of the data. The number and relative complexity of the issues involved in assessing trends from the publicly accessible database relate to database structure and documentation and the evolution of the Radionuclide Rule. This contributes to the inability of water system managers and state regulators to readily or reliably determine if combined-Ra concentrations were increasing at various scales of interest, such as regional and local levels. Information about water resource management practices is especially beneficial in finer-scale groundwater data analysis, because each well has a unique construction, operation and sampling history.

Some limitations of this study include the assumptions that factors such as seasonal variation in water demand, local geology, or well construction do not impact overall long-term trends. It is recognized that seasonal demand for municipal pumping and the subsequent impact on hydraulic gradients can change concentrations of natural contaminants within an aquifer system. Local geology is difficult to examine in terms of long-term contaminant trends but is important to consider for local-scale geochemistry. It is also recognized that newly constructed wells or recent well reconstruction can impact contaminant concentration in the long-term trend. Nonetheless, in this study, analysis of the data sets provided insight into broad, long-term trends in combined-Ra concentrations in the MCOAS in Wisconsin. Knowledge of long-term combined-Ra trends in the MCOAS may assist water resource managers in making better-informed decisions. Continued increasing combined-Ra trends in the MCOAS may result in (1) less potable water for communities or (2) substantial additional costs associated with radionuclide treatment of groundwater or the installation of surface water infrastructure. Water utilities must address combined-Ra exceedances to ensure public health and to remain in compliance with USEPA regulations, while also considering associated costs and effectiveness of various approaches to reducing combined-Ra levels in pumped groundwater used for drinking. The results of this study suggest an increase in combined-Ra activity has occurred in public water supply wells in the regionally unconfined and confined portions of the MCOAS over the past decade. Many factors affect combined-Ra activities in drinking water, including complex local- and regional-scale hydrologic processes and flow paths, and rock-water geochemical and physical conditions. While these complexities make it difficult to accurately predict combined-Ra activity within a well field, knowledge of increasing trends can inform decision-making for water resource managers and regulators.

ACKNOWLEDGEMENT

The authors thank the Wisconsin Geological and Natural History Survey and the Wisconsin Department of Natural Resources (Madison, Wisconsin) for their assistance with this work. The authors also thank Peter Schoephoester, Assistant Director and Information Manager at WGNHS, for providing and explaining data sets including the Wisconsin wells geodatabase, bedrock geology, geologic logs, and well construction reports. Funding for this project is provided by the Wisconsin Groundwater Research and Monitoring Program as well as the Wisconsin Department of Natural Resources. M.M. is supported by funding from the Grainger Wisconsin Distinguished Graduate Fellowship while A.P. is supported by the National Science Foundation Graduate Research Fellowship Program under Grant No. DGE-1747503. Any opinions, findings, and conclusions or recommendations expressed in this material are those of the author(s) and do not necessarily reflect the views of the National Science Foundation. Support was also provided by the Graduate School and the Office of the Vice Chancellor for Research and Graduate Education at the University of Wisconsin–Madison with funding from the Wisconsin Alumni Research Foundation.

REFERENCES

Arnold, T. L., Bexfield, L. M., Musgrove, M., Lindsey, B. D., Stackelberg, P. E., Barlow, J. R. B., ... Belitz, K. (2017). *Groundwater-quality data from the National Water-Quality Assessment Project, January through December 2014 and select quality-control data from May 2012 through December 2014.* U.S. Geological Survey Report 1063 (p. 96). https://doi.org/10.3133/ds1063

Behm, D. (2018). EPA approves $116 million in low-cost loans to Waukesha for Lake Michigan water supply project. *Milwaukee Journal Sentinal*. Retrieved from https://www.jsonline.com/story/news/local/milwaukee/2018/11/02/epa-approves-116-million-low-cost-loans-waukesha-water-project/1851639002/

Bronaugh, D., & Werner, A. (2013). *zyp: Zhang + Yue-Pilon trends package*. Retrieved from https://cran.r-project.org/package=zyp

Cohn, P., Skinner, R., Burger, S., Falgiano, J., & Klotz, J. (2003). *Radium in drinking water and the incidence of osteosarcoma*. Trenton, NJ: New Jersey Department of Environmental Protection. https://doi.org/10.7282/T3H70GKK

Dieter, C. A., Maupin, M. A., Caldwell, R. R., Harris, M. A., Ivahnenko, T. I., Lovelace, J. K., ... Linsey, K. S. (2018). *Estimated use of water in the United States in 2015*. U.S. Geological Survey Information Circular 1441 (p. 76). https://doi.org/10.3133/cir1441

Evans, R. D. (1933). Radium poisoning: A review of present knowledge. *American Journal of Public Health and the Nations Health*, *23*(10), 1017–1023. https://doi.org/10.2105/AJPH.23.10.1017-b

Gilkeson, R. H., Specht, S. A., Cartwright, K., Griffin, R. A., & Larson, T. E. (1978). *Geologic studies to identify the source for high levels of radium and barium in Illinois ground-water supplies: A preliminary report*.

Great Lakes-St. Lawrence River Basin Water Resources Council. (2016). *Final decision* (2016-1).

Grundl, T., & Cape, M. (2006). Geochemical factors controlling radium activity in a sandstone aquifer. *Groundwater*, *44*(4), 518–527. https://doi.org/10.1111/j.1745-6584.2006.00162.x

Guse, C. E., Marbella, A. M., George, V., & Layde, P. M. (2002). Radium in Wisconsin drinking water: An analysis of osteosarcoma risk. *Archives of Environmental Health: An International Journal*, *57*(4), 294–303. https://doi.org/10.1080/00039890209601412

International Atomic Energy Agency. (2014). *The environmental behaviour of radium: Revised edition*. Technical reports series no. 476 (pp. 44–51). https://doi.org/10.1016/0883-2927(92)90073-C

Komsta, L. (2013). *mblm: Median-based linear models*. Retrieved from https://CRAN.R-project.org/package=mblm

Mathews, M., Gotkowitz, M., & Ginder-Vogel, M. (2018). Effect of geochemical conditions on radium mobility in discrete intervals within the Midwestern Cambrian-Ordovician aquifer system. *Applied Geochemistry*, *97*, 238–246. https://doi.org/10.1016/j.apgeochem.2018.08.025

Mays, C. W., Rowland, R. E., & Stehney, A. F. (1985). Cancer risk from the lifetime intake of Ra and U isotopes. *Health Physics*, *48*(5), 635–647. https://doi.org/10.1097/00004032-198505000-00005

Perrone, D., & Jasechko, S. (2019). Deeper well drilling an unsustainable stopgap to groundwater depletion. *Nature Sustainability*, *2*(8), 773–782. https://doi.org/10.1038/s41893-019-0325-z

R Core Team. (2018). *R: A language and environment for statistical computing (version 3.5.1)*. Vienna, Austria: Author. Retrieved from http://www.R-project.org/

Sen, P. K. (1968). Estimates of regression coefficient based on Kendall's tau. *Journal of the American Statistical Association*, *63*(324), 1279–1289. https://doi.org/10.1080/01621459.1968.10480934

Siegel, D. I. (1989). *Geochemistry of the Cambrian-Ordovician aquifer system in the northern Midwest, United States*. U.S. Geological Survey Professional Paper 1405-D.

Stackelberg, P. E., Szabo, Z., & Jurgens, B. C. (2018). Radium mobility and the age of groundwater in public-drinking-water supplies from the Cambrian-Ordovician aquifer system, north-central USA. *Applied Geochemistry*, *89*, 34–48. https://doi.org/10.1016/j.apgeochem.2017.11.002

Szabo, Z., dePaul, V. T., Fischer, J. M., Kraemer, T. F., & Jacobsen, E. (2012). Occurrence and geochemistry of radium in water from principal drinking-water aquifer systems of the United States. *Applied Geochemistry*, *27*(3), 729–752. https://doi.org/10.1016/j.apgeochem.2011.11.002

Theil, H. (1992). A rank-invariant method of linear and polynomial regression analysis. In B. Raj & J. Koerts (Eds.), *Henri Theil's contributions to economics and econometrics: Econometric theory and methodology* (pp. 345–381). Dordrecht: Springer Netherlands.

U.S. Environmental Protection Agency. (2000). National primary drinking water regulations. *Federal Register*, *65*(236), 76708–76753. https://www.govinfo.gov/content/pkg/FR-2000-12-07/pdf/00-30421.pdf

U.S. Environmental Protection Agency. (2001). *Radionuclides rule: A quick reference guide*. Retrieved from https://nepis.epa.gov/Exe/ZyPDF.cgi?Dockey=30006644.txt

Weaver, T. R., & Bahr, J. (1991). Geochemical evolution in the Cambrian-Ordovician sandstone aquifer, eastern Wisconsin: 1. Major ion and radionuclide distribution. *Groundwater*, *29*(3), 350–356. https://doi.org/10.1111/j.1745-6584.1991.tb00525.x

Wilson, J. T. (2012). *Water-quality assessment of the Cambrian-Ordovician aquifer system in the Northern Midwest, United States*. U.S. Geological Survey Scientific Investigations Report 2011-5229 (p. 154).

Wisconsin Department of Natural Resources. (2013). *Radium in drinking water*. Retrieved from http://dnr.wi.gov/files/PDF/pubs/DG/DG0008.pdf

Wisconsin Department of Natural Resources. (2018). *Public drinking water system data*. Retrieved from https://dnr.wi.gov/dwsviewer

Wisconsin Department of Natural Resources. (2019). *Wisconsin public water systems 2018 annual drinking water report*. Retrieved from https://dnr.wi.gov/topic/DrinkingWater/

Young, H. L., & Siegel, D. I. (1992). *Hydrogeology of the Cambrian-Ordovician aquifer system in the Northern Midwest, United States*. U.S. Geological Survey Professional Paper 1405-B 99.

SUPPORTING INFORMATION

Additional supporting information may be found online in the Supporting Information section at the end of this article.

How to cite this article: Dematatis M, Plechacek A, Mathews M, et al. Spatial and temporal variability of radium in the Wisconsin Cambrian–Ordovician aquifer system. *AWWA Wat Sci*. 2020;e1171. https://doi.org/10.1002/aws2.1171

Supplementary Information

Spatial and temporal variability of radium in the Wisconsin Cambrian-Ordovician aquifer system

Marie Dematatis[1], Amy Plechacek[2], Madeleine Mathews[2], Daniel Wright[1], Florence Udenby[3], Madeline Gotkowitz[4,5], Matthew Ginder-Vogel[1,2*]

1. Department of Civil and Environmental Engineering, University of Wisconsin-Madison, Madison, WI 53706, United States
2. Environmental Chemistry and Technology, Department of Civil and Environmental Engineering, University of Wisconsin-Madison, Madison, WI 53706, United States
3. Wisconsin Department of Natural Resources, Madison, WI 53707, United States
4. Montana Bureau of Mines and Geology, Butte, MT 59701, United States
5. Current Affiliation: Montana Bureau of Mines and Geology, Butte, MT 59701, United States

*Corresponding author. Tel.: (608) 262-0768; E-mail address: matt.ginder-vogel@wisc.edu

Table of Contents

Supporting Methods

Data Sources and Selection:

Groundwater combined radium data were accessed from the WI DNR's publicly available drinking water quality dataset for municipal wells, located at https://dnr.wi.gov/topic/Groundwater/grn.html. Sample summary count reports were generated by searching and downloading sample analytical data from: https://dnr.wi.gov/dwsviewer/ContamResult/Search.

The well database provided by the Wisconsin Geological and Natural History Survey (WGNHS) used includes well locations, and therefore is not available to the public for security reasons. The Wisconsin bedrock geology geospatial dataset used to create regional datasets was downloaded from: https://wgnhs.wisc.edu/pubs/000390/.

Geologic logs and well construction reports were retrieved from the Wisconsin Geological and Natural History Survey (WGNHS). The information and exact locations of public wells are not available to the public for security reasons. Wells sampled for combined radium within the geographic extent of the Maquoketa Shale were classified as regionally confined or regionally unconfined based on the lithologic information of the well open interval. Geologic logs were utilized when available because they contain stratigraphic interpretations, listing the presence and depth of specific geologic formations such as the Maquoketa Shale. The well open interval (well casing bottom depth to well bottom depth) was compared to the depth and thickness of the Maquoketa Shale. Well construction reports were utilized when geologic logs were not available by interpreting geologic descriptions and associated depths. Well construction reports were compared to nearby geologic logs to confirm that geologic description interpretations matched approximate formation depths in geologic logs. When a radium sampling

record did not include an associated geologic log or well construction report, it was excluded from analyses.

Data for regional-scale analysis was filtered to for samples categorized as “Raw Water” type. A “Raw Water” sample is collected directly from a tap at a wellhead before any treatment. For the local-scale analysis, “Raw Water”, “Investigation,” “Check,” and “Grab” sample types were included. “Investigation” refers to a sample that is taken for some purpose other than regulatory compliance; “Check” samples are samples collected to verify the results of a measurement; and “Grab” samples refer to samples collected all at one time. The data for the local-scale analysis was further filtered to ensure samples representative of the aquifer system by eliminating samples collected following radionuclide treatment, iron removal, or filtration, and samples consisting of blended water from multiple wells.

Statistics:

Nonparametric Theil-Sen linear regression, a single median method, computes slopes of lines crossing all possible pairs of points when x-coordinates differ. After calculating these slopes, the slope estimator is calculated as the median of the slopes. It can be substantially more robust than simple linear regression (i.e. ordinary least squares) for skewed and heteroscedastic data (Sen, 1968; Siegel, 1982; Theil, 1992; Wilcox, 2001). It is thus likely to be preferable in the conditions of sparse, irregular temporal sampling present in the study dataset.

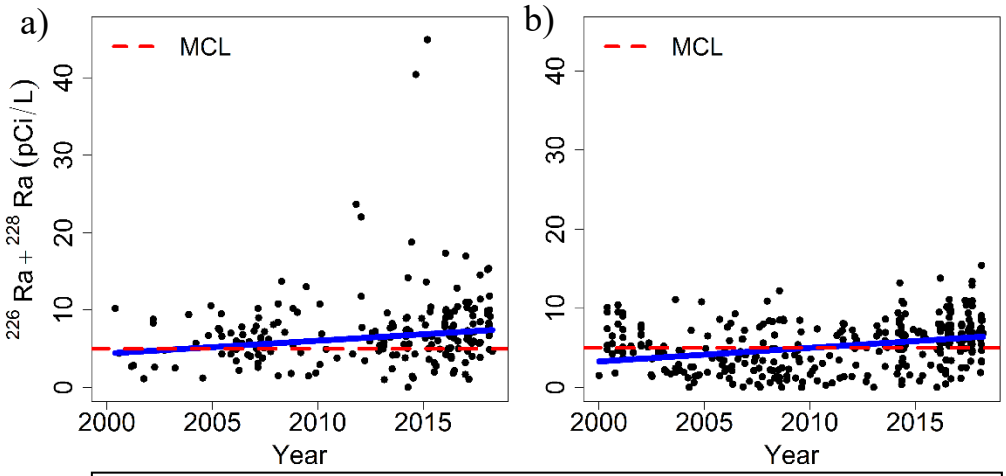

a)	b)
p < 0.001, n = 211	p < 0.001, n = 340
m = 0.1659	m = 0.1717
95% CI: [0.07559, 0.2567]	95% CI: [0.1110, 0.2321]

Figure S1. Combined radium (^{226}Ra + ^{228}Ra) data for wells drawing from the a) the region of the Midwestern Cambrian-Ordovician aquifer system confined by Maquoketa Shale, and b) the regionally unconfined portion of Midwestern Cambrian-Ordovician aquifer system. Theil-Sen linear regressions are denoted by the blue lines. The associated p-value, number of samples (n), regression slope (m), and 95% confidence interval (CI) are noted below. Results demonstrated an increasing trend in Ra for wells in both regions.

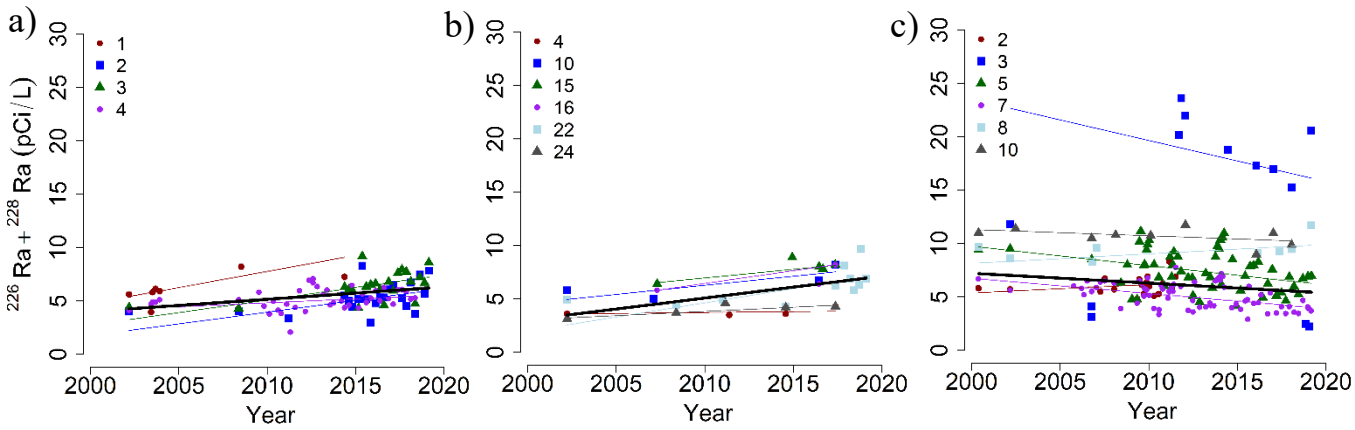

a)	b)	c)
p < 0.001, n = 98	p < 0.001, n = 35	p < 0.001, n = 176
m = 0.1157	m = 0.2052	m = -0.09241
95% CI: [0.05758, 0.1706]	95% CI: [0.09845, 0.3242]	95% CI: [-0.1689, -0.001231]

Figure S2. Combined radium (^{226}Ra + ^{228}Ra) data for water utility wells drawing from the regionally-confined Midwestern Cambrian-Ordovician aquifer system in the Wisconsin municipalities of a) Sussex, b) Brookfield, and c) Waukesha. Legend indicates local well identification number by color and shape; color also indicates Theil Sen linear regression associated with each respective well. Theil Sen linear regressions including all wells are denoted by bold black lines with the associated *p*-value, number of samples (*n*), regression slope (*m*), and 95% confidence interval (CI) noted below.

Table S1. Combined radium measurements used in the regional-scale analysis. Wisconsin Unique Well Number is represented by WUWN.

WUWN	County	Ra activity (pCi/L)	Sample Date
AC338	Outagamie	6.2	8/24/2017
AC715	Waukesha	7.9	8/8/2013
AJ774	Waukesha	7.1	8/6/2012
AR350	Clark	1.5	1/3/2000
AT090	Sauk	1.6	6/26/2002
AT091	Brown	40.4	8/27/2014
AT091	Brown	44.9	3/18/2015
AT099	Barron	3.7	6/2/2014
AX007	Racine	7.7	6/11/2013
AX007	Racine	7.5	4/1/2014
AX007	Racine	8.1	2/10/2015
AX007	Racine	8.3	1/12/2016
AX007	Racine	6.5	2/6/2017

AX007	Racine	6.7	2/20/2018
AY325	Jefferson	6.0	3/26/2012
AY338	Walworth	7.0	11/18/2005
AY338	Walworth	6.0	2/21/2006
AY365	Rock	0.6	2/14/2008
AY377	Fond du Lac	6.9	3/16/2016
AY377	Fond du Lac	8.5	9/18/2017
AY377	Fond du Lac	7.6	2/27/2018
AY378	Fond du Lac	5.1	4/11/2016
AY378	Fond du Lac	3.9	9/18/2017
AY378	Fond du Lac	6.9	2/26/2018
AY379	Fond du Lac	5.0	4/11/2016
AY379	Fond du Lac	5.8	9/19/2017
AY379	Fond du Lac	4.9	2/26/2018
BA125	Waukesha	4.6	10/11/2007
BA125	Waukesha	6.6	8/20/2012
BA125	Waukesha	5.0	2/11/2013
BA125	Waukesha	5.6	2/6/2014
BA125	Waukesha	5.0	4/8/2015
BA125	Waukesha	4.2	2/1/2016
BA125	Waukesha	6.1	3/9/2017
BA125	Waukesha	7.5	3/5/2018
BF185	Brown	12.2	7/28/2008
BF185	Brown	8.1	8/3/2011
BF185	Brown	6.4	2/21/2012
BF185	Brown	6.8	4/17/2013
BF185	Brown	7.3	12/2/2014
BF185	Brown	6.2	6/1/2015
BF186	Brown	8.5	7/28/2008
BF186	Brown	8.0	8/25/2011
BF186	Brown	6.4	2/21/2012
BF186	Brown	7.0	4/17/2013
BF186	Brown	7.7	5/7/2014
BF186	Brown	6.8	6/1/2015
BF187	Brown	8.4	10/9/2008
BF187	Brown	6.0	8/3/2011
BF187	Brown	4.9	2/21/2012
BF187	Brown	4.5	4/17/2013
BF187	Brown	7.1	5/7/2014
BF187	Brown	6.6	6/1/2015
BF188	Brown	8.8	5/7/2014

BF190	Brown	9.5	11/28/2000
BF190	Brown	9.0	2/20/2001
BF190	Brown	6.6	5/19/2014
BF191	Brown	4.2	8/22/2000
BF191	Brown	3.7	2/20/2001
BF191	Brown	5.6	5/19/2014
BF192	Brown	4.7	11/28/2000
BF192	Brown	4.4	2/20/2001
BF193	Brown	6.5	8/22/2000
BF193	Brown	5.1	2/20/2001
BF193	Brown	3.2	5/19/2014
BF194	Brown	10.4	11/28/2000
BF194	Brown	9.4	2/20/2001
BF194	Brown	0.9	5/19/2014
BF195	Brown	8.0	11/28/2000
BF195	Brown	7.3	2/20/2001
BF195	Brown	4.8	5/19/2014
BF196	Brown	5.5	8/22/2000
BF196	Brown	6.3	2/20/2001
BF196	Brown	6.7	5/19/2014
BF197	Brown	10.9	5/19/2014
BF201	Brown	6.5	7/15/2014
BF204	Brown	9.3	7/15/2014
BF206	Brown	5.2	1/2/2002
BF206	Brown	2.5	3/17/2014
BF207	Brown	7.9	1/2/2002
BF207	Brown	4.8	3/17/2014
BF208	Brown	6.7	1/2/2002
BF208	Brown	6.9	3/17/2014
BF209	Brown	6.6	1/2/2002
BF209	Brown	5.3	3/17/2014
BF211	Brown	14.2	4/15/2014
BF214	Brown	8.5	7/15/2009
BF214	Brown	7.4	5/11/2010
BF214	Brown	6.9	6/15/2011
BF214	Brown	5.6	3/14/2012
BF214	Brown	6.9	8/8/2013
BF214	Brown	8.1	3/31/2014
BF215	Brown	8.6	8/8/2013
BF215	Brown	8.5	3/31/2014
BF216	Brown	1.4	6/26/2014

BF229	Buffalo	6.9	2/24/2015
BF257	Calumet	4.3	1/28/2016
BF257	Calumet	5.7	4/26/2017
BF257	Calumet	15.4	2/14/2018
BF587	Dodge	0.4	6/15/2016
BF587	Dodge	3.3	8/21/2017
BF601	Dodge	5.6	5/7/2014
BF601	Dodge	6.6	6/3/2015
BF601	Dodge	6.9	4/7/2016
BF601	Dodge	6.0	5/25/2017
BF611	Dodge	1.5	9/27/2005
BF611	Dodge	2.0	12/20/2005
BF612	Dodge	4.5	12/20/2005
BF619	Dodge	6.7	3/25/2014
BF619	Dodge	5.5	5/27/2015
BF619	Dodge	10.5	8/23/2016
BF619	Dodge	4.7	2/13/2017
BF619	Dodge	9.2	3/12/2018
BF624	Dodge	4.2	10/1/2013
BF624	Dodge	3.8	2/26/2014
BF624	Dodge	3.6	4/14/2015
BF624	Dodge	6.0	8/30/2016
BF624	Dodge	5.7	8/31/2017
BF624	Dodge	4.6	4/17/2018
BF635	Dodge	2.6	3/10/2016
BF635	Dodge	1.1	3/8/2017
BF796	Fond du Lac	7.7	3/29/2016
BF796	Fond du Lac	6.4	9/18/2017
BF796	Fond du Lac	9.1	2/27/2018
BF797	Fond du Lac	10.1	5/25/2000
BF797	Fond du Lac	5.7	3/29/2016
BF797	Fond du Lac	6.9	9/19/2017
BF797	Fond du Lac	4.7	2/27/2018
BF798	Fond du Lac	4.3	3/16/2016
BF798	Fond du Lac	5.4	9/18/2017
BF798	Fond du Lac	3.3	2/27/2018
BF799	Fond du Lac	7.4	5/25/2000
BF799	Fond du Lac	5.5	3/16/2016
BF799	Fond du Lac	10.9	9/19/2017
BF799	Fond du Lac	7.5	2/27/2018
BF800	Fond du Lac	5.3	5/25/2000

BF800	Fond du Lac	3.7	6/29/2009
BF800	Fond du Lac	2.3	3/29/2016
BF800	Fond du Lac	4.4	9/18/2017
BF800	Fond du Lac	3.2	2/27/2018
BF801	Fond du Lac	4.8	5/25/2000
BF801	Fond du Lac	2.1	5/8/2007
BF801	Fond du Lac	7.1	3/16/2016
BF801	Fond du Lac	4.7	9/18/2017
BF801	Fond du Lac	5.4	2/27/2018
BF802	Fond du Lac	6.6	4/11/2016
BF802	Fond du Lac	11.4	9/19/2017
BF802	Fond du Lac	11.8	2/26/2018
BF803	Fond du Lac	10.2	5/25/2000
BF803	Fond du Lac	9.2	4/11/2016
BF803	Fond du Lac	8.5	9/19/2017
BF803	Fond du Lac	8.0	2/26/2018
BF804	Fond du Lac	9.5	3/16/2016
BF804	Fond du Lac	14.5	9/18/2017
BF804	Fond du Lac	10.0	2/26/2018
BF805	Fond du Lac	9.5	5/25/2000
BF805	Fond du Lac	13.8	3/16/2016
BF805	Fond du Lac	13.4	9/18/2017
BF805	Fond du Lac	15.4	2/26/2018
BF806	Fond du Lac	7.4	3/16/2016
BF806	Fond du Lac	6.9	9/18/2017
BF806	Fond du Lac	8.5	2/26/2018
BF808	Fond du Lac	1.8	6/8/2016
BF808	Fond du Lac	11.0	3/7/2017
BF880	Grant	3.4	5/25/2011
BF928	Green Lake	10.2	7/5/2016
BF929	Green Lake	8.0	3/22/2016
BF963	Iowa	2.7	8/6/2014
BF983	Jefferson	1.5	5/11/2015
BG191	Lafayette	1.6	9/30/2014
BG194	Lafayette	4.9	6/23/2014
BG195	Lafayette	6.5	3/11/2013
BG195	Lafayette	7.1	3/17/2015
BG195	Lafayette	6.4	9/20/2016
BG195	Lafayette	10.3	9/19/2017
BG340	Marinette	6.1	4/11/2017
BG346	Marinette	5.9	7/31/2013

BG346	Marinette	9.4	9/7/2016
BG346	Marinette	7.2	7/11/2017
BG429	Milwaukee	7.4	3/12/2014
BG440	Milwaukee	4.8	9/24/2002
BG440	Milwaukee	5.9	10/4/2006
BG440	Milwaukee	5.4	3/6/2007
BG440	Milwaukee	5.4	12/13/2012
BG440	Milwaukee	5.3	2/18/2013
BG440	Milwaukee	5.0	4/8/2014
BG440	Milwaukee	4.9	10/21/2015
BG453	Milwaukee	8.9	3/12/2014
BG454	Milwaukee	6.6	3/12/2014
BG505	Oconto	6.0	3/28/2016
BG505	Oconto	5.3	3/14/2017
BG507	Oconto	4.3	10/29/2002
BG507	Oconto	4.3	1/28/2003
BG508	Oconto	4.5	10/29/2002
BG508	Oconto	5.2	1/28/2003
BG509	Oconto	4.2	10/29/2002
BG509	Oconto	5.1	1/28/2003
BG574	Outagamie	10.0	7/26/2016
BG574	Outagamie	8.6	7/26/2017
BG575	Outagamie	7.1	7/26/2016
BG575	Outagamie	7.5	7/26/2017
BG576	Outagamie	7.5	7/26/2016
BG576	Outagamie	6.5	7/26/2017
BG578	Outagamie	6.6	7/26/2016
BG578	Outagamie	6.4	7/26/2017
BG579	Outagamie	8.4	2/1/2008
BG579	Outagamie	9.6	8/30/2016
BG579	Outagamie	6.0	8/15/2017
BG580	Outagamie	5.7	8/30/2016
BG580	Outagamie	10.6	8/15/2017
BG581	Outagamie	10.3	8/30/2016
BG581	Outagamie	5.9	8/15/2017
BG738	Racine	6.5	6/11/2013
BG738	Racine	9.0	4/1/2014
BG738	Racine	6.4	2/10/2015
BG738	Racine	7.9	1/12/2016
BG738	Racine	7.3	2/6/2017
BG738	Racine	7.6	2/20/2018

BG746	Racine	9.4	11/19/2003
BG808	Rock	1.7	2/26/2014
BH177	Walworth	4.3	6/17/2005
BH177	Walworth	4.9	2/21/2006
BH178	Walworth	4.3	11/18/2005
BH178	Walworth	3.4	2/21/2006
BH246	Washington	7.3	12/27/2006
BH246	Washington	9.7	3/16/2016
BH246	Washington	10.3	2/1/2017
BH359	Waukesha	6.7	10/27/2004
BH359	Waukesha	5.3	5/31/2007
BH375	Waukesha	5.0	2/6/2007
BH375	Waukesha	6.7	6/14/2016
BH375	Waukesha	8.2	5/17/2017
BH380	Waukesha	6.4	4/24/2007
BH380	Waukesha	8.9	12/9/2014
BH380	Waukesha	8.0	6/14/2016
BH380	Waukesha	8.2	5/17/2017
BH381	Waukesha	5.8	4/24/2007
BH381	Waukesha	6.4	6/14/2016
BH381	Waukesha	8.2	5/17/2017
BH395	Waukesha	7.1	6/10/2008
BH395	Waukesha	6.0	6/21/2012
BH421	Waukesha	3.1	3/1/2007
BH424	Waukesha	7.3	5/20/2014
BH429	Waukesha	23.6	10/31/2011
BH429	Waukesha	22.0	1/26/2012
BH429	Waukesha	18.8	6/17/2014
BH429	Waukesha	17.3	1/26/2016
BH429	Waukesha	17.0	1/11/2017
BH429	Waukesha	15.2	1/23/2018
BH434	Waukesha	9.1	3/3/2016
BH434	Waukesha	9.2	5/15/2017
BH434	Waukesha	9.5	1/23/2018
BH436	Waukesha	10.8	2/18/2008
BH436	Waukesha	10.8	2/9/2010
BH436	Waukesha	11.8	1/26/2012
BH436	Waukesha	9.0	1/27/2016
BH436	Waukesha	11.0	1/11/2017
BH436	Waukesha	9.9	1/23/2018
BH443	Waukesha	8.1	11/27/2007

BH443	Waukesha	8.4	2/11/2008
BH543	Winnebago	8.3	3/26/2008
BH543	Winnebago	9.5	2/23/2016
BH543	Winnebago	11.0	5/18/2017
BH544	Winnebago	4.9	3/26/2008
BH544	Winnebago	5.7	5/10/2016
BH544	Winnebago	4.9	5/18/2017
BO040	Jefferson	1.2	5/6/2009
BO040	Jefferson	0.8	3/23/2015
BO307	Sauk	4.8	5/6/2009
BO307	Sauk	2.8	9/30/2015
BO679	Racine	7.2	9/25/2012
BO679	Racine	5.0	9/6/2016
BO679	Racine	7.2	6/6/2017
BP229	Outagamie	10.9	12/28/2007
BP229	Outagamie	13.2	4/14/2014
BP229	Outagamie	11.1	8/17/2016
BP229	Outagamie	12.9	9/18/2017
BP229	Outagamie	8.7	2/20/2018
BP724	Eau Claire	5.3	7/16/2014
BP724	Eau Claire	4.2	5/11/2015
BP724	Eau Claire	8.8	8/17/2016
BP724	Eau Claire	10.4	6/6/2017
CL048	Brown	10.2	3/6/2007
CL048	Brown	13.6	2/25/2015
CL048	Brown	12.8	8/11/2016
CL048	Brown	10.2	6/13/2017
CM075	Dane	0.3	5/15/2014
CO448	Dodge	5.8	2/26/2016
CO448	Dodge	6.8	3/15/2017
DG402	Outagamie	6.1	8/12/2016
DG402	Outagamie	7.7	8/24/2017
DW152	Jefferson	9.4	3/12/2014
DW152	Jefferson	8.0	2/11/2016
DW152	Jefferson	5.9	2/6/2017
EJ765	Sauk	0.0	1/14/2016
EM264	Monroe	6.3	7/25/2016
EM264	Monroe	6.1	8/8/2017
EM276	Waukesha	13.7	4/18/2008
EQ931	Walworth	7.2	5/18/2004
EQ931	Walworth	7.9	8/9/2016

EQ931	Walworth	6.1	6/20/2017
FD551	Brown	5.4	1/2/2002
FH501	Fond du Lac	6.7	6/24/2014
FX351	Walworth	7.4	5/10/2005
FX351	Walworth	5.7	5/30/2006
FX370	Waukesha	10.4	5/14/2015
FX374	Waukesha	8.8	3/13/2002
FX374	Waukesha	8.3	7/16/2013
FX374	Waukesha	9.8	6/28/2016
FX374	Waukesha	6.8	3/7/2017
FX375	Waukesha	8.3	3/13/2002
FX375	Waukesha	2.4	7/16/2013
FX375	Waukesha	2.2	6/28/2016
FX375	Waukesha	1.1	3/7/2017
FX376	Waukesha	2.6	4/8/2002
FX377	Waukesha	2.5	3/30/2003
HJ128	Waukesha	4.0	10/27/2006
HJ128	Waukesha	3.8	5/24/2007
HJ128	Waukesha	5.4	11/5/2008
HJ128	Waukesha	4.5	3/12/2009
HJ128	Waukesha	3.8	12/2/2010
HJ128	Waukesha	4.3	8/31/2011
HJ128	Waukesha	4.7	11/28/2012
HJ128	Waukesha	4.2	7/25/2013
HJ128	Waukesha	4.3	8/13/2014
HJ128	Waukesha	6.0	9/16/2015
HJ128	Waukesha	5.1	4/25/2016
HJ128	Waukesha	4.0	5/3/2017
HJ196	Outagamie	7.8	7/26/2016
HJ196	Outagamie	6.8	3/26/2018
HN161	Brown	4.9	4/14/2014
HR251	Outagamie	1.1	9/16/2016
HR251	Outagamie	2.5	3/15/2017
HR251	Outagamie	1.9	2/12/2018
HW895	Outagamie	5.3	8/12/2016
HW895	Outagamie	5.5	8/24/2017
IE266	Brown	0.0	4/15/2014
IE861	Walworth	5.7	3/24/2004
IE861	Walworth	6.6	6/16/2005
IE861	Walworth	5.4	2/21/2006
KL362	Brown	2.9	6/10/2014

KW593	Calumet	1.2	7/15/2014
LT992	Brown	3.3	5/27/2014
LW772	Brown	6.1	10/30/2006
LW772	Brown	4.9	5/6/2008
LW772	Brown	5.4	6/10/2009
LW772	Brown	5.0	9/11/2013
LW772	Brown	3.4	6/21/2016
LW772	Brown	5.9	9/11/2017
MG104	Trempealeau	5.6	5/19/2002
MK423	Dodge	5.7	3/3/2016
MK423	Dodge	6.0	3/22/2017
MM157	Waukesha	4.4	7/31/2000
MM157	Waukesha	3.2	7/14/2015
MM157	Waukesha	3.8	5/6/2016
MM157	Waukesha	3.2	1/3/2017
MO407	Dodge	1.8	10/9/2000
MZ718	Dane	1.4	7/11/2002
NV230	Polk	3.7	9/21/2005
NV230	Polk	4.1	12/19/2006
NV231	Polk	1.2	3/24/2004
NV236	Chippewa	3.3	5/16/2007
NV239	Saint Croix	2.4	8/9/2007
NV242	Pierce	2.2	2/20/2008
NV243	Saint Croix	2.1	4/3/2008
NY868	Waukesha	2.7	2/28/2001
NY871	Dane	1.1	10/3/2001
NZ392	Waukesha	1.9	11/30/2009
NZ392	Waukesha	2.8	8/18/2015
NZ643	Walworth	7.9	1/30/2007
NZ643	Walworth	6.5	12/11/2012
OG942	Waukesha	2.8	4/9/2001
OG942	Waukesha	2.0	7/14/2015
OG942	Waukesha	4.0	5/6/2016
OG942	Waukesha	1.7	1/3/2017
OH469	Brown	7.5	1/2/2002
OH469	Brown	6.9	3/17/2014
RA584	Rock	3.6	7/10/2002
RE564	Dodge	4.7	10/23/2003
RG653	Dane	1.7	5/30/2003
RG653	Dane	2.6	6/24/2004
RG654	Juneau	1.4	7/28/2004

RG655	Walworth	2.6	5/13/2004
RG693	Outagamie	3.4	12/12/2005
RG700	Dane	2.2	2/14/2003
RL254	Marinette	5.3	7/31/2013
RL254	Marinette	6.8	9/7/2016
RL254	Marinette	10.9	7/11/2017
RL259	Winnebago	3.2	7/8/2009
RL260	Winnebago	7.0	8/6/2009
RT720	Eau Claire	2.1	11/11/2003
RV159	Trempealeau	0.0	4/14/2004
RV162	Trempealeau	0.0	4/13/2004
RW901	Jefferson	4.4	8/21/2001
RX268	Jefferson	5.2	7/10/2001
RY206	Dodge	5.1	5/1/2002
SA144	Rock	1.9	3/26/2003
SA190	Rock	1.9	8/18/2003
SA852	Outagamie	11.1	8/20/2003
SA852	Outagamie	8.6	9/28/2005
SA852	Outagamie	7.6	2/7/2006
SA852	Outagamie	8.0	10/22/2007
SA852	Outagamie	9.7	9/16/2016
SA852	Outagamie	7.8	3/21/2017
SA852	Outagamie	7.4	2/12/2018
SB744	Monroe	1.6	10/7/2004
SB757	Grant	3.6	1/21/2010
SB777	Waukesha	2.6	3/1/2007
SH979	Clark	1.5	9/9/2004
SI612	Marathon	0.6	7/7/2004
SK038	Jefferson	1.2	7/20/2004
SO618	Columbia	3.0	12/4/2006
SO619	Columbia	0.4	5/8/2006
SO621	Sauk	3.2	4/22/2008
SO622	Richland	4.1	4/16/2009
SO641	Outagamie	5.6	7/18/2016
SO641	Outagamie	4.5	2/28/2017
SQ101	Wood	3.4	9/20/2016
SQ101	Wood	6.8	3/21/2017
SQ102	Wood	6.5	3/1/2005
SQ102	Wood	8.0	3/21/2017
SR722	Ozaukee	5.0	12/22/2005
SR722	Ozaukee	6.2	9/4/2007

SR722	Ozaukee	3.4	3/28/2012
SR722	Ozaukee	1.0	2/27/2013
SS417	Racine	10.5	12/9/2004
SS417	Racine	9.5	6/7/2005
SZ294	Waukesha	2.2	4/11/2006
TJ178	Jefferson	1.1	3/10/2006
TJ210	La Crosse	2.2	7/10/2008
TK529	Waukesha	0.8	2/26/2007
TM595	Dane	0.1	11/6/2006
TO502	Dane	4.5	9/21/2006
TP746	Iowa	2.9	10/14/2003
TP817	Outagamie	4.6	12/4/2003
TQ116	Clark	2.4	8/20/2003
TQ317	Waukesha	4.2	9/11/2006
TQ317	Waukesha	4.2	3/12/2007
TQ323	Winnebago	10.8	11/16/2004
TQ323	Winnebago	9.3	6/20/2006
TQ325	Dodge	4.9	1/25/2005
TQ325	Dodge	6.1	10/18/2006
TQ325	Dodge	4.8	3/10/2016
TQ325	Dodge	4.7	3/8/2017
TQ327	Waukesha	1.9	2/24/2005
TQ446	Marathon	1.9	1/15/2004
TT889	Rock	3.7	5/18/2005
TT956	Kenosha	7.6	4/19/2005
TT956	Kenosha	7.2	6/27/2007
TT956	Kenosha	7.7	2/8/2012
TT956	Kenosha	5.8	2/25/2013
TT956	Kenosha	7.6	5/10/2016
TT956	Kenosha	6.5	2/20/2017
TT957	Rock	7.2	11/28/2006
TT957	Rock	7.6	8/14/2007
TT957	Rock	6.6	5/6/2008
TT957	Rock	7.2	7/21/2011
TT973	Rock	3.7	9/21/2005
TT975	Dodge	3.8	9/22/2005
TU107	Outagamie	2.1	6/16/2016
TU107	Outagamie	2.5	6/6/2017
TU514	Sheboygan	1.8	9/26/2008
TU527	Kenosha	6.9	3/11/2010
TU539	Outagamie	10.6	6/17/2014

TU539	Outagamie	7.5	6/16/2016
TU539	Outagamie	10.7	6/6/2017
TU539	Outagamie	8.5	3/13/2018
TV642	Outagamie	4.2	10/24/2006
TV642	Outagamie	3.4	10/11/2007
UB015	Kenosha	5.1	6/19/2007
UL988	Saint Croix	1.4	6/11/2008
UO874	La Crosse	1.2	5/7/2008
UO912	La Crosse	1.0	12/3/2008
UV413	Waukesha	3.0	2/9/2010
UV414	Waukesha	4.9	5/27/2010
UY738	Clark	0.0	8/10/2009
UY766	Clark	0.7	8/31/2009
UY773	Clark	0.0	8/18/2009
VD077	Rock	0.3	10/7/2010
VK897	Walworth	10.2	10/30/2008
VK897	Walworth	13.0	6/18/2009
VL002	Sawyer	2.3	2/8/2006
VL269	Rock	2.8	11/10/2005
VL852	Waukesha	7.8	5/30/2006
VL960	Jefferson	5.9	3/16/2006
VL961	Marinette	2.6	7/31/2013
VL961	Marinette	7.3	9/7/2016
VL961	Marinette	9.4	7/11/2017
VL965	Racine	6.8	6/15/2006
VL966	Outagamie	8.1	4/6/2006
VL966	Outagamie	5.6	10/22/2007
VL966	Outagamie	7.2	1/13/2012
VL966	Outagamie	7.9	9/15/2016
VL966	Outagamie	6.3	3/13/2017
VL966	Outagamie	6.1	2/12/2018
VM097	Rock	2.1	4/25/2006
VM098	Rock	2.7	4/25/2006
VX766	Eau Claire	4.0	11/4/2008
VX766	Eau Claire	4.0	11/4/2008
VX770	Barron	0.0	9/3/2008
WG311	Calumet	9.9	1/28/2016
WG311	Calumet	10.0	4/26/2017
WG311	Calumet	7.6	2/14/2018
WH972	Walworth	9.0	3/14/2007
WI033	Rock	3.6	8/10/2006

WJ282	Walworth	0.0	8/28/2007
WJ283	Jackson	0.4	7/18/2007
WJ286	Trempealeau	3.8	6/8/2007
WJ910	Washington	9.7	1/13/2009
WJ910	Washington	5.0	3/16/2016
WJ910	Washington	6.2	2/1/2017
WJ910	Washington	7.8	2/5/2018
WK637	Jefferson	1.5	2/18/2008
WK743	Monroe	1.3	10/4/2007
WK858	Dane	0.8	5/13/2010
WK859	Columbia	0.6	1/27/2011
WL581	Outagamie	1.3	7/29/2008
WL768	Walworth	3.9	6/19/2007
WL773	Dane	2.5	9/9/2008
WL776	Jackson	1.4	12/2/2008
WM410	Marinette	0.8	7/23/2008
WM753	Winnebago	8.6	9/30/2008
WN837	Dane	2.3	1/7/2009
WO060	Ozaukee	1.5	7/28/2009
WO236	Trempealeau	4.7	6/11/2009
WP527	La Crosse	1.6	1/13/2010
WP561	Sauk	2.1	2/18/2010
WP601	Dane	2.5	3/30/2010
WQ168	Sauk	2.8	3/14/2012
WW467	Juneau	0.7	9/6/2012
XA110	Waukesha	9.6	4/22/2013
XA110	Waukesha	9.8	5/7/2015
XA110	Waukesha	10.0	2/4/2016
XA110	Waukesha	7.2	1/5/2017
XA110	Waukesha	8.3	2/15/2018
YE608	Grant	3.0	8/11/2010
YE615	Dane	6.6	4/20/2011
YE971	Waupaca	4.0	12/13/2010
YE971	Waupaca	6.1	7/16/2015
YE971	Waupaca	4.8	1/21/2016
YE971	Waupaca	5.8	3/27/2017
YE971	Waupaca	6.9	1/8/2018
YF448	Rock	1.2	6/8/2011
YG024	Barron	1.4	8/19/2011
YG119	Dane	0.0	1/15/2013
YG586	Columbia	1.5	10/2/2012

YG656	Monroe	1.4	1/4/2012
YH168	Dodge	7.8	3/12/2013
YH168	Dodge	1.7	6/15/2016
YH168	Dodge	8.0	8/21/2017
YI080	Columbia	5.0	9/13/2012

Table S2. Combined radium measurements used in the local-scale analysis. Wisconsin Unique Well Number is represented by WUWN.

WUWN	System Name	Ra activity (pCi/L)	Sample Date
AJ774	SUSSEX VILLAGE HALL & WATER UTILITY	4.10	3/12/2002
AJ774	SUSSEX VILLAGE HALL & WATER UTILITY	4.70	6/10/2003
AJ774	SUSSEX VILLAGE HALL & WATER UTILITY	4.90	7/9/2003
AJ774	SUSSEX VILLAGE HALL & WATER UTILITY	4.90	9/9/2003
AJ774	SUSSEX VILLAGE HALL & WATER UTILITY	5.10	12/3/2003
AJ774	SUSSEX VILLAGE HALL & WATER UTILITY	5.10	5/20/2008
AJ774	SUSSEX VILLAGE HALL & WATER UTILITY	5.80	7/15/2009
AJ774	SUSSEX VILLAGE HALL & WATER UTILITY	4.50	10/27/2009
AJ774	SUSSEX VILLAGE HALL & WATER UTILITY	3.77	2/15/2010
AJ774	SUSSEX VILLAGE HALL & WATER UTILITY	4.95	5/11/2010
AJ774	SUSSEX VILLAGE HALL & WATER UTILITY	4.14	8/16/2010
AJ774	SUSSEX VILLAGE HALL & WATER UTILITY	3.80	10/18/2010
AJ774	SUSSEX VILLAGE HALL & WATER UTILITY	4.70	2/8/2011

AJ774	SUSSEX VILLAGE HALL & WATER UTILITY	2.07	4/25/2011
AJ774	SUSSEX VILLAGE HALL & WATER UTILITY	4.36	8/1/2011
AJ774	SUSSEX VILLAGE HALL & WATER UTILITY	5.94	10/26/2011
AJ774	SUSSEX VILLAGE HALL & WATER UTILITY	4.00	2/29/2012
AJ774	SUSSEX VILLAGE HALL & WATER UTILITY	6.95	5/15/2012
AJ774	SUSSEX VILLAGE HALL & WATER UTILITY	6.69	8/6/2012
AJ774	SUSSEX VILLAGE HALL & WATER UTILITY	7.07	8/6/2012
AJ774	SUSSEX VILLAGE HALL & WATER UTILITY	6.33	10/29/2012
AJ774	SUSSEX VILLAGE HALL & WATER UTILITY	5.60	3/4/2013
AJ774	SUSSEX VILLAGE HALL & WATER UTILITY	6.00	5/21/2013
AJ774	SUSSEX VILLAGE HALL & WATER UTILITY	4.60	7/22/2013
AJ774	SUSSEX VILLAGE HALL & WATER UTILITY	4.81	10/1/2013
AJ774	SUSSEX VILLAGE HALL & WATER UTILITY	5.00	3/13/2014
AJ774	SUSSEX VILLAGE HALL & WATER UTILITY	4.35	5/20/2014
AJ774	SUSSEX VILLAGE HALL & WATER UTILITY	4.59	8/18/2014
AJ774	SUSSEX VILLAGE HALL & WATER UTILITY	6.44	10/21/2014
AJ774	SUSSEX VILLAGE HALL & WATER UTILITY	4.33	3/3/2015
AJ774	SUSSEX VILLAGE HALL & WATER UTILITY	5.65	5/19/2015
AJ774	SUSSEX VILLAGE HALL & WATER UTILITY	4.85	8/10/2015
AJ774	SUSSEX VILLAGE HALL & WATER UTILITY	5.25	11/11/2015
AJ774	SUSSEX VILLAGE HALL & WATER UTILITY	5.92	2/17/2016
AJ774	SUSSEX VILLAGE HALL & WATER UTILITY	4.98	5/19/2016
AJ774	SUSSEX VILLAGE HALL & WATER UTILITY	6.24	8/10/2016
AJ774	SUSSEX VILLAGE HALL & WATER UTILITY	5.24	11/15/2016
AJ774	SUSSEX VILLAGE HALL & WATER UTILITY	4.70	2/15/2017
AJ774	SUSSEX VILLAGE HALL & WATER UTILITY	6.03	5/23/2017
AJ774	SUSSEX VILLAGE HALL & WATER UTILITY	6.06	8/15/2017
AJ774	SUSSEX VILLAGE HALL & WATER UTILITY	5.86	11/14/2017
AJ774	SUSSEX VILLAGE HALL & WATER UTILITY	5.15	2/14/2018
AJ774	SUSSEX VILLAGE HALL & WATER UTILITY	5.27	5/15/2018
BA144	BROOKFIELD WATER UTILITY	3.14	3/25/2002
BA144	BROOKFIELD WATER UTILITY	3.70	5/20/2008
BA144	BROOKFIELD WATER UTILITY	4.60	2/28/2011
BA144	BROOKFIELD WATER UTILITY	4.20	7/29/2014
BA144	BROOKFIELD WATER UTILITY	4.30	5/17/2017
BH375	BROOKFIELD WATER UTILITY	5.80	3/25/2002
BH375	BROOKFIELD WATER UTILITY	5.00	2/6/2007
BH375	BROOKFIELD WATER UTILITY	6.70	6/14/2016
BH375	BROOKFIELD WATER UTILITY	8.20	5/17/2017
BH380	BROOKFIELD WATER UTILITY	6.40	4/24/2007
BH380	BROOKFIELD WATER UTILITY	8.90	12/9/2014

BH380	BROOKFIELD WATER UTILITY	8.00	6/14/2016
BH380	BROOKFIELD WATER UTILITY	7.80	8/31/2016
BH380	BROOKFIELD WATER UTILITY	8.20	5/17/2017
BH381	BROOKFIELD WATER UTILITY	5.80	4/24/2007
BH381	BROOKFIELD WATER UTILITY	6.40	6/14/2016
BH381	BROOKFIELD WATER UTILITY	8.20	5/17/2017
BH387	BROOKFIELD WATER UTILITY	4.90	3/25/2002
BH387	BROOKFIELD WATER UTILITY	4.40	5/20/2008
BH387	BROOKFIELD WATER UTILITY	4.90	1/4/2011
BH387	BROOKFIELD WATER UTILITY	4.30	7/29/2014
BH387	BROOKFIELD WATER UTILITY	6.20	5/17/2017
BH387	BROOKFIELD WATER UTILITY	8.10	11/14/2017
BH387	BROOKFIELD WATER UTILITY	6.90	3/14/2018
BH387	BROOKFIELD WATER UTILITY	5.80	6/4/2018
BH387	BROOKFIELD WATER UTILITY	6.30	9/24/2018
BH387	BROOKFIELD WATER UTILITY	6.30	9/24/2018
BH387	BROOKFIELD WATER UTILITY	9.70	10/29/2018
BH387	BROOKFIELD WATER UTILITY	9.70	10/29/2018
BH387	BROOKFIELD WATER UTILITY	6.90	2/12/2019
BH424	SUSSEX VILLAGE HALL & WATER UTILITY	5.60	3/11/2002
BH424	SUSSEX VILLAGE HALL & WATER UTILITY	3.95	6/10/2003
BH424	SUSSEX VILLAGE HALL & WATER UTILITY	5.80	7/9/2003
BH424	SUSSEX VILLAGE HALL & WATER UTILITY	6.10	9/9/2003
BH424	SUSSEX VILLAGE HALL & WATER UTILITY	5.90	12/3/2003
BH424	SUSSEX VILLAGE HALL & WATER UTILITY	8.20	7/14/2008
BH424	SUSSEX VILLAGE HALL & WATER UTILITY	7.25	5/20/2014
BH425	SUSSEX VILLAGE HALL & WATER UTILITY	4.02	3/11/2002
BH425	SUSSEX VILLAGE HALL & WATER UTILITY	4.00	5/20/2008
BH425	SUSSEX VILLAGE HALL & WATER UTILITY	3.37	3/15/2011
BH425	SUSSEX VILLAGE HALL & WATER UTILITY	5.51	5/20/2014
BH425	SUSSEX VILLAGE HALL & WATER UTILITY	4.99	8/18/2014
BH425	SUSSEX VILLAGE HALL & WATER UTILITY	4.44	10/21/2014
BH425	SUSSEX VILLAGE HALL & WATER UTILITY	5.16	3/3/2015
BH425	SUSSEX VILLAGE HALL & WATER UTILITY	8.25	5/19/2015
BH425	SUSSEX VILLAGE HALL & WATER UTILITY	5.14	8/10/2015
BH425	SUSSEX VILLAGE HALL & WATER UTILITY	2.96	11/11/2015
BH425	SUSSEX VILLAGE HALL & WATER UTILITY	4.79	2/17/2016
BH425	SUSSEX VILLAGE HALL & WATER UTILITY	5.31	5/19/2016
BH425	SUSSEX VILLAGE HALL & WATER UTILITY	5.30	8/10/2016
BH425	SUSSEX VILLAGE HALL & WATER UTILITY	6.11	11/15/2016
BH425	SUSSEX VILLAGE HALL & WATER UTILITY	6.47	2/16/2017

BH425	SUSSEX VILLAGE HALL & WATER UTILITY	5.23	8/15/2017
BH425	SUSSEX VILLAGE HALL & WATER UTILITY	4.51	11/14/2017
BH425	SUSSEX VILLAGE HALL & WATER UTILITY	6.72	2/14/2018
BH425	SUSSEX VILLAGE HALL & WATER UTILITY	3.75	5/15/2018
BH425	SUSSEX VILLAGE HALL & WATER UTILITY	7.48	8/22/2018
BH425	SUSSEX VILLAGE HALL & WATER UTILITY	5.66	11/27/2018
BH425	SUSSEX VILLAGE HALL & WATER UTILITY	7.83	2/21/2019
BH426	SUSSEX VILLAGE HALL & WATER UTILITY	4.40	3/11/2002
BH426	SUSSEX VILLAGE HALL & WATER UTILITY	4.30	5/20/2008
BH426	SUSSEX VILLAGE HALL & WATER UTILITY	6.30	5/20/2014
BH426	SUSSEX VILLAGE HALL & WATER UTILITY	6.10	8/18/2014
BH426	SUSSEX VILLAGE HALL & WATER UTILITY	6.02	10/21/2014
BH426	SUSSEX VILLAGE HALL & WATER UTILITY	4.32	3/3/2015
BH426	SUSSEX VILLAGE HALL & WATER UTILITY	9.19	5/19/2015
BH426	SUSSEX VILLAGE HALL & WATER UTILITY	6.34	8/10/2015
BH426	SUSSEX VILLAGE HALL & WATER UTILITY	6.51	11/11/2015
BH426	SUSSEX VILLAGE HALL & WATER UTILITY	6.62	2/17/2016
BH426	SUSSEX VILLAGE HALL & WATER UTILITY	6.05	5/19/2016
BH426	SUSSEX VILLAGE HALL & WATER UTILITY	4.58	8/10/2016
BH426	SUSSEX VILLAGE HALL & WATER UTILITY	6.78	11/15/2016
BH426	SUSSEX VILLAGE HALL & WATER UTILITY	5.95	2/15/2017
BH426	SUSSEX VILLAGE HALL & WATER UTILITY	7.61	5/23/2017
BH426	SUSSEX VILLAGE HALL & WATER UTILITY	7.94	8/15/2017
BH426	SUSSEX VILLAGE HALL & WATER UTILITY	7.73	11/14/2017
BH426	SUSSEX VILLAGE HALL & WATER UTILITY	6.80	2/14/2018
BH426	SUSSEX VILLAGE HALL & WATER UTILITY	4.72	5/15/2018
BH426	SUSSEX VILLAGE HALL & WATER UTILITY	7.21	8/22/2018
BH426	SUSSEX VILLAGE HALL & WATER UTILITY	6.68	11/27/2018
BH426	SUSSEX VILLAGE HALL & WATER UTILITY	8.59	2/21/2019
BH429	WAUKESHA WATER UTILITY	11.80	3/4/2002
BH429	WAUKESHA WATER UTILITY	3.10	10/12/2006
BH429	WAUKESHA WATER UTILITY	4.10	10/12/2006
BH429	WAUKESHA WATER UTILITY	20.18	9/12/2011
BH429	WAUKESHA WATER UTILITY	23.64	10/31/2011
BH429	WAUKESHA WATER UTILITY	22.00	1/26/2012
BH429	WAUKESHA WATER UTILITY	18.76	6/17/2014
BH429	WAUKESHA WATER UTILITY	17.32	1/26/2016
BH429	WAUKESHA WATER UTILITY	16.95	1/11/2017
BH429	WAUKESHA WATER UTILITY	15.22	1/23/2018
BH429	WAUKESHA WATER UTILITY	2.47	11/8/2018
BH429	WAUKESHA WATER UTILITY	2.21	1/17/2019

BH429	WAUKESHA WATER UTILITY	20.58	3/7/2019
BH431	WAUKESHA WATER UTILITY	9.40	5/22/2000
BH431	WAUKESHA WATER UTILITY	9.50	3/4/2002
BH431	WAUKESHA WATER UTILITY	8.50	10/12/2006
BH431	WAUKESHA WATER UTILITY	6.30	6/4/2008
BH431	WAUKESHA WATER UTILITY	8.00	10/14/2008
BH431	WAUKESHA WATER UTILITY	4.77	1/21/2009
BH431	WAUKESHA WATER UTILITY	4.75	5/7/2009
BH431	WAUKESHA WATER UTILITY	10.18	6/23/2009
BH431	WAUKESHA WATER UTILITY	11.15	7/20/2009
BH431	WAUKESHA WATER UTILITY	7.96	9/23/2009
BH431	WAUKESHA WATER UTILITY	8.02	10/12/2009
BH431	WAUKESHA WATER UTILITY	9.43	11/17/2009
BH431	WAUKESHA WATER UTILITY	9.89	12/8/2009
BH431	WAUKESHA WATER UTILITY	10.30	1/11/2010
BH431	WAUKESHA WATER UTILITY	8.03	4/20/2010
BH431	WAUKESHA WATER UTILITY	6.83	7/27/2010
BH431	WAUKESHA WATER UTILITY	6.02	11/17/2010
BH431	WAUKESHA WATER UTILITY	8.74	3/15/2011
BH431	WAUKESHA WATER UTILITY	6.86	4/19/2011
BH431	WAUKESHA WATER UTILITY	8.01	5/10/2011
BH431	WAUKESHA WATER UTILITY	9.23	6/3/2011
BH431	WAUKESHA WATER UTILITY	8.76	8/23/2011
BH431	WAUKESHA WATER UTILITY	7.39	10/28/2011
BH431	WAUKESHA WATER UTILITY	6.80	3/23/2012
BH431	WAUKESHA WATER UTILITY	6.78	6/16/2012
BH431	WAUKESHA WATER UTILITY	5.11	7/1/2012
BH431	WAUKESHA WATER UTILITY	4.51	11/13/2012
BH431	WAUKESHA WATER UTILITY	7.20	3/20/2013
BH431	WAUKESHA WATER UTILITY	6.84	6/21/2013
BH431	WAUKESHA WATER UTILITY	5.86	8/1/2013
BH431	WAUKESHA WATER UTILITY	8.75	10/7/2013
BH431	WAUKESHA WATER UTILITY	9.78	11/19/2013
BH431	WAUKESHA WATER UTILITY	9.51	12/18/2013
BH431	WAUKESHA WATER UTILITY	10.36	1/14/2014
BH431	WAUKESHA WATER UTILITY	6.16	2/6/2014
BH431	WAUKESHA WATER UTILITY	10.55	3/4/2014
BH431	WAUKESHA WATER UTILITY	10.98	4/3/2014
BH431	WAUKESHA WATER UTILITY	8.50	9/23/2014
BH431	WAUKESHA WATER UTILITY	4.14	12/9/2014
BH431	WAUKESHA WATER UTILITY	5.61	3/10/2015

BH431	WAUKESHA WATER UTILITY	6.96	6/10/2015
BH431	WAUKESHA WATER UTILITY	7.87	9/22/2015
BH431	WAUKESHA WATER UTILITY	7.95	12/4/2015
BH431	WAUKESHA WATER UTILITY	8.27	3/10/2016
BH431	WAUKESHA WATER UTILITY	4.93	6/9/2016
BH431	WAUKESHA WATER UTILITY	6.23	9/20/2016
BH431	WAUKESHA WATER UTILITY	7.57	12/21/2016
BH431	WAUKESHA WATER UTILITY	5.11	3/16/2017
BH431	WAUKESHA WATER UTILITY	5.38	6/28/2017
BH431	WAUKESHA WATER UTILITY	4.63	9/27/2017
BH431	WAUKESHA WATER UTILITY	6.87	12/7/2017
BH431	WAUKESHA WATER UTILITY	5.98	3/13/2018
BH431	WAUKESHA WATER UTILITY	5.23	6/14/2018
BH431	WAUKESHA WATER UTILITY	6.72	9/13/2018
BH431	WAUKESHA WATER UTILITY	6.91	12/26/2018
BH431	WAUKESHA WATER UTILITY	6.97	3/7/2019
BH433	WAUKESHA WATER UTILITY	6.69	5/22/2000
BH433	WAUKESHA WATER UTILITY	5.60	3/4/2002
BH433	WAUKESHA WATER UTILITY	6.00	10/5/2005
BH433	WAUKESHA WATER UTILITY	5.80	3/16/2006
BH433	WAUKESHA WATER UTILITY	5.20	5/2/2006
BH433	WAUKESHA WATER UTILITY	6.50	7/13/2006
BH433	WAUKESHA WATER UTILITY	5.50	10/12/2006
BH433	WAUKESHA WATER UTILITY	5.89	1/16/2007
BH433	WAUKESHA WATER UTILITY	6.40	4/10/2007
BH433	WAUKESHA WATER UTILITY	6.50	7/9/2007
BH433	WAUKESHA WATER UTILITY	6.30	1/21/2008
BH433	WAUKESHA WATER UTILITY	3.90	6/4/2008
BH433	WAUKESHA WATER UTILITY	4.41	5/7/2009
BH433	WAUKESHA WATER UTILITY	6.48	6/23/2009
BH433	WAUKESHA WATER UTILITY	6.23	8/12/2009
BH433	WAUKESHA WATER UTILITY	5.08	9/23/2009
BH433	WAUKESHA WATER UTILITY	5.76	10/12/2009
BH433	WAUKESHA WATER UTILITY	5.67	11/17/2009
BH433	WAUKESHA WATER UTILITY	6.78	12/8/2009
BH433	WAUKESHA WATER UTILITY	5.14	1/11/2010
BH433	WAUKESHA WATER UTILITY	3.91	4/14/2010
BH433	WAUKESHA WATER UTILITY	3.33	7/28/2010
BH433	WAUKESHA WATER UTILITY	3.79	8/3/2010
BH433	WAUKESHA WATER UTILITY	6.06	9/16/2010
BH433	WAUKESHA WATER UTILITY	5.74	10/14/2010

BH433	WAUKESHA WATER UTILITY	4.88	2/1/2011
BH433	WAUKESHA WATER UTILITY	5.50	3/1/2011
BH433	WAUKESHA WATER UTILITY	5.86	4/12/2011
BH433	WAUKESHA WATER UTILITY	5.51	5/10/2011
BH433	WAUKESHA WATER UTILITY	6.16	6/3/2011
BH433	WAUKESHA WATER UTILITY	7.76	7/7/2011
BH433	WAUKESHA WATER UTILITY	5.98	10/24/2011
BH433	WAUKESHA WATER UTILITY	3.72	3/23/2012
BH433	WAUKESHA WATER UTILITY	4.66	6/24/2012
BH433	WAUKESHA WATER UTILITY	3.59	7/1/2012
BH433	WAUKESHA WATER UTILITY	6.38	8/1/2012
BH433	WAUKESHA WATER UTILITY	4.02	11/13/2012
BH433	WAUKESHA WATER UTILITY	4.04	3/20/2013
BH433	WAUKESHA WATER UTILITY	4.43	6/14/2013
BH433	WAUKESHA WATER UTILITY	4.19	7/1/2013
BH433	WAUKESHA WATER UTILITY	4.16	9/3/2013
BH433	WAUKESHA WATER UTILITY	6.50	10/7/2013
BH433	WAUKESHA WATER UTILITY	6.67	11/19/2013
BH433	WAUKESHA WATER UTILITY	6.81	12/18/2013
BH433	WAUKESHA WATER UTILITY	6.57	1/14/2014
BH433	WAUKESHA WATER UTILITY	7.15	2/6/2014
BH433	WAUKESHA WATER UTILITY	6.91	3/4/2014
BH433	WAUKESHA WATER UTILITY	5.91	4/3/2014
BH433	WAUKESHA WATER UTILITY	3.98	9/3/2014
BH433	WAUKESHA WATER UTILITY	4.31	12/9/2014
BH433	WAUKESHA WATER UTILITY	3.85	3/10/2015
BH433	WAUKESHA WATER UTILITY	4.61	6/10/2015
BH433	WAUKESHA WATER UTILITY	4.75	7/28/2015
BH433	WAUKESHA WATER UTILITY	2.91	8/6/2015
BH433	WAUKESHA WATER UTILITY	5.98	9/1/2015
BH433	WAUKESHA WATER UTILITY	4.40	12/4/2015
BH433	WAUKESHA WATER UTILITY	4.46	3/10/2016
BH433	WAUKESHA WATER UTILITY	5.19	5/5/2016
BH433	WAUKESHA WATER UTILITY	3.41	9/20/2016
BH433	WAUKESHA WATER UTILITY	5.37	11/8/2016
BH433	WAUKESHA WATER UTILITY	3.47	3/16/2017
BH433	WAUKESHA WATER UTILITY	4.08	6/28/2017
BH433	WAUKESHA WATER UTILITY	3.43	9/27/2017
BH433	WAUKESHA WATER UTILITY	4.08	12/7/2017
BH433	WAUKESHA WATER UTILITY	3.55	3/13/2018
BH433	WAUKESHA WATER UTILITY	3.44	6/14/2018

BH433	WAUKESHA WATER UTILITY	4.67	9/13/2018
BH433	WAUKESHA WATER UTILITY	4.04	12/26/2018
BH433	WAUKESHA WATER UTILITY	3.92	1/2/2019
BH433	WAUKESHA WATER UTILITY	3.70	3/1/2019
BH434	WAUKESHA WATER UTILITY	9.70	5/22/2000
BH434	WAUKESHA WATER UTILITY	8.60	3/4/2002
BH434	WAUKESHA WATER UTILITY	8.30	10/23/2006
BH434	WAUKESHA WATER UTILITY	9.60	1/16/2007
BH434	WAUKESHA WATER UTILITY	9.13	3/3/2016
BH434	WAUKESHA WATER UTILITY	9.24	5/15/2017
BH434	WAUKESHA WATER UTILITY	9.47	1/23/2018
BH434	WAUKESHA WATER UTILITY	11.69	3/7/2019
BH436	WAUKESHA WATER UTILITY	11.00	5/22/2000
BH436	WAUKESHA WATER UTILITY	11.40	6/24/2002
BH436	WAUKESHA WATER UTILITY	11.40	6/24/2002
BH436	WAUKESHA WATER UTILITY	10.50	10/12/2006
BH436	WAUKESHA WATER UTILITY	10.80	2/18/2008
BH436	WAUKESHA WATER UTILITY	10.75	2/9/2010
BH436	WAUKESHA WATER UTILITY	11.75	1/26/2012
BH436	WAUKESHA WATER UTILITY	8.97	1/27/2016
BH436	WAUKESHA WATER UTILITY	10.98	1/11/2017
BH436	WAUKESHA WATER UTILITY	9.88	1/23/2018
EQ944	WAUKESHA WATER UTILITY	5.80	5/22/2000
EQ944	WAUKESHA WATER UTILITY	5.70	3/4/2002
EQ944	WAUKESHA WATER UTILITY	5.50	4/10/2007
EQ944	WAUKESHA WATER UTILITY	6.70	7/9/2007
EQ944	WAUKESHA WATER UTILITY	5.70	1/21/2008
EQ944	WAUKESHA WATER UTILITY	4.81	5/7/2009
EQ944	WAUKESHA WATER UTILITY	6.63	6/23/2009
EQ944	WAUKESHA WATER UTILITY	6.13	8/12/2009
EQ944	WAUKESHA WATER UTILITY	5.26	9/23/2009
EQ944	WAUKESHA WATER UTILITY	5.90	10/12/2009
EQ944	WAUKESHA WATER UTILITY	6.33	11/17/2009
EQ944	WAUKESHA WATER UTILITY	6.89	12/8/2009
EQ944	WAUKESHA WATER UTILITY	6.00	1/11/2010
EQ944	WAUKESHA WATER UTILITY	5.10	4/20/2010
EQ944	WAUKESHA WATER UTILITY	5.27	7/26/2010
EQ944	WAUKESHA WATER UTILITY	6.22	10/13/2010
EQ944	WAUKESHA WATER UTILITY	8.31	2/28/2011
EQ944	WAUKESHA WATER UTILITY	5.75	4/19/2011
EQ944	WAUKESHA WATER UTILITY	6.88	7/7/2011

IZ383	BROOKFIELD WATER UTILITY	3.60	3/25/2002
IZ383	BROOKFIELD WATER UTILITY	4.50	5/20/2008
IZ383	BROOKFIELD WATER UTILITY	3.50	5/23/2011
IZ383	BROOKFIELD WATER UTILITY	3.60	7/29/2014
IZ383	BROOKFIELD WATER UTILITY	4.30	5/17/2017
VL852	SUSSEX VILLAGE HALL & WATER UTILITY	7.20	5/9/2006
VL852	SUSSEX VILLAGE HALL & WATER UTILITY	7.80	5/30/2006
VL852	SUSSEX VILLAGE HALL & WATER UTILITY	1.37	9/27/2007
VL852	SUSSEX VILLAGE HALL & WATER UTILITY	7.00	12/20/2007

References

Sen, P. K. (1968). Estimates of Regression Coefficient Based on Kendall's tau. *Journal of the American Statistical Association, 63*(324), 1279-1289. doi:10.1080/01621459.1968.10480934

Siegel, A. F. (1982). Robust Regression Using Repeated Medians. *Biometrika, 69*(1), 242-244.

Theil, H. (1992). A Rank-Invariant Method of Linear and Polynomial Regression Analysis. In B. Raj & J. Koerts (Eds.), *Henri Theil's Contributions to Economics and Econometrics: Econometric Theory and Methodology* (pp. 345-381). Dordrecht: Springer Netherlands.

Wilcox, R. R. (2001). Theil-Sen estimator. *Fundamentals of modern statistical methods. New York: Springer-Verlag*, 207-210.